University of South Carolina
Scholar Commons

Theses and Dissertations

6-30-2016

Molecular Cues Of Pattern-Recognition-Receptor Pathways In Redox-Toxicity-Driven Environmental NAFLD

Suvarthi Das
University of South Carolina

Follow this and additional works at: https://scholarcommons.sc.edu/etd

 Part of the Environmental Public Health Commons

Recommended Citation

Das, S.(2016). *Molecular Cues Of Pattern-Recognition-Receptor Pathways In Redox-Toxicity-Driven Environmental NAFLD.* (Doctoral dissertation). Retrieved from https://scholarcommons.sc.edu/etd/3406

This Open Access Dissertation is brought to you by Scholar Commons. It has been accepted for inclusion in Theses and Dissertations by an authorized administrator of Scholar Commons. For more information, please contact dillarda@mailbox.sc.edu.

www.manaraa.com

MOLECULAR CUES OF PATTERN-RECOGNITION-RECEPTOR PATHWAYS IN REDOX-TOXICITY-DRIVEN ENVIRONMENTAL NAFLD

by

Suvarthi Das

Bachelor of Science
University of Calcutta, 2006

Master of Science
University of Calcutta, 2008

Submitted in Partial Fulfillment of the Requirements

For the Degree of Doctor of Philosophy in

Environmental Health Sciences

The Norman J. Arnold School of Public Health

University of South Carolina

2016

Accepted by:

Saurabh Chatterjee, Major Professor

Gregory Michelotti, Committee Member

Alan Decho, Committee Member

Sean Norman, Committee Member

Lacy Ford, Senior Vice Provost and Dean of Graduate Studies

www.manaraa.com

© Copyright by Suvarthi Das, 2016
All Rights Reserved.

www.manaraa.com

DEDICATION

To all those unrecognized or under-recognized missionaries, who for times immemorial, have dedicated their lives for healing the ailments of the human kind, and have strived for the betterment and advancement of Science.

www.manaraa.com

ACKNOWLEDGEMENTS

I owe everything that amounted to my Ph.D. dissertation, first and foremost, to my Ph.D. advisor and 'mentor in the true sense', Dr. Saurabh Chatterjee. Not to mention my committee members, Drs. Gregory Michelotti, Alan Decho and Sean Norman, whose advice and guidance were invaluable. Nothing of this would have been possible without my wonderful colleagues and my friends in Columbia, who have become more like family and have boosted up my morale every now and then. Last but not the least, I am grateful to my family, friends, teachers and well-wishers back in India whose unwavering faith in me kept me going, when the days were not so sunny and bright.

***** I cannot thank my parents nearly enough, for being great visionaries in bringing me up and educating me, the way they did. *****

www.manaraa.com

ABSTRACT

With the pandemic proportions of obesity and a correlative increase in fatty liver disease, there was a dire need to explore the missing link between the changed environment and progression of NAFLD in obesity. My research implies that environmental toxin bromodichloromethane induces early liver lesions in obesity, and is mediated by the synchronous insult of oxidative stress and increased levels of the adipokine leptin. In a two-pronged approach to investigate the molecular cues, I looked at the role of Purinergic receptor X7 and Toll 4 receptor. Both rodent models and cell-based systems were used. Also, in order to validate my findings in humans, I used diseased liver samples and corresponding age-matched controls. All diseased samples, and toxin-primed cell systems tested positive for oxidative stress markers. My first set of findings strongly suggest that P2X7r is a key regulator of autophagy-induced metabolic oxidative stress and early liver inflammation. In the second part of my investigation, I observed that toll 4 receptor recruitment to raft-zones of the liver cell membranes is crucial for its induction and inflammation in NAFLD. Most importantly, instead of the well-established stimulator of toll-receptor 4, LPS, I show that peroxynitrite which is elevated in the system as a result of the free radical chemistry, post environmental toxin exposure, is a potent inducer of TLR4-mediated inflammation in the disease. High-end confocal microscopy and immunofluorescence imaging techniques were utilized in addition to quantifying gene expressions, and immunoblotting proteins. Also, in a first-ever report in any model of

www.manaraa.com

NAFLD I used a peroxynitite-scavenging molecule FBA, showing positive remediation of NAFLD symptoms. This could be a very promising treatment regimen for redox-toxicity driven NAFLD. In conclusion, this novel disease model of NAFLD, helps us better understand the environmental link to the disease in presence of obesity, and exemplifies the molecular cues as potential therapeutic targets for alleviation of this silent-killer.

www.manaraa.com

PREFACE

Obesity is a widespread disease/ syndrome in the modern world. Steatosis of liver (fatty liver) is common in approximately seventy-five percent of obese subjects and around twenty percent of these individuals develop inflammatory liver disease. Non-alcoholic fatty liver disease (NAFLD) is a spectrum where the liver progresses from fat accumulation, to necroinflammation, to scarring of liver tissue (fibrosis). The advanced stage of the NAFLD spectrum, nonalcoholic steatohepatitis (NASH), is marked by necroinflammation, release of proinflammatory cytokines and some degrees of fibrosis. NASH if untreated, can lead to cirrhosis, hepatocellular carcinoma and autoimmune disorders owing to the highly inflamatory microenvironment. The progression of steatosis to steatohepatitis can be very rapid and is characterized by infiltration of macrophages, activation of Kupffer cells (resident macrophages in the liver), apoptosis leading to necrosis, Mallory Body formation, and degeneration of hepatocytes.

This progression can be promoted by a second hit, brought on by reductive metabolism of environmental toxicants in water, diet and air. Our laboratory has shown evidence of NASH being caused by reductive metabolism of disinfection byproducts via CYP2E1, in presence of high fat diet. Chlorine-based disinfectants have played a critical role in protecting drinking water supplies from water-borne infectious diseases for nearly a century.

Bromodichloromethane belongs to a wide range of chemicals known as trihalomethanes, which are formed after chlorine, is added to the water for disinfection. The possible

www.manaraa.com

exposure routes to BDCM are by ingestion (through drinking water), by inhalation and/or by dermal absorption. Reports suggest that the maximum exposure can occur through oral and dermal route. BDCM is metabolized by the CYP450 enzyme primarily present in the microsomes of hepatocytes. The toxic effects of BDCM are mediated by the reductive free radical metabolism of this compound by CYP2E1, an isoform of cytochrome P450 enzyme, forming highly toxic hydroxenonenal adducts that cause hepatocellular necrosis (Das S et al, Toxicol Appl Pharm; Seth R et al, Tox Sciences, Chatterjee Lab, 2013). Also, since this model of NASH is derived from chronic exposure to drinking water disinfection byproduct and is an example of ad libitum exposure, I have used the phrase redox-toxicity driven environmental NAFLD or NASH (Seth R et al, Chatterjee Lab, Toxicological Sciences, 2013).

www.manaraa.com

TABLE OF CONTENTS

DEDICATION iii

ACKNOWLEDGEMENTS iv

ABSTRACT v

PREFACE vii

LIST OF TABLES xi

LIST OF FIGURES xii

CHAPTER 1: INTRODUCTION 1

CHAPTER 2: PROINFLAMMATORY ADIPOKINE LEPTIN MEDIATES DISINFECTION BYPRODUCT BROMODICHLOROMETHANE-INDUCED EARLY STEATOHEPATITIC INJURY IN OBESITY 8

2.1 INTRODUCTION 10

2.2 MATERIALS AND METHODS 13

2.3 RESULTS 19

2.4 DISCUSSION 29

CHAPTER 3: PURINERGIC RECEPTOR X7 IS A KEY MODULATOR OF METABOLIC OXIDATIVE STRESS- MEDIATED AUTOPHAGY AND INFLAMMATION IN EXPERIMENTAL NONALCOHOLIC STEATOHEPATITIS 36

3.1 INTRODUCTION 38

3.2 MATERIALS AND METHODS 40

3.3 RESULTS 47

www.manaraa.com

3.4 Discussion 61

Chapter 4: NADPH Oxidase-Derived Peroxynitrite Drives Inflammation In Mice And Human Nonalcoholic Steatohepatitis Via TLR4-Lipid Raft Recruitment ...67

4.1 Introduction 69

4.2 Materials And Methods 72

4.3 Results 76

4.4 Discussion 95

Chapter 5: Conclusion 107

References 118

Appendix A – License Agreement for Chapter 2 128

Appendix B – License Agreement for Chapter 3 129

Appendix C-License Agreement For Chapter 4 130

www.manaraa.com

LIST OF TABLES

Table 2.1 Histology Activity Index 24

Table 4.1 NASH CRN scores for NASH model.....105

www.manaraa.com

LIST OF FIGURES

Figure 2.1 Diet induced obesity potentiates oxidative stress following BDCM exposure in mice 21

Figure 2.2 Diet induced obesity and BDCM co-exposure increases leptin expression and contribute to early steatohepatitic lesions 23

Figure 2.3 BDCM exposure-induced oxidative stress is mediated by leptin in diet induced obese mice and in isolated Kupffer cells 25

Figure 2.4 BDCM co-exposure in diet induced obese mice causes Kupffer cell activation and is mediated by leptin 28

Figure 2.5 BDCM and leptin mediated cell death mechanisms in diet induced obese liver 30

Figure 3.1 Oxidative stress in diet and BDCM co-exposed model, and MCD model is mediated by CYP2E1 48

Figure 3.2 High-fat diet and BDCM co-exposure, and MCD diet increase expression of P2X7r 51

Figure 3.3 Metabolic oxidative stress influences autophagy protein profiles in NASH ... 53

Figure 3.4 P2X7 receptor deletion modulates autophagy in NASH 55

Figure 3.5 Immunodetection of late autophagic gene and chaperone protein 57

Figure 3.6 LAMP2A and Bodipy colocalization in high-fat diet and BDCM co-exposed model and MCD model 58

Figure 3.7 P2X7 receptor modulates inflammation in NASH 60

Figure 3.8 Fibrosis and necrotic damage are mediated by P2X7r in response to DAMPs in both high-fat fed and BDCM co-exposed model and MCD model 62

www.manaraa.com

Figure 4.1 NADPH oxidase activation and peroxynitrite-mediated tyrosine nitration 78

Supplementary Figure 4.1 Immunofluorescence images for NADPH oxidase activation in MCD rodent model and human samples.....80

Figure 4.2 NADPH oxidase and peroxynitrite – driven TLR4 recruitment to lipid rafts in hepatic cell-membranes 82

Supplementary Figure 4.2 NADPH oxidase and peroxynitrite – driven TLR4 recruitment to lipid rafts in hepatic cell-membranes including MCD rodent model and human samples 84

Figure 4.3 NADPH oxidase and peroxynitrite–driven NFkB translocation and DNA-binding via TLR4 signaling 86

Figure 4.4 NADPH oxidase and peroxynitrite–driven hepatic sinusoidal injury via TLR4 signaling.....87

Supplementary Figure 4.3 Hepatic sinusoidal injury in MCD rodent model and human samples.....89

Supplementary Figure 4.4 Quantitative real time PCR analyses of mRNA levels of ICAM-1 and E-Selectin in NASH models.....91

Supplementary Figure 4.5 Quantitative real time PCR analyses of mRNA levels of proinflammatory mediators in Human control and Human NASH livers 92

Figure 4.5 TLR4 signaling-mediated cytokine release and Kupffer cell activation 94

Supplementary Figure 4.6 Quantitative real time PCR analyses of mRNA levels of TNF-α, IL-6 and Lcn2 in NASH models.....96

Supplementary Figure 4.7 Quantitative real time PCR analyses of mRNA levels of SAA1, IL-1β and MCP-1 in NASH models 98

Supplementary Figure 4.8 Immunodetection of IL-1β, MCP-1 AND CD68 in MCD rodent models and human samples 100

Figure 4.6 Immunohistochemistry images for α-SMA in rodent NASH models and human samples.....102

Supplementary Figure 4.9 Western blot analysis of alpha smooth muscle actin (α-SMA) in liver homogenates from rodent models of NASH and human NASH livers.....104

www.manaraa.com

CHAPTER 1

INTRODUCTION

During the past decade, rates of obesity including childhood and adolescent obesity have been on the rise, and associated co-morbidities like Non-alcoholic fatty liver disease are looming large. Risk factors such as diet composition, excess caloric intake, decreased exercise, genetics, and the built environment are perceived as causes of obesity and associated co-morbidities (1) (2). Obesity is considered as a low inflammatory condition, following a number of studies in the last decade (3). The increased blood levels of proinflammatory cytokines and adipokines such as leptin influence the inflammatory state in obesity (4). Obesity associated co-morbidities include lung, liver and cardiovascular complications (2). In parallel, it is perceived that with increased obesity there is also an increase in liver disorders like non alcoholic steatohepatitis, cirrhosis and in extreme cases hepatocarcinoma (5). I felt a dire need to find the missing link between the changes in the environment and the increasing incidences of fatty liver disease in obesity, and hence my research in this field. I investigated one of the most common sources of environmental toxicant, drinking water. Several hypotheses have been put forward for the progression of fatty liver to inflammatory liver disease in obesity. The two hit hypothesis and the multi factorial hypothesis point to a secondary assault apart from obesity to be a relevant cause for liver diseases (6, 7). In recent literature, our laboratory and others have shown that CCl_4 exposure, albeit in lower doses can sensitize obese liver to hepatotoxicity and development

www.manaraa.com

of early steatohepatitic injury (4, 8). A recent study from Cave M *et al.* shows the involvement of the built environment in development of liver diseases in humans (9). The study explicitly shows the association of polychlorinated biphenyls and heavy metals to non alchoholic steatohepatitis in American adults. Lately the involvement of cytochrome P450s in the metabolism of these environmental toxicants has been an active area of research (10, 11). The role of CYP2E1 has been extensively studied and it has been found to have a close association with reactive oxygen species generation and development of steatohepatitic injury (12). Research by our Principal Investigator has shown previously that free radical metabolism of the model toxin CCl_4 by CYP2E1 causes the release of damage associated molecular patterns (DAMPS) and increased release of leptin from both hepatic and adipose tissues (8). These studies assume significance since both reactive oxygen species (ROS) and leptin have been found to exacerbate the progression of steatosis to steatohepatitis in obesity (12), (13) Similar to CCl_4, which produces trihalomethyl radicals upon metabolism by CYP2E1, several trihalomethanes have been found to be metabolized by CYP2E1 to produce noxious free radicals (14-16). The disinfection byproducts of drinking water which are formed from reaction with the bromine in water following chlorine disinfection, produce ROS (16). Although direct exposure to high doses of environmental toxins is rare, low exposures from the environment are far more common. These doses may be well-tolerated by normal healthy individuals but can be potential risk factors for inflammatory liver injuries such as steatohepatitis in obese persons. This risk assumes significance in terms of public health because there is presently an alarming rise in obesity in the United States alone. The National Toxicological program identifies several disinfection byproducts for drinking water that are hepatotoxic (16-18) and are bioactivated

www.manaraa.com

by liver cytochrome p450 enzymes leading to generation of free radicals (15, 16). The resulting oxidative stress from the reductive metabolism of $CHBrCl_2$ can lead to amplification of hepatotoxicity by triggering host innate immune responses. Innate immune events such as activation of macrophages through secretion of an array of cytokines can amplify the risk of developing full-blown inflammatory disease like early steatohepatitic injury leading to fibrosis and cirrhosis if exposed on a chronic basis.

Leptin is a 167-amino acid protein discovered in 1994 by positional cloning of the ob gene (2) (2, 19). Though it is considered to be an anorexigenic hormone, its levels are elevated in obesity as a result of resistance to its actions in the hypothalamus, a condition called central resistance (20). Leptin is thought to contribute, in part, to NASH development in obesity through its proinflammatory actions on sinusoidal epithelial cells and Kupffer cells (4, 21-23). Recent lines of evidence support a role of the elevated levels of leptin found in obesity in generating reactive oxygen and reactive nitrogen species and subsequent free radical formation (24). Free radical production appears to contribute to the progression of steatohepatitis and its resultant hepatotoxicity (25). The presence of high levels of leptin in obesity certainly makes it a prime candidate for amplifying the risk of NASH progression as both a first and second hit, which not only satisfies the two hit hyposthesis, but also is in line with the multi hit paradigm(7). My studies as noted in Chapter 2, and other studies from our laboratory have demonstrated that leptin mediates the effect on NASH progression through peroxynitrite formation and Kupffer cell activation in a toxin model of NASH.

Nonalcoholic steatohepatitis (NASH) is associated with metabolic oxidative stress, often ascribed to enhanced oxidation of membrane lipids, mitochondrial uncoupling of the

www.manaraa.com

electron transport chain and higher cytochrome P450 enzyme activity (11, 26, 27). Metabolic oxidative stress leads to cellular stress and induce cell death mechanisms which modulate inflammatory microenvironment in NASH (8, 28).

Cell death mechanisms in disease pathogenesis are synonymous with necrosis, autophagy and apoptosis, however much attention is recently focused on the various roles of autophagy in cellular processes, inflammation, energy homeostasis and immunity (29, 30). In spite of increased attention on autophagy, the mechanisms that control autophagy in NASH remain unclear. Autophagy is a central eukaryotic process with many cytoplasmic homeostatic roles (30). It is a critical pathway for degradation of intracellular components by lysosomes and has established roles in hepatic lipid metabolism, insulin sensitivity and cellular injury (31). Autophagy, dependent upon the involvement of the cellular components has been classified into macro, micro and chaperone mediated autophagy (CMA). It is crucial though, that these processes rely on formation of autophagosomes, increased levels of LC3B, fusion of autophagosome with the lysosome and degradation of the cellular cargo by lysosomal enzymes (31-34). Given the importance of autophagy in cellular homeostasis and disease pathogenesis it is also important to study both the inducers and regulators of autophagy in a pathological state like NASH. One of the key components of the inflammatory microenvironment in various disease pathologies is the ionotrophic purinergic receptors (P2 receptors) which respond to the damage associated molecular patterns (DAMPs) (35, 36). There is an increased focus on a subclass of these receptors (P2X7 receptor) which bind ATP with high affinity and is known to regulate inflammation in early steatohepatitic injury in mice (8). Apart from the binding to ATP, P2X7 receptor (P2X7r) has been shown to increase NADPH oxidase activity,

www.manaraa.com

increase Kupffer cell-MHC class II expression and regulate inflammation (8). With increased focus on purinergic receptors, inflammosome activation and autophagy in NASH, I explored the possibility of P2X7r as a key regulator of autophagy and the resultant inflammation in NASH, as recorded in my first-authored manuscript in Chapter 3.

Nonalcoholic steatohepatitis (NASH) has been studied extensively in preclinical models and humans. NASH manifestations range from an early sinusoidal endothelial dysfunction, inflammation followed by a defective tissue repair resulting in fibrosis(37-42). Inefficient tissue perfusion in the fatty tissue mostly associated with fatty liver and subsequent NASH progression can result in recruitment of other cell types including Kupffer cells, sinusoidal endothelial cells and circulating lymphocytes, making it a perfect microenvironment for forming an inflammatory foci (43).

Recent research reports identify an emerging role of toll like receptor 4 in NASH pathogenesis(44, 45). Several endogenous mediators like gut derived endotoxin and nuclear factor HMGB-1 has been implicated to activate TLR4 signaling leading to NASH severity(46, 47). After its discovery in the 1980s, toll like receptor signaling has been in the forefront of innate immune signaling and disease pathophysiology (48). TLR4, one of the many TLRs discovered since then plays a pivotal role in cytokine release along with its adaptor molecules myeloid differentiation primary response gene 88 (MyD88) and TIR-domain-containing adapter-inducing interferon-β **(**TRIF). MyD88 was found to work as an adaptor for inflammatory signaling pathways downstream of members of the TLR and interleukin-1 (IL-1) receptor families(49). Activation of the TLR4 pathway leads to a variety of functional outputs, including the activation of nuclear factor-kappa B (NFκB), mitogen-activated protein kinases, and activator protein 1, making MyD88 a central node

www.manaraa.com

of inflammatory pathways(49) . Lipopolysaccharide of gram negative bacterial cell walls is a strong ligand for TLR4 on the cell membrane. MD-2 is associated with Toll-like receptor 4 (TLR4) on the cell surface and enables TLR4 to respond to LPS (50). Deficiency of MyD88 or TLR4 in mice have attenuated the development of the disease(51). Though oxidative stress via NADPH oxidase has been shown to drive NASH pathogenesis especially fibrogenesis and Kupffer cell activation, there is no direct evidence of a single mechanism where a specific oxidative species can drive the recruitment of TLR4-mediated inflammation in NASH(13, 24, 52). I , in my study recorded in Chapter therefore aim to identify a single intracellular reactive nitrative species that may play a distinct role in developing the inflammatory pathogenesis in NASH via TLR4 recruitment to hepatic lipid rafts, an early yet distinct process in TLR4 activation and downstream signaling. One of the common sources of generation of toxic superoxide radicals may be NADPH oxidase isoforms which can be found in both phagocytic and non-phagocytic cells(53). Liver has been shown to be a rich source of various NOX isoforms, being present in phagocytic Kupffer cells, stellate cells and sinusoidal endothelial cells (39, 52, 54). Out of the various NOX isoforms NOX2 is primarily present in Kupffer cells and stellate cells whereas NOX1 and NOX4 have been found in other liver cell types(52). NOX2 is comprised of several subunits which includes the gp91, p22 (membrane subunits), p67, p47 and Rac1 (cytosolic subunits)(53). Upon receipt of proper signals, the cytosolic subunits align with their membrane counterparts to form an active NADPH oxidase complex which produce superoxide radicals to be released in the extracellular space(53). Several laboratories including us have shown the involvement of NOX2 in NASH development(13, 24, 54). NOX2 stimulation by high leptin results in peroxynitrite generation thus causing Kupffer

www.manaraa.com

cell activation in NASH(13). NOX2 has also been shown to facilitate recruitment of toll-like receptor 4 to lipid rafts and to help in receptor dimerization and its association with MD2 in several inflammatory diseases(55). Since there is no evidence of the molecular events that follow NADPH oxidase activation concerning the type of reactive species formation and the mechanisms that link TLR4 activation, I investigated the role of peroxynitrite in TLR4 activation in NASH.

www.manaraa.com

CHAPTER 2

PROINFLAMMATORY ADIPOKINE LEPTIN MEDIATES DISINFECTION BYPRODUCT BROMODICHLOROMETHANE-INDUCED EARLY STEATOHEPATITIC INJURY IN OBESITY

Das S, Kumar A, Seth RK, Tokar EJ, Kadiiska MB, Waalkes MP, Mason RP, Chatterjee S. *Toxicology and Applied Pharmacology*, 2013 Jun 15; 269(3):297-306.
Reprinted here with permission of publisher.

www.manaraa.com

Running title: Toxin-associated steatohepatitis in obesity due to bromodichloromethane exposure

Key words:, Adipocytokines, Kupffer cell, oxidative stress, lipid peroxidation, tyrosine nitration, necrosis, tumor necrosis factor, OB/OB mice.

Author for correspondence:

*Dr. Saurabh Chatterjee, Ph.D. [1]Environmental Health and Disease Laboratory, Department of Environmental Health Sciences, University of South Carolina, Columbia 29208 USA. Email: schatt@mailbox.sc.edu; Tel: 803-777-8120; Fax: 803-777-3391**Grant Support:** This work has been supported by NIH pathway to Independence Award (4R00ES019875-02 to Saurabh Chatterjee) and the Intramural Research Program of the National Institutes of Health and the National Institute of Environmental Health Sciences (Z01 ES050139-13 to Ronald P. Mason)

Conflict of interest: The authors declare no conflict of interest

Abstract:

Today's developed world faces a major public health challenge in a rise in obese population and an increased incidence in fatty liver disease. There is a strong association among diet induced obesity, fatty liver disease and development of nonalcoholic steatohepatitis but the environmental link to disease progression remains unclear. Here we demonstrate that water disinfection byproduct bromodichloromethane-induced early steatohepatitic lesions in obesity, is mediated by increased oxidative stress and leptin which act in synchrony to potentiate disease progression. Low acute exposure of bromodichloromethane (BDCM), in

www.manaraa.com

diet induced obesity produced oxidative stress as shown by increased lipid peroxidation, protein free radical and nitrotyrosine formation and elevated leptin levels. Exposed obese mice showed histopathological signs of early steatohepatitic injury and necrosis. Spontaneous knockout mice for leptin or systemic leptin receptor knockout mice had significantly decreased oxidative stress and TNF-α levels. Co-incubation of leptin and BDCM caused Kupffer cell activation as shown by increased MCP-1 release and NADPH oxidase membrane assembly, a phenomenon that was decreased in Kupffer cells isolated from leptin receptor knockout mice. There was a significant increase in Kupffer cell activation marker CD68 in livers of obese mice that were BDCM exposed and showed increased necrosis as assessed by levels of isocitrate dehydrogenase, an event that was decreased in the absence of leptin or its receptor. In conclusion our results show that disinfection byproduct BDCM exposure in diet induced obesity augments steatohepatitic injury by potentiating effects of leptin on oxidative stress, kupffer cell activation and cell death in the liver.

2.1 INTRODUCTION

Childhood and adolescent rates of obesity and overweight have assumed pandemic proportions in the last decade. Risk factors such as diet composition, excess caloric intake, decreased exercise, genetics, and the built environment are perceived as causes of obesity and associated co-morbidities (1) (2). Obesity is considered as a low inflammatory condition, following a number of studies in the last decade (3). The increased blood levels of proinflammatory cytokines and adipokines such as leptin influence the inflammatory state in obesity (4). Obesity associated co-morbidities include lung, liver and cardiovascular complications (2). In parallel, it is perceived that with increased obesity

www.manaraa.com

there is also an increase in liver disorders like nonalcoholic steatohepatitis, cirrhosis and in extreme cases hepatocarcinoma (5). Several hypotheses have been put forward for the progression of fatty liver to inflammatory liver disease in obesity. The two hit hypothesis and the multi factorial hypothesis point to a secondary assault apart from obesity to be a relevant cause for liver diseases (6, 7). In recent literature, we and others have shown that CCl_4 exposure, albeit in lower doses can sensitize obese liver to hepatotoxicity and development of early steatohepatitic injury (4, 8). A recent study from Cave M *et al.* shows the involvement of the built environment in development of liver diseases in humans (9). The study explicitly shows the association of polychlorinated biphenyls and heavy metals to non alchoholic steatohepatitis in American adults. Lately the involvement of cytochrome p 450s in the metabolism of these environmental toxicants has been an active area of research (10, 11). The role of CYP2E1 has been extensively studied and it has been found to have a close association with reactive oxygen species generation and development of steatohepatitic injury(12). Our research has shown previously that free radical metabolism of the model toxin CCl_4 by CYP2E1 causes the release of damage associated molecular patterns (DAMPS) and increased release of leptin from both hepatic and adipose tissues(8). These studies assume significance since both reactive oxygen species (ROS) and leptin have been found to exacerbate the progression of steatosis to steatohepatitis in obesity(12), ((13) Similar toCCl_4, which produces trihalomethyl radicals upon metabolism by CYP2E1, several trihalomethanes have been found to be metabolized by CYP2E1 to produce noxious free radicals (14-16). The disinfection byproducts of drinking water which are formed from reaction with the bromine in water following chlorine disinfection, produce ROS (16). Although direct exposure to high doses of environmental toxins is rare, low exposures from

www.manaraa.com

the environment are far more common. These doses may be well-tolerated by normal healthy individuals but can be potential risk factors for inflammatory liver injuries such as steatohepatitis in obese persons. This risk assumes significance in terms of public health because there is presently an alarming rise in obesity in the United States alone. The National Toxicological program identifies several disinfection byproducts for drinking water that are hepatotoxic (16-18) and are bioactivated by liver cytochrome p450 enzymes leading to generation of free radicals (15, 16). The resulting oxidative stress from the reductive metabolism of $CHBrCl_2$ can lead to amplification of hepatotoxicity by triggering host innate immune responses. Innate immune events such as activation of macrophages through secretion of an array of cytokines can amplify the risk of developing full-blown inflammatory disease like early steatohepatitic injury leading to fibrosis and cirrhosis if exposed on a chronic basis.

Leptin is a 167-amino acid protein discovered in 1994 by positional cloning of the ob gene (2) (2, 19). Though it is considered to be an anorexigenic hormone, its levels are elevated in obesity as a result of resistance to its actions in the hypothalamus, a condition called central resistance (20). Leptin is thought to contribute, in part, to NASH development in obesity through its proinflammatory actions on sinusoidal epithelial cells and Kupffer cells (4, 21-23). Recent lines of evidence support a role of the elevated levels of leptin found in obesity in generating reactive oxygen and reactive nitrogen species and subsequent free radical formation (24). Free radical production appears to contribute to the progression of steatohepatitis and its resultant hepatotoxicity(25). The presence of high levels of leptin in obesity certainly makes it a prime candidate for amplifying the risk of NASH progression as both a first and second hit, which not only satisfies the two hit

www.manaraa.com

hyposthesis, but also is in line with the multi hit paradigm(7). Our own studies have demonstrated that leptin mediates the effect on NASH progression through peroxynitrite formation and Kupffer cell activation in a toxin model of NASH.

Our study tests the hypothesis that low bromodichloromethane exposure, which has been studied for the formation of dihalomethyl radicals in ESR studies, produces ROS in obese liver and the resultant oxidative stress links early steatohepatic injury. We also examine the role of leptin in mediating the progression of simple steatosis to early staetohepatitic injury following acute BDCM exposure. We show here, in a first ever report, the direct role of BDCM in inducing steatohepatitic injury in obese mice liver through the involvement of increased leptin resulting in Kupffer cell activation, TNF-α release and cell death.

2.2 MATERIALS AND METHODS

Materials: The spin trap 5,5-dimethyl-1-pyrroline N-oxide (DMPO) was obtained from Dojindo Molecular Technologies, Kumamoto, Japan. Bromodichloromethane, Collagenase Type IV, apocynin and gadolinium chloride ($GdCl_3$) were purchased from Sigma Chemical Company, St Louis, MO. Tempol was purchased from Sigma. Mouse recombinant leptin and neutralizing antibody to mouse leptin were purchased from R&D Systems,(R&D Systems Inc, Minneapolis, MN). All other chemicals were of analytical grade and were purchased from Sigma Chemical Company or Roche Molecular Biochemicals (Mannheim, Germany). All aqueous solutions were prepared using water passed through a Picopure 2UV Plus system (Hydro Services and Supplies, Inc., RTP, NC) equipped with a 0.2 μm pore size filter.

www.manaraa.com

Obese mice: Custom DIO adult male, pathogen-free, 10-week-old mice with a C57BL6/J background (Jackson Laboratories, Bar Harbor, Maine) were used as models of diet-induced obesity. The mice were fed with a high fat diet (60% kcal) from 6 weeks until 16 weeks. All experiments were conducted in the 16-week age group. Age-matched lean controls were fed with a diet having 10% kcal fat. The animals were housed one to a cage before any experimental use. Mice that contained the disrupted OB gene (leptin) (B6.V-Lep<ob>/J) (Jackson Laboratories) and disrupted DB gene (leptin receptor) (B6.BKS(D)-Lepr<db>/J) were fed with a high fat diet and treated identically to DIO obese mice. Mice had ad libitum access to food and water and were housed in a temperature-controlled room at 23-24 °C with a 12-hour light/dark cycle. All animals were treated in strict accordance with the NIH Guide for the Humane Care and Use of Laboratory Animals, and the experiments were approved by the institutional review board both at NIEHS and the University of South Carolina at Columbia.

Induction of liver injury in obese mice: DIO mice or high fat-fed gene-specific knockout mice at 16 weeks were administered Bromodichloromethane (2.0mmoles/kg, diluted in olive oil) through the intraperitoneal route.

Isolation of Kupffer cells: Kupffer cells were isolated as per the protocol by Froh, et al. (Current Protocols in Toxicology, 14.4.1-14.4.12, 2002) with some modifications. Briefly, mice were anesthetized and their livers were perfused initially by sterile HBSS and later by 0.03% collagenase at a flow rate of 5 ml/minute. Following perfusion, the liver was dissected and incubated with 0.03% collagenase for another 30 minutes at 37°C. The tissue was minced and cells were extracted with a syringe piston. The cell suspension was filtered through a 75µ cell strainer (BD Falcon). The resultant single cell suspension was

www.manaraa.com

centrifuged at 50g for 3 minutes to obtain parenchymal cells (mostly hepatocytes). The supernatant was further centrifuged at 650xg and the pellet was resuspended in 10 ml of HBSS. The suspension was loaded on a Percoll gradient and centrifuged at 1500 g for 15 minutes to obtain the Kupffer cells. The isolated cells were plated onto 32mm^2 plastic dishes for adherence. Qualitative screening for Kupffer cells was carried out with immunoreactivity against the CD68 antibody. Cultures with >80% CD68-positive cells were used for experiments.

Kupffer cell culture: 10^5 isolated Kupffer cells were cultured in 24 well plates with 5 mM BDCM and 100 µg/ml recombinant leptin. Following 24 h incubation, the supernatant was collected for analysis of cytokines, and cell lysates were used for DMPO nitrone adduct and Nitrotyrosine immunoreactivity.

Enzyme-linked immunosorbent assay: Immunoreactivity for DMPO nitrone adducts and nitrotyrosine was detected in liver homogenates and Kupffer cell lysates using standard ELISA (56). TNF-α and MCP-1release was estimated in serum using ELISA kits from BD Pharmingen and Thermo Scientific, respectively, following the manufacturer's protocols.

Histopathology: For each animal, sections of liver were collected and fixed in 10% neutral buffered formalin. For histological examinations, formalin-fixed liver sections were stained with hematoxylin/eosin and observed under a light microscope.

TUNEL Assay:

Liver tissue from mice were fixed overnight in 10% neutral-buffered formalin (Sigma Aldrich, Missouri, USA) and paraffin-embedded sections (5 µm thickness, courtesy

www.manaraa.com

Instrumentation Resource Facility, School of Medicine, University of South Carolina, USA) prepared from them were used for TUNEL staining. TACS 2TdT DAB in situ Apoptosis Detection Kit was supplied by Trevigen Inc. Maryland, USA. Stained sections were imaged under high power (40X, 25.2X magnification) using BX43 microscope and DP73 camera from Olympus America Inc., Pennsylvania, USA.

Western Blotting:

100mg of tissue from each liver sample was homogenized in 1ml of RIPA buffer (Sigma Aldrich) using dounce homogenizer. Homogenate was centrifuged, the supernatant was diluted 1:10 and used for western blotting. We used Novex (Invitrogen, California,USA) 4 – 12% bis-tris gradient gel. Rabbit anti-mouse primary antibodies against isocitrate dehydrogenase (IDH) and β-actin (positive control); and goat anti-rabbit HRP-conjugated secondary antibody were obtained from AbCam plc (Massachussetts, USA). The dilutions used were: anti-IDH – 1:1000, anti-β-actin – 1:500, secondary antibody – 1:10000. Trans – Blot Turbo transfer system (Bio-Rad Laboratories Inc., California, USA) and precut nitrocellulose blotting membrane/filter paper sandwiches (Bio-Rad) were used to perform a 7-minute transfer. Pierce ECL Western Blotting substrate (Thermo Fisher Scientific Inc., Illinois, USA) was used. BioMax MS Films and cassettes (with intensifying screen) were from Kodak.

Real-Time Reverse Transcription–Polymerase Chain Reaction Analysis: Gene expression levels in tissue samples were measured by real-time reverse transcription–polymerase chain reaction analysis. Tissue samples (85-100 mg) were taken from each liver and individually homogenized using a Tissue Tearor variable speed homogenizer.

www.manaraa.com

Total RNA was isolated from homogenates with the use of TRIzol reagent (Invitrogen, Carlsbad, CA) according to the manufacturer's instructions and purified with the use of RNeasy mini kit columns (Qiagen, Valencia, CA). Purified RNA was reverse transcribed to complementary DNA with the use of Moloney murine leukemia virus reverse transcriptase (Applied Biosystems, Foster City, CA) reverse transcriptase and oligo-dT primers. Gene-specific primers were designed with the use of Primer Express 3.0 software (Applied Biosystems, Foster City, CA).

The ABsolute SYBR Green ROX Mix (ABgene, Rockford, IL) was used for amplifications. Amplification conditions were as follows: 15 minutes at 95^{o}C, followed by 40 cycles of 95^{o}C for 1 minute and 60^{o}C for 1 minute. Cycle time (Ct) values for the selected genes were normalized to values for 18S in the same sample. For each liver, tissue samples were collected and tested separately with triplicate Ct values collected each time. DIO mouse liver was used as the control for comparison with all other livers. Ct values for all controls were set at 100%. The sequences for the primers used for RT-PCR are provided in 5' to 3' orientation.

TNF:Forward – AGCCCACGTCGTAGCAAACCACCAA,

Reverse – AACACCCATTCCCTTCACAGAGCAAT.

Mcp-1:Forward - CTTCTGGGCCTGCTGTTCA

Reverse – CCAGCCTACTCATTGGGATCA

. CD68: Forward- GCTACATGGCGGTGGAGTACAA

Reverse – ATGATGAGAGGCAGCAAGATGG.

www.manaraa.com

Immuno-spin trapping of DMPO-protein radicals from cell lysates using ELISA: Kupffer cell lysates for use in ELISA for the detection of DMPO-protein nitrone adducts were prepared using a cell sonicator. Since buffers contain traces of metals and other contaminants that could form DMPO-protein radicals, we compared chelexed phosphate buffer (pH 7.4) containing 100 μM DTPA and RIPA buffer. Results from the pilot experiments found no significant difference in the chemiluminescence signal from these experiments, and all subsequent lysates were prepared in RIPA buffer (0.05 g sodium deoxycholate, 100 μL Triton X-100 and 10 μL of 10% SDS in 10 mL of 0.1 M PBS) containing protease inhibitors (Complete, Mini Protease Inhibitor Cocktail Tablets, Roche Applied Science, Indianapolis, IN). Following a 30 min incubation of the samples in ice, they were centrifuged at 20000 × g for 20 min. The soluble material (supernatant) was stored at 4° C until use.

Confocal laser scanning microscopy (Zeiss LSM 510 UV Meta): DIO obese mice were administered carbon tetrachloride to induce metabolic oxidative stress. DMPO was injected in two doses of 1 g/kg at 2 h and 1 h prior to sacrifice. Livers were fixed in 10% neutral buffered formalin and soaked in 30% sucrose for 24 h. The frozen sections (10 micron) were cryocut using a frozen tissue processor (Leica Instruments, Bannockburn, IL) at the immunohistochemistry core facility at NIEHS. Tissue slices were then treated with 0.5% SDS (5 minutes) for antigen retrieval, permeabilized, and blocked (2% nonfat dry milk, Pierce Biomedical, Rockford, IL). An antibody specific to DMPO nitrone adducts and Alexafluor 568 goat anti-rabbit secondary antibody (Molecular Probes, now Invitrogen, Carlsbad, CA) were used as primary and secondary antibodies, respectively. Anti-nitrotyrosine antibody was from Abcam. Confocal images were taken on a Zeiss

www.manaraa.com

LSM710-UV meta (Carl Zeiss, Inc., Oberkochen, Germany) using a Plan-NeoFluor 40X/1.3/40XxOil DIC objective with different zoom levels.

Macrophage depletion by $GdCl_3$: Mice were injected with gadolinium chloride (10mg/kg) through the i.v. route, 24 h prior toBDCM treatment, as described by Rai et al(1).

Statistical analyses: All in vivo experiments were repeated three times with 3 mice per group (N=3; data from each group of three mice was pooled). All in vitro experiments were repeated three times, and the statistical analysis was carried out by analysis of variance (ANOVA) followed by the Bonferroni posthoc correction for intergroup comparisons. Quantitative data from Western blots as depicted by the relative intensity of the bands were analyzed by performing a Student's t test. $P<0.05$ was considered statistically significant.

2.3 RESULTS

Bromodichloromethane acute exposure sensitizes obese liver to increased free radical stress. We have shown previously that free radical metabolism of a "second hit" like CCl_4 produces lipid peroxidation and protein radical formation in obesity (8). BDCM is known to be metabolized by CYP2E1 and produces dihalomethyl radicals (16). To investigate the role of BDCM exposure in causing increased free radical stress in obesity, lipid peroxidation was analyzed in the obese liver. 4-hydroxynonenal, (4-HNE) a peroxidation product of lipids was measured in whole liver homogenates. Results showed that there was a significant increase in 4-HNE adducts in DIO+BDCM group as compared to lean control , lean control + BDCM and DIO groups at 6 hours post exposure ($P<0.05$) (Fig. 2.1A).

www.manaraa.com

Further, we analyzed whether the lipid peroxidation led to protein radical formation and tyrosine nitration in the obese liver. Results showed that there was a significant increase in the protein radical-adduct formation in DIO+BDCM group as compared to lean control, lean control+BDCM and DIO groups ($P<0.05$) (Fig. 2.1B). The protein radical adducts localized in the centrolobular region of the liver (Zone 3), a typical hallmark of radical based liver injury (16) (Fig. 2.1C). To find whether the protein radicals were primarily due to tyrosine radicals, immunoreactivity against nitrotyrosine was analyzed. Results showed that DIO+BDCM group had greater immunoreactivity to 3-nitrotyrosine in the centrolobular region when analyzed by confocal laser scanning microscopy, as compared to lean control mice treatedwith BDCM (Fig. 2.1D). The CYP2E1 protein levels were also increased significantly in DIO+BDCM group when compared to lean control, lean control+BDCM and DIO only groups. The HNE adducts and protein radical formation was abrogated following use of CYP2E1 inhibitor Diallylsulfide (Data not shown).Since higher CYP2E1 levels and resultant metabolic oxidative stress by CYP2E1 yields noxious free radicals following BDCM exposure as shown here, the results were indicative of potentiation of free radical formation in obesity.

BDCM acute exposure causes increased leptin levels and contributes to early steatohepatitic lesions in obesity. We have shown previously that CYP2E1 metabolism and increased free radical formation led to heightened leptin levels in liver (Chatterjee S et al, 2012, Journal of Hepatology). To investigate whether BDCM exposure led to increased leptin production at the liver and adipose tissues, western blot analysis was performed with both liver and adipose tissues in mice exposed to BDCM. Results showed that treatment

www.manaraa.com

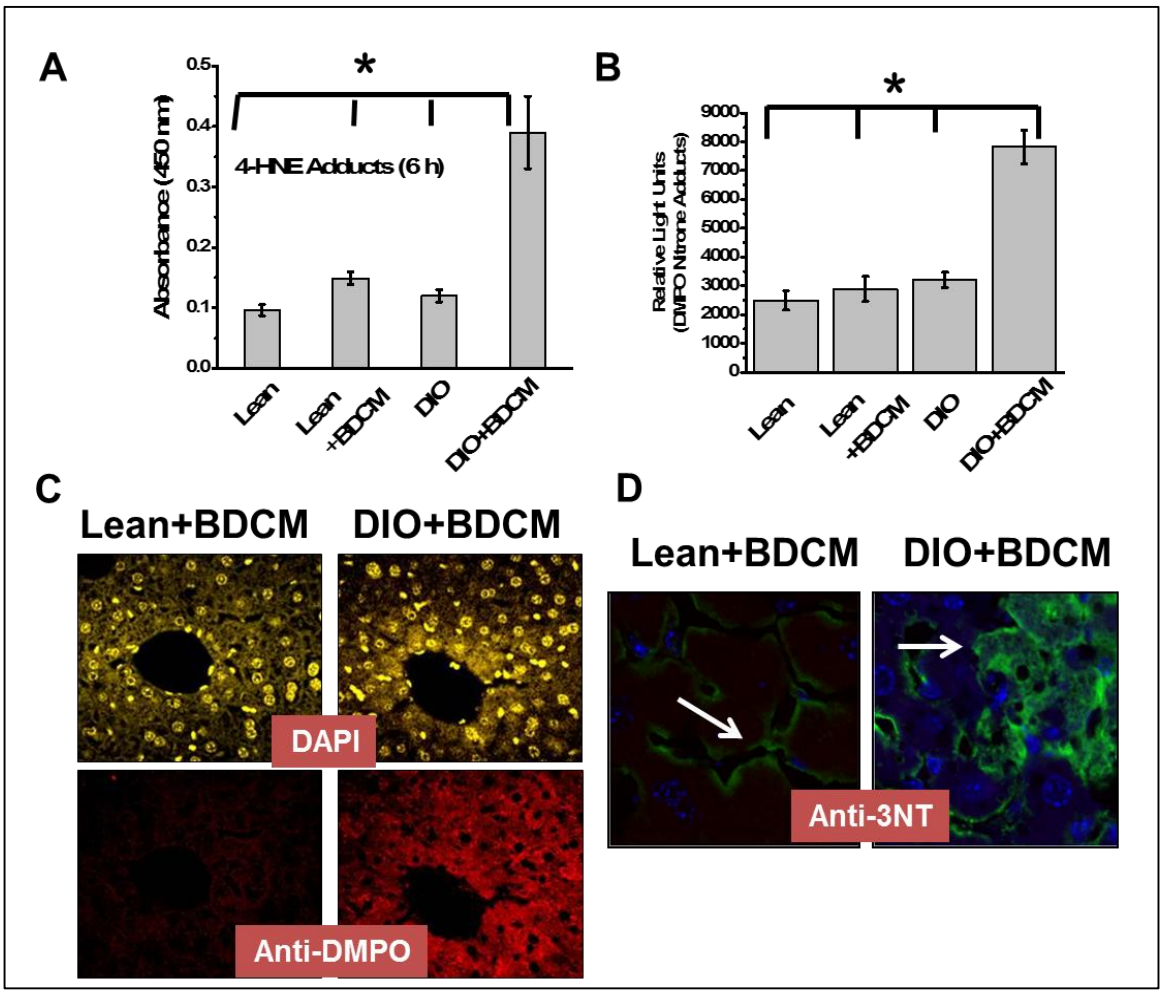

Figure 2.1 Diet induced obesity potentiates oxidative stress following BDCM exposure in mice. A. Immunoreactivity of 4-hydroxynonenal (4-HNE) adducts in mice liver homogenates as detected by ELISA. B. Immuno-spin trapping of DMPO nitrone adducts, a measure of protein radical formation in mice liver homogenates following BDCM exposure, as detected by ELISA. C. Immunolocalization of DMPO nitrone adducts in the centolobular region (Zone III) following BDCM exposure. Anti-DMPO immunoreactivity is shown in red staining, as detected by confocal laser scanning microscopy. D. Immunolocalization of 3-nitrotyrosine adducts, detected by confocal laser scanning microscopy in mice exposed to BDCM as shown in green stain. Nuclear stain (DAPI) is shown in blue. Results are expressed as mean±SE. Statistical significance was tested using ANOVA, with Bonferroni posthoc correction. *($P<0.05$)

of BDCM significantly increased leptin levels in both liver and adipose tissues of DIO mice as compared to lean control, lean control+BDCM and DIO only mice ($P<0.05$) (Fig. 2.2A).

www.manaraa.com

BDCM exposure also significantly elevated plasma ALT and LDH levels in DIO+BDCM mice as compared to lean control, lean control+BDCM and DIO only mice ($P<0.05$) (Fig. 2.2B). This result also emphasizes liver injury with significant non programmed cell death as indicated by elevated LDH levels(Fig. 2.2B). To characterize the early steatohepatitc lesions in obesity following BDCM exposure, liver histopathology was examined and scored as per the histology activity index (HAI) index. Results showed that there was significant elevation of HAI scores in DIO+BDCM mice as compared to lean controls (Table 2.1). Examination of liver tissue revealed significant leukocyte infiltration, increased steatosis and ballooning degeneration at 48 hours post BDCM exposure (Fig. 2.2C).

Increased leptin in obesity mediates protein radical and nitrotyrosine formation in vivo and in isolated Kupffer cells. Leptin, a proinflammatory adipokine has been shown to participate in the inflammatory process associated with steatohepatitic lesions in obesity(4, 57). Leptin resistance is key to progression of disease in obesity (57). We have shown that CYP2E1 metabolism of CCl_4elevates serum leptin levels (Chatterjee S et al, 2012, Journal of Hepatology, In Press). To investigate whether increased leptin in obesity and following BDCM exposure contributes to protein radical formation and free radical stress, we used mice with spontaneous knockout of leptin gene and the leptin receptor knockout models (lepr-/-). DMPO-nitrone adduct formation, which exemplifies protein radical adducts, was significantly decreased in OB/OB mice and leptin receptor knockout mice as compared to DIO mice treated with BDCM (Fig. 2.3A). 3-nitrotyrosine immunoreactivity was significantly decreased in OB/OB mice and in mice that are leptin

www.manaraa.com

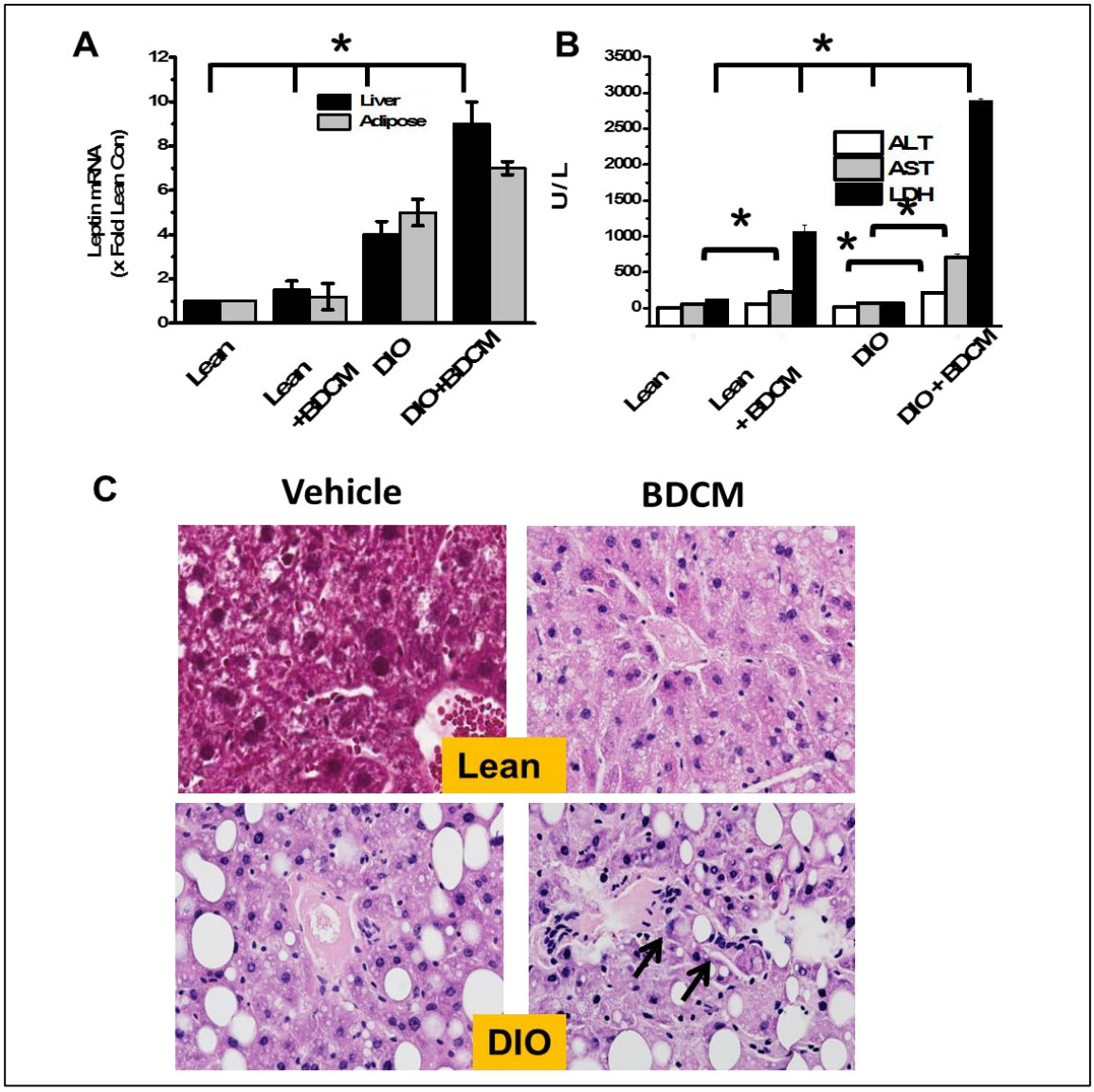

Figure 2.2 Diet induced obesity and BDCM co-exposure increases leptin expression and contribute to early steatohepatitic lesions. A. Leptin mRNA expression in adipose and liver tissues in mice exposed to BDCM. Results are shown as an index of fold increase over lean control group. B. Serum levels of liver enzymes, markers of tissue injury and necrosis. Serum levels of AST, ALT and LDH, a marker of tissue necrosis are shown in mice that were exposed to BDCM. C. HE stained paraffin embedded liver tissue section of mice exposed to BDCM. Arrow heads indicate increased leukocyte infiltration, a marker of inflammatory microenvironment. Results are expressed as mean±SE. Statistical significance was tested using ANOVA, with Bonferroni posthoc correction. *($P<0.05$)

www.manaraa.com

Table 2.1 Histology Activity Index

Groups	Lean Control	Lean Control +BDCM	DIO	DIO+BDCM
Confluent Necrosis:	0	1	1	3±1
Parenchymal Injury	0	1	1	3±1
Portal Inflammation:	0	1	1	4±2
Grade (Inflammation):	4±1	7±3	8±2	15±4
Stage (Fibrosis):	0	0	1	1

Table 2.1 Assessment of inflammation scores using Histology Activity Index. H&E slides were analyzed for each group namely, Lean control, Lean control+BDCM, DIO and DIO+BDCM and ranked blindfoldedly. Inflammation was ranked based on the leukocyte infiltration and presence of necrosis with a progressive rank from 0 to 10, with 0 being minimal on the scale. Results are expressed as mean±SE

Receptor deficient as compared to DIO mice treated with BDCM (Fig. 2.3B). To show the involvement of Kupffer cells in leptin mediated protein radical formation and the mechanisms that underlie redox stress, isolated Kupffer cells from DIO mice were incubated with recombinantleptin and BDCM. Results showed that Kupffer cells that were incubated with leptin and exposed to BDCM had significantly elevated protein radical formation, as compared to apocynin (NADPH oxidase inhibitor)- treated, Tempol (Superoxide Dismutase-mimetic compound) -treated, Kupffer cells from mice that were deficient in leptin receptor and cells treated with excess DMPO (spin trap for free radicals) (Fig. 2.3C). Confocal laser scanning images also showed decreased protein radical formation in isolated Kupffer cells from leptin receptor deficient mice as compared to DIO

www.manaraa.com

and DIO+BDCM treated groups (Fig. 2.3D). deficient mice as compared to DIO and DIO+BDCM treated groups (Fig. 2.3D). The results clearly showed that leptin was fundamental in the potentiation of the free radical stress mediated by lipid peroxidation and superoxide release from either CYP2E1 or NADPH oxidase (Kupffer cells) in obese mice.

Increased leptin and BDCM metabolism in obesity activates Kupffer cells and p67 translocation, a measure of NADPH oxidase membrane assembly and activation. It has been shown by us and others that adipocytokine leptin activates Kupffer cells in acute and chronic liver injury (23, 58), Chatterjee S et al, 2012, Journal of Hepatology In press). Kupffer cell activation is marked by increased release of TNF-α and monocyte chemoattractant protein-1 (16, 58, 59). Further Kupffer cell has functional NADPH oxidase and releases superoxide flux upon activation (Chatterjee S et al, J Hepatology, 2012, In Press). Results showed that isolated Kupffer cells, incubated with BDCM and leptin had significant elevation of TNF-α levels in the supernatant at 24 h as compared to cells isolated from DIO only mice ($P<0.05$), while apocynin, Tempol and excess DMPO significantly decreased the release of TNF-α levels as compared to BDCM and leptin incubated cells ($P<0.05$) (Fig. 2.4A). Further, cells isolated from leptin receptor knockout mice had significant decrease in TNF-α levels as compared to the DIO+BDCM+Leptin group (Fig. 2.4A). Real time q-pcr analysis showed a significant increase in CD68, the activation marker for Kupffer cells in DIO+BDCM group as compared to lean control, lean +BDCM andDIO group. The expression of CD68 was significantly lower in leptin receptor knockout and leptin knockout mice livers as compared to DIO+BDCM group ($P<0.05$) (Fig. 2.4B). $GdCl_3$-treated livers of DIO+BDCM group also showed a significant decrease in CD68 mRNA expression as compared to DIO+BDCM group, showing that the CD68

www.manaraa.com

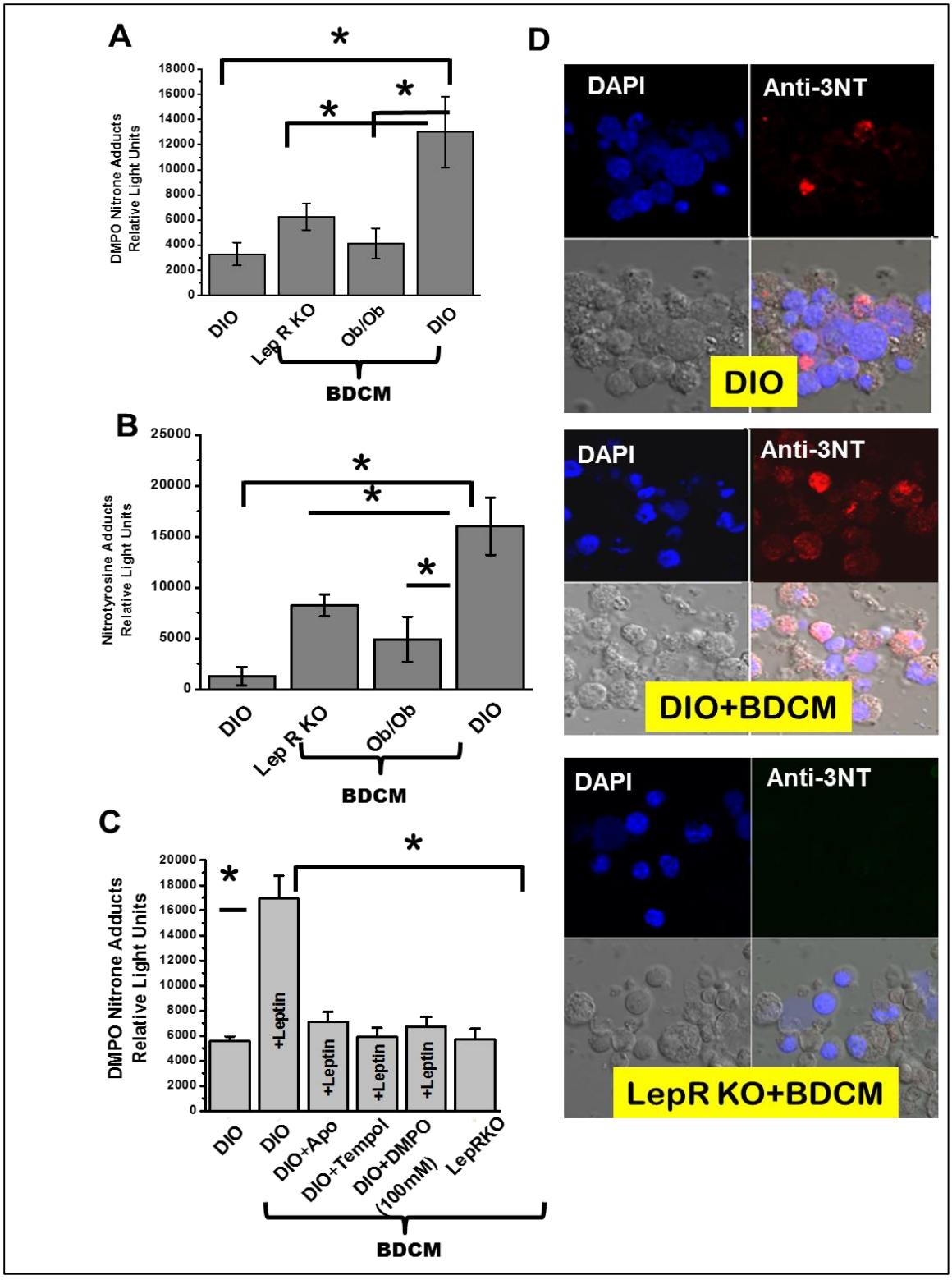

Figure 2.3 BDCM exposure-induced oxidative stress is mediated by leptin in diet induced obese mice and in isolated Kupffer cells..A Immunoreactivity of protein radical adducts as assessed by ELISA in liver homogenates from BDCM exposed diet induced obese mice,

www.manaraa.com

leptin receptor and leptin knockout mice. B. Immunoreactivity of protein nitrotyrosine adducts as assessed by ELISA in liver homogenates from BDCM exposed diet induced obese mice, leptin receptor and leptin knockout mice. C. Kupffer cell protein radical adducts following co-incubation of BDCM and leptin, in the presence or absence of NADPH oxidase inhibitor apocynin or superoxide dismutase mimetic, Tempol or in the presence of excess spin trap DMPO or in cells isolated from leptin receptor deficient mice. D. Immunolocalization of DMPO-nitrone adducts in isolated Kupffer cells from diet induced obese mice and leptin receptor knockout mice, as assessed by confocal laser scanning microscope. Anti-DMPO staining is marked by red and nuclear stain in blue. Results are expressed as mean±SE. Statistical significance was tested using ANOVA, with Bonferroni posthoc correction. *($P<0.05$)

expression was strictly from macrophage origin ($P<0.05$) (Fig. 2.4B). TNF-α and MCP-1 protein levels in livers of DIO +BDCM had a significant increase as measured by western blot analysis (Fig. 2.4C) and band quantification (Supplementary Fig. 2.1) when compared to lean control, lean +BDCM and DIO groups. Protein levels of these proteins decreased significantly in leptin receptor knockout and leptin knockout mice livers as compared to the DIO+BDCM group ($P<0.05$). P67 phox subunit of NADPH oxidase needs to translocate to the membrane to align with the GP91 phox subunit for its activation and superoxide production. Western blot analysis of membrane fractions of liver homogenates of DIO mice that were treated with BDCM and fed with high fat diet had a significant increase in p67 translocation as compared to to lean control, lean +BDCM, DIO, leptin receptor knockout and leptin knockout mice ($P<0.05$) (Fig. 2.4D). These results clearly show the synergistic effect of leptin and BDCM exposure in promoting Kupffer cell activation and NADPH oxidase membrane assembly, two crucial events in progression of steatosis to early steatohepatitic lesions in obesity.

BDCM exposure synergizes with leptin in promoting non-programmed cell death and progression of steatosis to early steatohepatitic lesions. One of the key events

www.manaraa.com

in early steatohepatitic injury is necrosis and degeneration of hepatocytes (25). To investigate the role of BDCM exposure to high fat fed mice in cell death, levels of hepatocyte necrotic marker, isocitrate dehydrogenase were measured. Results from western blot analyzes indicated that isocitrate dehydrogenase was significantly increased in DIO+BDCM group as compared to lean control, DIO only and lean control+BDCM groups ($P<0.05$) (Fig. 2.5A and 2.5B) . Leptin receptor knockout or leptin knockout liver homogenates had significant decrease in the isocitrate dehydrogenase levels as compared to DIO+BDCM group ($P<0.05$) (Fig. 2.5A and 2.5B). To evaluate whether there was late stage apoptosis following BDCM treatment and it was influenced by the increased leptin levels, in situ TUNEL assay was performed. Results from immunohistochemistry for TUNEL labeling showed that there was increased apoptosis in DIO mice as compared to either DIO+BDCM or leptin receptor knockout or leptin knockout mice (Fig. 2.5C). The number of TUNEL positive nuclei were significantly higher in DIO mice as compared DIO+BDCM or leptin receptor knockout or leptin knockout mice ($P<0.05$) (Fig. 2.5D). The results assume significance since programed cell death induction as compared to necrosis might be viewed as a survival mechanism of hepatocytes in toxin-mediated injury (60). Further, the finding of significant increases in Isocitrate Dehydrogenase in DIO+BDCM group (Fig. 2.5A) confirmed necrotic injury and non-programed cell death following a synergistic role of BDCM and leptin.

2.4 DISCUSSION

Acute BDCM exposure in mice that were high fat fed led to increased oxidative stress, increased expression of leptin, liver inflammation through Kupffer cell activation, NADPH oxidase membrane assembly, cytokine release and non-programmed cell death following

www.manaraa.com

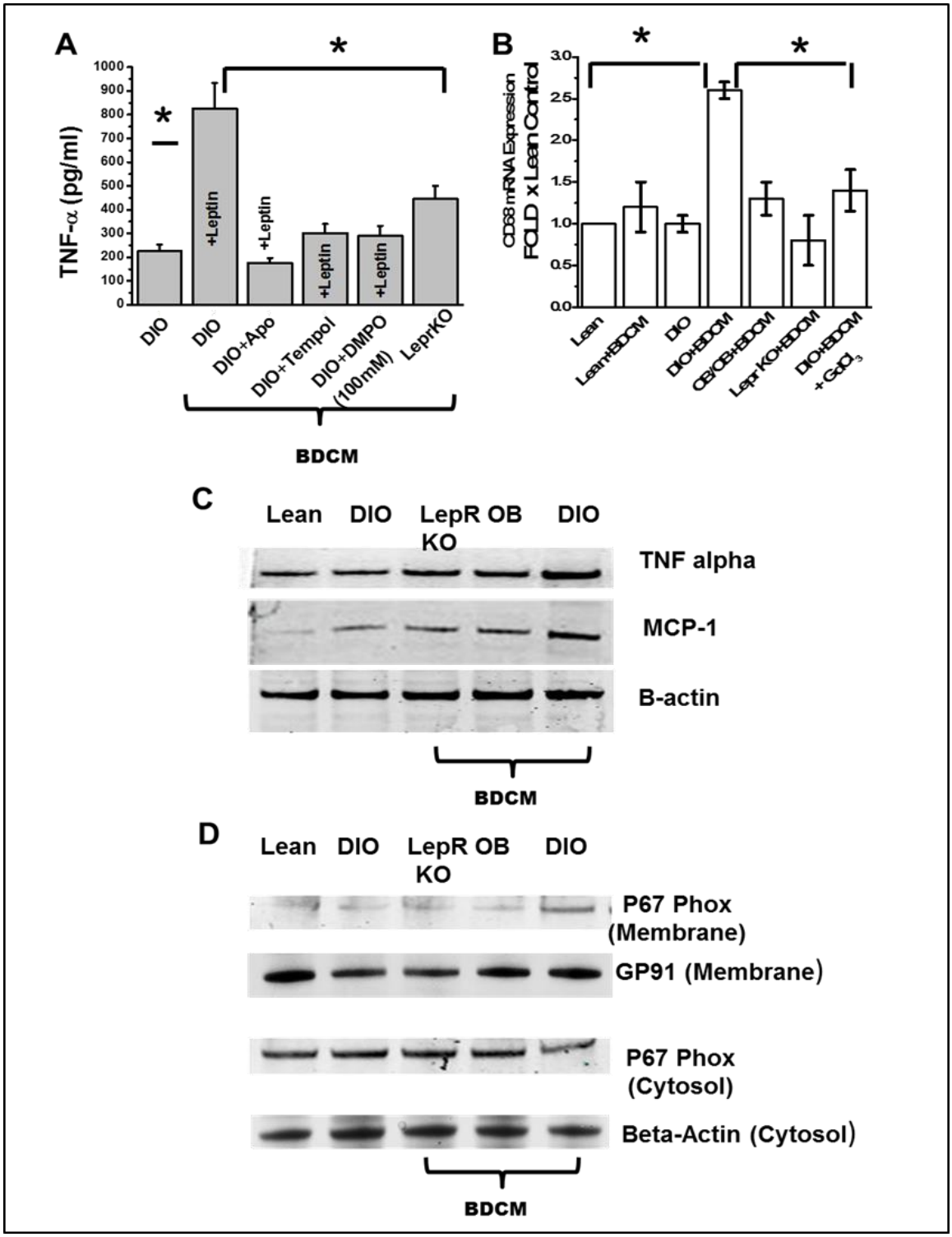

Figure 2.4 BDCM co-exposure in diet induced obese mice causes Kupffer cell activation and is mediated by leptin. A. TNF-α levels in supernatants of isolated Kupffer cells following co-incubation with BDCM and leptin in the presence or absence of NADPH oxidase inhibitor apocynin or superoxide dismutase mimetic, Tempol or in the presence of

www.manaraa.com

excess spin trap DMPO or in cells isolated from leptin receptor deficient mice. B. CD68 mRNAexpression as assessed by quantitative real time PCR.. C. Western blot analysis of TNF-α and MCP-1 in liver homogenates of BDCM exposed diet induced obese mice or mice that lacked the leptin receptor or leptin. D. Membrane translocation of NADPH oxidase subunit P67 following BDCM exposure in diet induced obese mice and in mice that lack either the leptin receptor or leptin. Results are expressed as mean±SE. Statistical significance was tested using ANOVA, with Bonferroni posthoc correction. *($P<0.05$)

the reductive metabolism of this water disinfection byproduct. These events following BDCM exposure are hallmarks of early steatohepatitic injury in the liver and showed adherence to the two hit hypothesis and the multi hit paradigm (6, 7). The observations showed for the first time that an underlying condition of obesity can potentiate the risk of developing steatohepatitis following drinking water disinfection byproduct exposure. Assuming that more than 30% of the US population is obese, the results underline a serious public health problem not only in this country but in developed and developing nations where use of chlorine as a disinfectant is largely used.

In spite of stricter regulations of BDCM levels in drinking water, chlorine is a widely used disinfection agent across the civilized world. The general population is exposed to trihalomethanes through consumption of treated drinking water, beverages, and food products, inhalation of contaminated air, and dermal contact with treated water (17, 61). BDCM reductive metabolism by CYP2E1 causes free radical production and has been shown to generate PBN specific free radicals by ESR (15). CYP2E1 has been the primary cyp450 isoform to metabolize BDCM (16). We hypothesized that BDCM exposure and the resultant free radical generation starts an inflammatory cascade linking oxidative stress and the liver innate immune response. Results showed that BDCM formed 4HNE adducts, a lipid peroxidation product at 6 hours followed by protein free radical formation and stable, following free radical generation,

www.manaraa.com

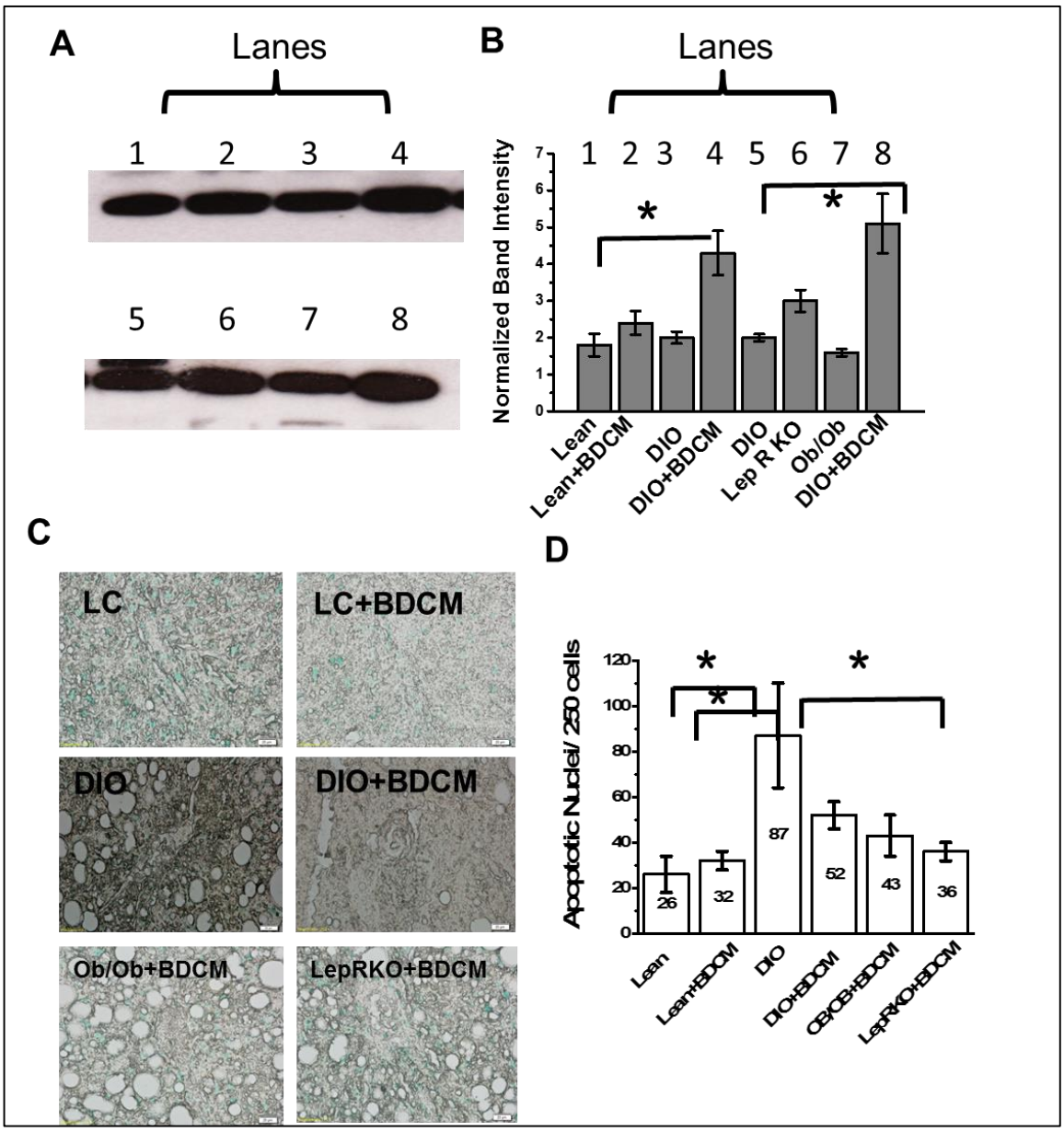

Figure 2.5 BDCM and leptin mediated cell death mechanisms in diet induced obese liver. A. Western blot analysis of isocitrate dehydrogenase, a hepatocyte necrosis marker in liver homogenates. Lanes 1-8 represent lean control, lean+BDCM, DIO, DIO+BDCM, DIO internal control, Leptin receptor knockout, OB/OB and DIO+BDCM (reference control) respectively. B. Band analysis of western blots shown in A. C. Histological examination of paraffin embedded liver tissue sections following TUNEL staining of BDCM exposed diet induced obese mice in the presence or absence of either leptin or leptin receptor. D. Numerical estimate of TUNEL positive nuclei in paraffin embedded liver tissue sections when assessed in 10x magnification from BDCM exposed DIO mice and in the absence of leptin or leptin receptor.

www.manaraa.com

following free radical generation, BDCM exposure also significantly increased leptin mRNA expression in both adipose tissue and liver of high fat fed mice (DIO) (Fig. 2.2A). This data was important to finding a strong correlation between obesity, BDCM-induced oxidative stress and altered histopathology in the liver. Increased leptin in DIO mice coupled with higher release of this adipokine following CCl_4 induced NASH caused immune cell activation and necrosis in the liver (Chatterjee S et al, Journal of Hepatology, in press). Similarly our finding that BDCM caused an increase of leptin mRNA in liver of obese mice, over and above the high leptin levels found in obesity, was crucial to find a causal effect in BDCM induced early steatohepatic lesions.

To prove the BDCM-leptin interplay in causing early NASH like symptoms, we used both OB/OB mice, a spontaneous knockout for leptin and DB/DB mice that have a systemic deletion of the leptin receptor isoform. Cellular effects of leptin are mediated by leptin receptor isoforms Ob (long) and Ob (short) and they belong to the IL-6 family of receptors and activate the JAK-STAT pathway for their downstream effects (62). Leptin is known to mediate oxidative stress by activating NADPH oxidase and formation of peroxynitrite (24); Chatterjee S et al, 2012, Journal of Hepatology, In press). Leptin also mediates Kupffer cell activation and thus triggers the release of innate immune mediators and T cell proliferation, through its actions on liver and other peripheral tissues (19, 63, 64). Our results of increased release of leptin following BDCM exposure allowed us to probe the significance of leptin in BDCM exposed early steatohepatitic lesions. Results showed that both whole liver homogenates and isolated Kupffer cells produced protein free radicals as measured by the immune-spin trapping technique (Fig. 2.3). The radicals further stabilized to form nitrotyrosine adducts, which are formed from either peroxynitrite

www.manaraa.com

metabolism or in a direct reaction of peroxidases in presence of nitric oxide (65). Nitrotyrosine formation is correlated with immune pathogenesis of many diseases. The significant formation of 3-nitrotyrosine indicated a prominent role of BDCM-Leptin interplay in the steatohepatitic lesions in DIO mice. Isolated Kupffer cells that were incubated with leptin and BDCM, showed increased oxidative stress but oxidative stress was significantly decreased in the presence of apocynin, an NADPH oxidase inhibitor or Tempol, an SOD mimetic compound or excess DMPO (Fig. 2.3C). Kupffer cells that lacked the leptin receptor isoforms had significant decrease in oxidative stress, suggesting that the presence of leptin, leptin receptor signaling coupled with BDCM was strongly associated with the Kupffer cell reactive oxygen species generation (Fig. 2.3C and D). Published literature indicates that oxidative stress in Kupffer cells leads to release of proinflammatory cytokines and chemokines that are central to inflammatory disease pathogenesis in fatty liver disease (24, 40). We and others have shown that Kupffer cell activation by leptin results in a poor outcome in fatty liver disease, leading to NASH like symptoms (23, 58) (13) . The release of proinflammatory cytokines and chemotactic proteins like TNF-α and MCP-1 from Kupffer cells lead to activation of inflammatory pathways that mediate disease progression in the liver(40). Our results showed that BDCM-leptin synchrony *in vivo* and *in vitro* led to TNF-α and MCP-1 release (Fig. 2.4). Further there was a significant increase in the CD68 protein in liver homogenates following BDCM exposure suggesting activation of Kupffer cells (Fig. 2.4). Kupffer cell activation was also confirmed by the use of Gdcl3-induced depletion of resident macrophages. $GdCl_3$-treated group showed significant decrease in CD68 expression as compared to DIO+BDCM group (Fig. 2.4B). Kupffer cell activation in liver disease to either alcohol treatment or NASH

www.manaraa.com

pathophysiology is crucial for disease progression. It has been presumed that inflammatory events in the Kupffer cells primarily trigger the increased antigen presentation, T cell proliferation and amplification of the inflammatory cascade (8, 23). Our results of increased oxidative stress, TNF-α and MCP-1 release and increased CD68 in liver confirm the Kupffer cell activation in BDCM exposure and show that it is leptin dependent

Kupffer cell activation and the resultant inflammatory events that follow in liver injury lead to cell death. There is evidence where damage associated molecular patterns have resulted in hepatocyte necrosis in CCl_4 mediated early steatohepatitis (8). Leptin, which is found in higher concentrations in obesity due to suspected central leptin resistance may contribute to the cell death patterns in the liver. NASH histopathology shows that hepatocyte necrosis is a key event in the pathogenesis of disease progression (8, 40, 66). We argued that BDCM-induced early steatohepatitic injury will cause hepatic cell death and is regulated by leptin and involves its receptor. We also hypothesized that absence of leptin would prevent non programmed cell death in hepatic microenvironment. Results showed that there was a significant increase in apoptotic nuclei in DIO group whereas DIO+BDCM group or the group that had absence of leptin or its receptor showed decreased apoptosis in the liver (Fig. 2.5C). Interestingly the levels of Isocitrate Dehydrogenase, a hepatocyte marker of necrosis increased significantly in DIO+BDCM group as compared to DIO alone or in groups that were devoid of leptin or leptin receptor (Fig. 2.5A and 2.5B). These results assumed significance since apoptosis and other programmed cell death patterns like autophagy are increasingly being recognized as cell survival mechanisms (60). Necrosis, as seen in DIO+BDCM group is a significant event in steatohepatitis of obesity

www.manaraa.com

and can also be perceived as leptin dependent in BDCM exposed early steatohepatitic lesions.

Taken together, we showed that BDCM exposure causes early steatohepatitic lesions in high fat diet induced obesity and is dependent on higher leptin levels in obesity but is exacerbated by the direct effects of BDCM on both adipose tissue and liver in producing higher expression of this adipokine. Though leptin is perceived as an anorexigenic hormone, a profound rise in the levels of this hormone in obesity due to central leptin resistance .The levels of leptin might rise further as a result of a direct effect of environmental contaminants like BDCM in causing more hepatic and adipose tissue expressions of this molecule, and thus sensitize the obese liver for heightened tissue injury. These events of hepatic tissue damage can lead to early steatohepatitic lesions and can predispose obese liver to more severe liver disease forms such as NASH and cirrhosis. Future studies on chronic exposure of low doses of BDCM might shed light on the disease progression of NASH and other inflammatory complications of the liver like autoimmune hepatitis and hepatocellular carcinoma. Thus, this first ever report on BDCM-exposed early steatohepatitic lesions in obesity might lead to answers to more complex public health questions on the environmental link to disease progression in obesity.

Footnote: **"**This article may be the work product of an employee or group of employees of the National Institute of Environmental Health Sciences (NIEHS), National Institutes of Health (NIH), however, the statements, opinions or conclusions contained therein do not necessarily represent the statements, opinions or conclusions of NIEHS, NIH or the United States government**."**

www.manaraa.com

Acknowledgements: The authors gratefully acknowledge James Clark, Tiwanda Marsh, Jeoffrey Hurlburt, Jeff Tucker and Ralph Wilson for excellent technical assistance. We also thank the Instrumentation resource facility (IRF) at the University of South Carolina School of Medicine for technical assistance.

www.manaraa.com

CHAPTER 3

PURINERGIC RECEPTOR X7 IS A KEY MODULATOR OF METABOLIC OXIDATIVE STRESS- MEDIATED AUTOPHAGY AND INFLAMMATION IN EXPERIMENTAL NONALCOHOLIC STEATOHEPATITIS

Das S, Seth RK, Kumar A, Kadiiska MB, Michelotti G, Diehl AM, Chatterjee S. *American Journal of Physiology Gastrointestinal and Liver Physiology* 2013 Dec; 305(12):G950-63
Reprinted here with permission of publisher

www.manaraa.com

Running title: P2X7 receptor as a therapeutic target in liver fibrosis

Key words: DMPO-nitrone adducts, lipid peroxidation, tyrosine nitration, Cytokines, CYP2E1, LC3B, Gabarap

Author for correspondence:

*Dr. Saurabh Chatterjee, Ph.D. [1]Environmental Health and Disease Laboratory, Department of Environmental Health Sciences, University of South Carolina, Columbia 29208 USA. Email: schatt@mailbox.sc.edu; Tel: 803-777-8120; Fax: 803-777-3391

Grant Support: This work has been supported by NIH pathway to Independence Award (4R00ES019875-02 to Saurabh Chatterjee), NIH R01 (R01DK053792 to Anna Mae Diehl) and the Intramural Research Program of the National Institutes of Health and the National Institute of Environmental Health Sciences.

Footnote: *"*This article may be the work product of an employee or group of employees of the National Institute of Environmental Health Sciences (NIEHS), National Institutes of Health (NIH), however, the statements, opinions or conclusions contained therein do not necessarily represent the statements, opinions or conclusions of NIEHS, NIH or the United States government*."*

Conflict of interest: The authors declare no conflict of interest.

Abstract: Recent studies indicate the metabolic oxidative stress, autophagy and inflammation are hallmarks of nonalcoholic steatohepatitis (NASH) progression. However the molecular mechanisms that link these important events in NASH remain unclear. In this study we investigated the mechanistic role of purinergic receptor X7 in modulating

www.manaraa.com

autophagy and resultant inflammation in NASH in response to metabolic oxidative stress. The study uses two rodent models of NASH. In one of them, a CYP2E1 substrate bromodichloromethane is used to induce metabolic oxidative stress and NASH. Methyl choline deficient diet feeding is used for the other NASH model. CYP2E1 and P2X7 receptor gene deleted mice are used to establish their roles in regulating metabolic oxidative stress and autophagy. Autophagy gene expression, protein levels, confocal microscopy based-immunolocalization of LAMP2A and histopathological analysis were performed. CYP2E1-dependent metabolic oxidative stress induced increases in P2X7 receptor expression, chaperone-mediated autophagy markers LAMP2A and Hsc 70 but caused depletion of LC3B protein levels. P2X7 receptor gene deletion significantly decreased LAMP2A and inflammatory indicators while significantly increasing LC3B protein levels as compared to wild type mice treated with BDCM. P2X7 receptor deleted mice were also protected from NASH pathology as evidenced by decreased inflammation and fibrosis. Our studies establish that P2X7 receptor is a key regulator of autophagy induced by metabolic oxidative stress in NASH, thereby modulating hepatic inflammation. Further our findings presented here forms a basis for P2X7 receptor as a potential therapeutic target in the treatment for NASH.

3.1 INTRODUCTION

Nonalcoholic steatohepatitis (NASH) is associated with metabolic oxidative stress, often ascribed to enhanced oxidation of membrane lipids, mitochondrial uncoupling of the electron transport chain and higher cytochrome P450 enzyme activity (11, 26, 27). Metabolic oxidative stress leads to cellular stress and induce cell death mechanisms which modulate inflammatory microenvironment in NASH (8, 28).

www.manaraa.com

Cell death mechanisms in disease pathogenesis are synonymous with necrosis, autophagy and apoptosis, however much attention is recently focused on the various roles of autophagy in cellular processes, inflammation, energy homeostasis and immunity (29, 30). In spite of increased attention on autophagy, the mechanisms that control autophagy in NASH remain unclear. Autophagy is a central eukaryotic process with many cytoplasmic homeostatic roles (30). It is a critical pathway for degradation of intracellular components by lysosomes and has established roles in hepatic lipid metabolism, insulin sensitivity and cellular injury (31). Autophagy, dependent upon the involvement of the cellular components has been classified into macro, micro and chaperone mediated autophagy (CMA). It is crucial though, that these processes rely on formation of autophagosomes, increased levels of LC3B, fusion of autophagosome with the lysosome and degradation of the cellular cargo by lysosomal enzymes (31-34). Interestingly, a recent investigation by Lin. et al., report pharmacological promotion of autophagy alleviated steatosis and injury in alcoholic and non-alcoholic fatty liver (67). Given the importance of autophagy in cellular homeostasis and disease pathogenesis it is also important to study both the inducers and regulators of autophagy in a pathological state like NASH. One of the key components of the inflammatory microenvironment in various disease pathologies is the ionotrophic purinergic receptors (P2 receptors) which respond to the damage associated molecular patterns (DAMPs) (35, 36). There is an increased focus on a subclass of these receptors (P2X7 receptor) which bind ATP with high affinity and is known to regulate inflammation in early steatohepatitic injury in mice (8). Apart from the binding to ATP, P2X7 receptor (P2X7r) has been shown to increase NADPH oxidase activity, increase Kupffer cell-MHC class II expression and regulate inflammation (8). With increased focus on purinergic

www.manaraa.com

receptors, inflammosome activation and autophagy in NASH, we explored the possibility of P2X7r as a key regulator of autophagy and the resultant inflammation in NASH.

The present study utilizes two distinct models of experimental NASH which have been established to produce pathology of full blown NASH. The toxin model of NASH utilizes co-administration of high fat diet and a low dose environmental toxin bromodichloromethane (BDCM) (68, 69). The diet-induced model exposes mice to methyl-choline deficient (MCD) diet for 8 weeks (70, 71). In a first ever report we show that in both models of NASH there was an increased metabolic oxidative stress, which caused higher expression of P2X7 receptors. Oxidative stress induced both early and late autophagy proteins and was dependent on the presence of P2X7 receptors. P2X7 receptor modulated LC3B protein depletion, an event which is crucial for autophagy. Further absence of P2X7 receptors significantly reduced downstream inflammosome activation and NASH pathophysiology. The present study also advances our understanding in considering P2X7receptor-linked autophagy pathways as potential therapeutic targets in NASH.

3.2 MATERIALS AND METHODS

Mouse model

Pathogen-free, custom DIO adult male mice with a C57BL/6J background (Jackson Laboratories, Bar Harbor, Maine) were used as models of toxin-induced non-alcoholic steatohepatitis (NASH). They were fed with a high fat diet (60% kcal) from 6 weeks to 16 weeks. All experiments were conducted at the completion of 16-weeks. The animals were housed one in each cage before any experimental use. Mice that contained the deleted

www.manaraa.com

CYP2E1 gene (cytochrome p450 knockout) (29/Sv-*Cyp2e1*^{tm1Gonz}/J) (Jackson Laboratories) and mice that contained the deleted P2X7r gene (purinergic receptor X7 knockout) (B6.129P2-P2rx7^{tm1Gab}/J) (Jackson Laboratories) were fed with a high fat diet and treated identically to DIO mice. The other set of mice were pathogen-free, adult male with a C57BL/6J background fed with methylcholine-deficient (MCD) diet and were used as models for diet-induced NASH. They were fed with MCD diet from 8 to 16 weeks. Mice that contained the disrupted P2X7r gene were also fed with methylcholine-deficient-diet. Mice had *ad libitum* access to food and water and were housed in a temperature-controlled room at 23-24°C with a 12-hour light/dark cycle. All animals were treated in strict accordance with the NIH Guide for the Humane Care and Use of Laboratory Animals, and the experiments were approved by the institutional review board both at NIEHS, Duke University and the University of South Carolina at Columbia.

Induction of liver injury in mice

DIO mice or high-fat-fed gene-specific knockout mice at 16 weeks were administered bromodichloromethane (BDCM) (2.0 mmoles/kg, diluted in olive oil) through the intra-peritoneal route. However, DIO mice treated with olive oil (diluent of BDCM) were used as control. After completion of the treatment, mice of all study groups were sacrificed for liver tissue and serum for the further experiments. MCD-diet-fed wildtype or gene specific knockout mice were sacrificed at 16 weeks for liver tissue for experiments. However, methylcholine-sufficient (MCS) diet-fed mice were used as control.

www.manaraa.com

Enzyme-linked immunosorbent assay (ELISA)

Immunoreactivity for DMPO-nitrone adduct was detected in liver homogenate using standard ELISA (56)

Histopathology:

Liver tissue sections from each mouse were fixed in 10% neutral buffered formalin. Formalin-fixed liver sections were stained with hematoxylin and eosin (H&E) and observed under the light microscope. Collagen content in liver tissue was evaluated using Sirius red–stained liver sections. Each liver section was stained with Picro-Sirius red (Sigma-Aldrich) and counterstained with fast green (Sigma-Aldrich).

Serum ALT, Alkaline Phosphatase and Albumin levels:

Blood from DIO, DIO+BDCM and P2X7 receptor deleted mice were collected by cardiac puncture and serum was separated by standard techniques. The serum ALT and alkaline phosphatase was measured at the clinical chemistry core. Albumin was measured using the commercially available kit (Alpha Diagnostic kit, San Antonio, TX).

Immunohistochemistry:

Formalin-fixed, paraffin-embedded liver tissue from all the mice groups were cut into 5 µm thick tissue sections. Each section was deparaffinized using standard protocol. Briefly, sections were incubated with xylene twice for 3 min, washed with xylene:ethanol (1:1) for 3 min and rehydrated through a series of ethanol (twice with 100 %, 95%, 70%, 50%), twice with distilled water and finally rinsed twice with phosphate buffered saline (PBS) (Sigma-Aldrich, St Louis, MO). Epitope retrieval of deparaffinized sections was carried

www.manaraa.com

out using epitope retrieval solution and steamer (IHC-world, Woodstock, MD) following manufacturer's protocol. The primary antibodies were (i) anti- 4-Hydroxynonenal, (ii) anti-3-Nitrotyrosine, (iii) anti-P2X7r, (iv) anti-GABARAP, (v) anti-LAMP-2A, (vi) anti-MHC II, (vii) anti-IL-1β (viii) anti-IFN-γ and (ix) anti-LC3B. Primary antibodies were purchased from AbCam Inc. (Massachussetts, USA), Millipore (Temecula, CA), R&D Systems (Minneapolis, MN) and used in 1:250 dilutions. Antigen specific immunohistochemistry (IHC) were performed using Vectastain Elite ABC kit (Vector Laboratories, Burlingame, CA) following manufacturer's protocols. 3,3' Diaminobenzedine (DAB) (Sigma-Aldrich) were used as a chromogen substrate. Sections were counter-stained by Mayer's hematoxylin (Sigma-Aldrich). Washing with PBS (Sigma-Aldrich) was performed thrice between the steps. Sections were mounted in Simpo mount (GBI Labs, Mukilteo, WA) and observed under 20X oil objective. Morphometric analysis was done using CellSens Software from Olympus America.

Western blotting:

30 mg of tissue from each liver sample was homogenized in 100 µl of RIPA buffer (Sigma Aldrich) with protease inhibitor (1X) (Pierce, Rockford, IL) using dounce homogenizer. The homogenate was centrifuged, the supernatant was diluted 1:5 and used for SDS PAGE and subjected to western blotting. Novex (Invitrogen, California, USA) 4–12% bis-tris gradient gel was used for SDS PAGE. Proteins were transferred to nitrocellulose membrane (i) using precut nitrocellulose/filter paper sandwiches (Bio-Rad Laboratories Inc., California, USA) and Trans – Blot Turbo transfer system (Bio-Rad) in case of low molecular weight proteins; and (ii) using wet transfer module from Invitrogen in case of high molecular weight proteins. 5% non-fat milk solution was used for blocking. Primary

www.manaraa.com

antibodies against Hsc 70, GABARAP, LC3B, LAMP-2A, Caspase-1, β-actin (all from AbCam Inc.), HMGB-1 (Millipore) at recommended dilutions; and compatible HRP-conjugated secondary antibodies were used. Pierce ECL Western Blotting substrate (Thermo Fisher Scientific Inc., Rockford, IL) was used. The blot was developed using BioMax MS Films and cassettes (with intensifying screen, Kodak). The images were subjected to densitometry analysis using Lab Image 2006 Professional 1D gel analysis software from KAPLEAN Bioimaging Solutions, Liepzig, Germany.

Quantitative Real Time Polymerase Chain Reaction (qRTPCR):

Gene expression levels in tissue samples were measured by two step qRTPCR. Total RNA was isolated from liver tissue by homogenization in TRIzol reagent (Invitrogen) according to the manufacturer's instructions and purified with the use of RNeasy mini kit columns (Qiagen, Valencia, CA). Purified RNA (1µg) was converted to cDNA using iScript cDNA synthesis kit (Bio-rad) following the manufacturer's standard protocol. qRTPCR was performed with the gene specific primers using SsoAdvanced SYBR Green supermix (Bio-rad) and CFX96 thermal cycler (Bio-rad). Threshold Cycle (Ct) values for the selected genes were normalized against 18S (internal control) values in the same sample. Each reaction was carried out in triplicates for each gene and for each tissue sample. DIO mouse liver sample was used as the control for comparison with all other liver samples in the toxin-induced NASH group and MCS-diet fed mouse liver sample was used as control for comparison with all other liver samples of the diet-induced NASH group. The relative fold change was calculated by the $2^{-\Delta\Delta Ct}$ method. The sequences for the primers used for Real time PCR are provided below in 5' to 3' orientation:

www.manaraa.com

Gene	***Primer sequence***
CYP2E1	Sense: GGCGCATCGTGGTCCTGCAT Antisense: CCGCACGTCCTTCCATGTGGG
P2X7r	Sense: GGGACGCTGAAGAACACCTT Antisense: CCTAACTTCGTCACCCCACC
GABARAP	Sense: AGAGGAGCATCCGTTCGAGA Antisense: CGAGCTTTGGGGGCTTTTTC
Atg-2A	Sense: AACATCCAACGTGCTAGGGG Antisense: GGACAGTGGGTGGATCTTGG
LC3B	Sense: GCTGTGAGGACAACAGCAAC Antisense: AGTGAGTGAGTGACCAGGGA
MHC II	Sense: TGATTCTGGGGGTCCTCGCCC Antisense: CGTGGTCGGCCTCAATGTCGT
LAMP2A	Sense: GTACCTGACAAGGCGACACA Antisense: CCCAAGAGACAGCGAATCCA
TGF-β	Sense: CTCACCGCGACTCCTGCTGC Antisense: TCGGAGAGCGGGAACCCTCG
COL-1-α-1	Sense: TGGACGATGGGGCTGGGGAG Antisense: GGGTGCCCAGTGGTCGCTTC
α-SMA	Sense: GGAGAAGCCCAGCCAGTCGC Antisense: ACCATTGTCGCACACCAGGGC
Hsc 70	Sense: AGTTGGCATTGATCTCGGCA Antisense: GTGTTGGTGGGGTTCATTGC

www.manaraa.com

Caspase-1	Sense: GGACCCTCAAGTTTTGCCCT Antisense: AACTTGAGCTCCAACCCTCG
IL-1β	Sense: CCTCGGCCAAGACAGGTCGC Antisense: TGCCCATCAGAGGCAAGGAGGA
TNF-α	Sense: CAACGCCCTCCTGGCCAACG Antisense: TCGGGGCAGCCTTGTCCCTT
IFN-γ	Sense: TGCGGGGTTGTATCTGGGGGT Antisense: GCGCTGGCCCGGAGTGTAGA
HMGB-1	Sense: GGACTCTCCTTTAACCGCCA Antisense: TTGTGATAGCCTTCGCTGGG

Confocal laser scanning microscopy (Zeiss LSM 510 UV Meta):

Frozen tissue sections after formalin fixation were analyzed by confocal microscopy using Zeiss LSM 510-UV meta (Carl Zeiss, Inc., Oberkochen, Germany) and a Plan-NeoFluor 40X/1.3 objective with different zoom levels. The primary antibody for LAMP-2A was obtained from AbCam Inc.; the Cy3-conjugated affinitipure secondary antibody was obtained from Jackson Immunoresearch. The BODIPY dye and DAPI used were supplied by Molecular Probes.

Statistical Analyses:

All *in vivo* experiments were repeated three times with 3 mice per group (N=3; data from each group of three mice were pooled). All *in vitro* experiments were repeated three times, and the statistical analysis was carried out by analysis of variance (ANOVA) followed by

www.manaraa.com

the Bonferroni posthoc correction for intergroup comparisons. Quantitative data from Western blots as depicted by the relative intensity of the bands were analyzed by performing a student's t test.$P<0.05$ was considered statistically significant.

3.3 RESULTS

Steatohepatitic injury in obese mice is associated with increased metabolic oxidative stress. Metabolic oxidative stress in obesity-induced steatohepatitic injury is caused following increased CYP2E1 activity, mitochondrial uncoupling of the electron transport chain or toxin metabolism following administration of hepatotoxic drugs (8, 10, 72, 73). We and others have shown that toxin-induced steatohepatitis models produce metabolic oxidative stress (8, 69, 74). The toxin and diet-induced steatohepatitic injury models that produce metabolic oxidative stress are relevant to clinical outcomes since NASH patients show oxidative stress, and has been hypothesized to augment disease progression (75). Our results demonstrate that CYP2E1 increases lipid peroxidation, oxidative and nitrosative stress upon steatohepatitic injury. 4-Hydroxynonenal (4-HNE), a marker for lipid peroxidation was found to be increased in liver tissues from both the toxin (DIO+BDCM) and diet models (MCD-diet fed mice) (Figs. 3.1A i-ii; iv-v; 3.1C) as compared to the respective controls (DIO and MC sufficient diet herein referred to as MCS diet). DIO mice with deletion of the CYP2E1 gene and administered BDCM showed decreased 4-hydroxynonenal adducts, when compared to DIO+BDCM only group (Figs. 3.1A ii-iii, 3.1C). Tyrosine nitration, a marker of oxidative and nitrosative stress, as evidenced by 3-nitrotyrosine (3NTyr) immunoreactivity was found to be increased in liver tissues from both the toxin (DIO+BDCM) and diet models (MCD-diet fed mice) (Figs. 3.1B i-ii; iv-v; 3.1D) as compared to the respective controls (DIO and MCS diet). DIO mice with deletion

www.manaraa.com

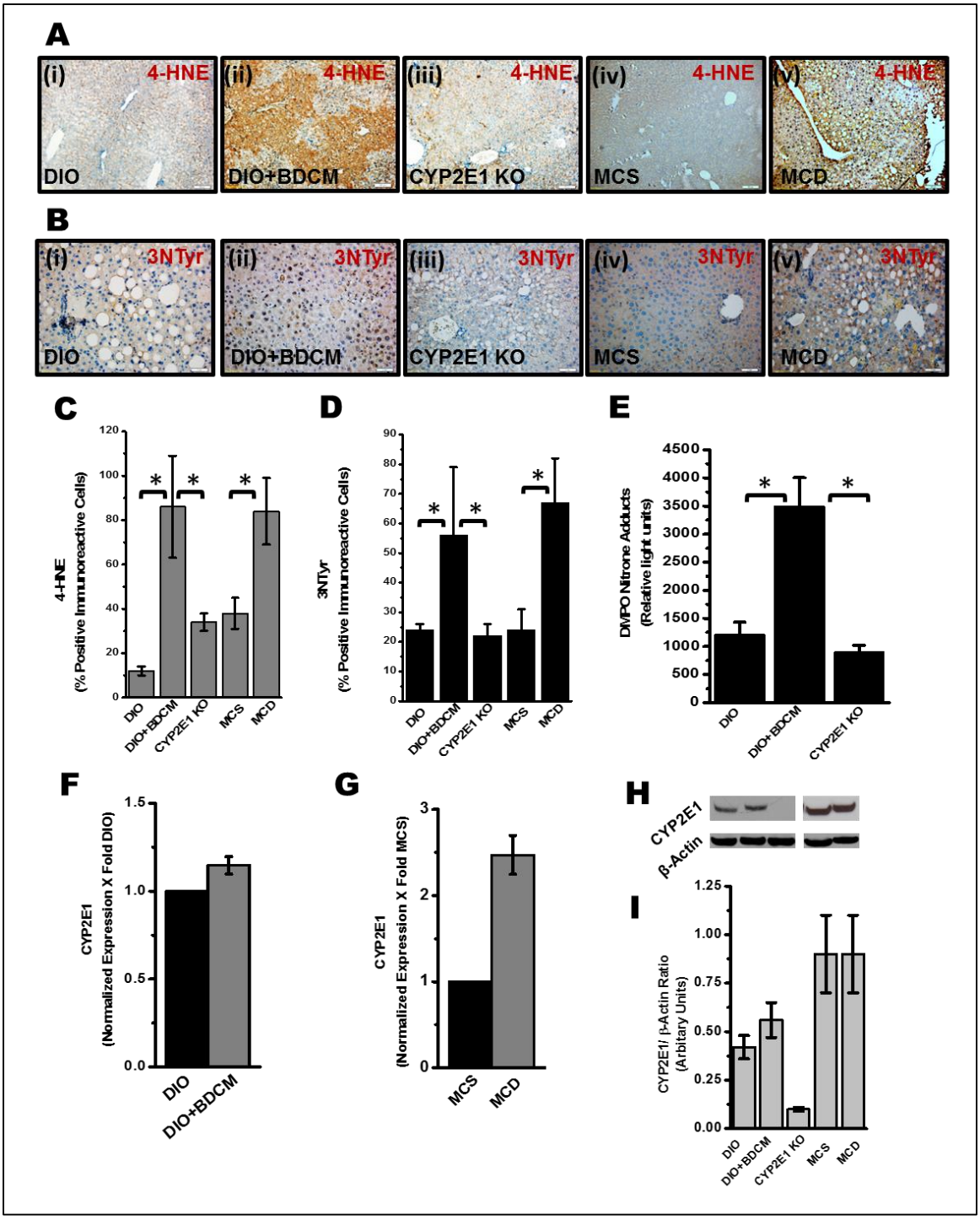

Figure 3.1 Oxidative stress in high-fat diet and BDCM co-exposed model and MCD model is mediated by CYP2E1A. 4-hydroxynonenal, (a marker of lipid peroxidation) immunoreactivity in liver slices from DIO, DIO+BDCM, CYP2E1 knockout, Methyl choline sufficient diet fed mice (MCS) and Methyl choline deficient diet fed mice(MCD)

www.manaraa.com

(i-v) . B. Nitrotyrosine immunoreactivity as shown by immunohistochemistry in liver slices (i-v; DIO, DIO+BDCM,CYP2E1 knockout, MCS and MCD Groups).C. Morphometry (percentage) of 4-hydroxynonenal reactive cells. D. Morphometry (percentage) of nitrotyrosine imunoreactive cells. E. DMPO-nitrone adducts, a marker of protein free radicals in toxin model of NASH as assessed by ELISA with anti-DMPO antibody. ($P<0.05$). F and G. CYP2E1 mRNA expression as measured by quantitative real time PCR ($P<0.05$) in toxin-induced and MCD models of NASH. H. Western blot analysis of CYP2E1 protein levels. Lanes 1-5 represent DIO, DIO+BDCM, CYP2E1 Knockout, MCS and MCD respectively. I. Band quantification of the immunoblots using normalization against beta-actin. The western analysis was done using liver homogenates from the respective groups. Representative immunoblot is shown.

of the CYP2E1 gene and administered BDCM showed decreased 3-nitrotyrosine immunoreactivity, when compared to DIO+BDCM only group (Figs. 3.1B ii-iii, 3.1D). To estimate the extent of protein radical formation and corresponding oxidation, DMPO-nitrone adducts were measured in the liver homogenates of the toxin-model of steatohepatitic injury. Results indicated that DMPO-nitrone adducts were significantly increased in DIO+BDCM group as compared to DIO only group ($P<0.05$)(Fig. 3.1E). CYP2E1 deleted mice fed with high fat diet and co-administered BDCM had a significant decrease in the nitrone adducts (Fig. 3.1E, $P<0.05$). Hepatic CYP2E1 mRNA expressions showed an increase in DIO+BDCM (not statistically significant) and MCD-diet treated mice as compared to DIO or MCS diet fed mice (Figs. 3.1F and G; $P<0.05$), suggesting that increased CYP2E1 expression might play a prominent role in the metabolic oxidative stress generation in steatohepatitic injury. The protein levels of CYP2E1 showed small increase in DIO+BDCM group when compared to DIO group (not statistically significant) but was unchanged in the MCS and MCD groups (Fig. 3.1H). Given the importance of P2X7 receptor in innate immunity, inflammation, cell death and disease pathogenesis in NASH following its activation, we investigated the role of metabolic oxidative stress in modulating the expression of hepatic P2X7 receptors, those might amplify inflammation. Gene expression was measured by qRTPCR. Results indicated that there was a significant

www.manaraa.com

increase in P2X7 receptor mRNA expression in DIO+BDCM group and MCD-diet fed group when compared to DIO and MCS-diet groups ($P<0.05$)(Figs. 3.2A and 3.2B). Deletion of the CYP2E1 gene in mice fed with high fat diet and exposed to BDCM, had significant decrease in the P2X7 receptor mRNA expression as compared to DIO+BDCM group ($P<0.05$)(Fig. 3.2A). Similar observations were found in the P2X7 receptor immunoreactivity in hepatic tissue. DIO+BDCM group and MCD-diet fed group had higher P2X7 receptor levels when compared to DIO only and MCS-diet groups (Figs. 3.2C, i-ii, iv-v). Mice that had the deletion of CYP2E1 gene but co-administered with high fat diet and BDCM had decreased levels of P2X7 receptors (Fig. 3.2C, iii). Hepatocytes, Kupffer cells and liver sinusoidal endothelial cells had increased expression of P2X7 receptor mRNA in the toxin model as compared to untreated samples.

CYP2E1-mediated metabolic oxidative stress in steatohepatitic injury induces macroautophagy and causes increased expression of chaperone-mediated autophagy-related proteins. To study the effect of metabolic oxidative stress on the induction of autophagy-related proteins in steatohepatitic injury, markers of macro and chaperone-mediated autophagy were analyzed. Results indicated that mRNA expressions of early autophagy genes GABARAP, Atg2A and LC3B; and components of the lysosomal translocation complex, LAMP2A and Hsc 70 were significantly elevated in DIO+BDCM group and MCD-diet fed group as compared to DIO and MCS-diet fed group respectively (Figs. 3.3A and 3.3B)($P<0.05$). Mice that had a deletion of CYP2E1 gene and were co-exposed to high fat diet and BDCM had a significant decrease in early autophagy markers GABARAP, Atg2A and LC3B as compared to DIO+BDCM group, while there was no

www.manaraa.com

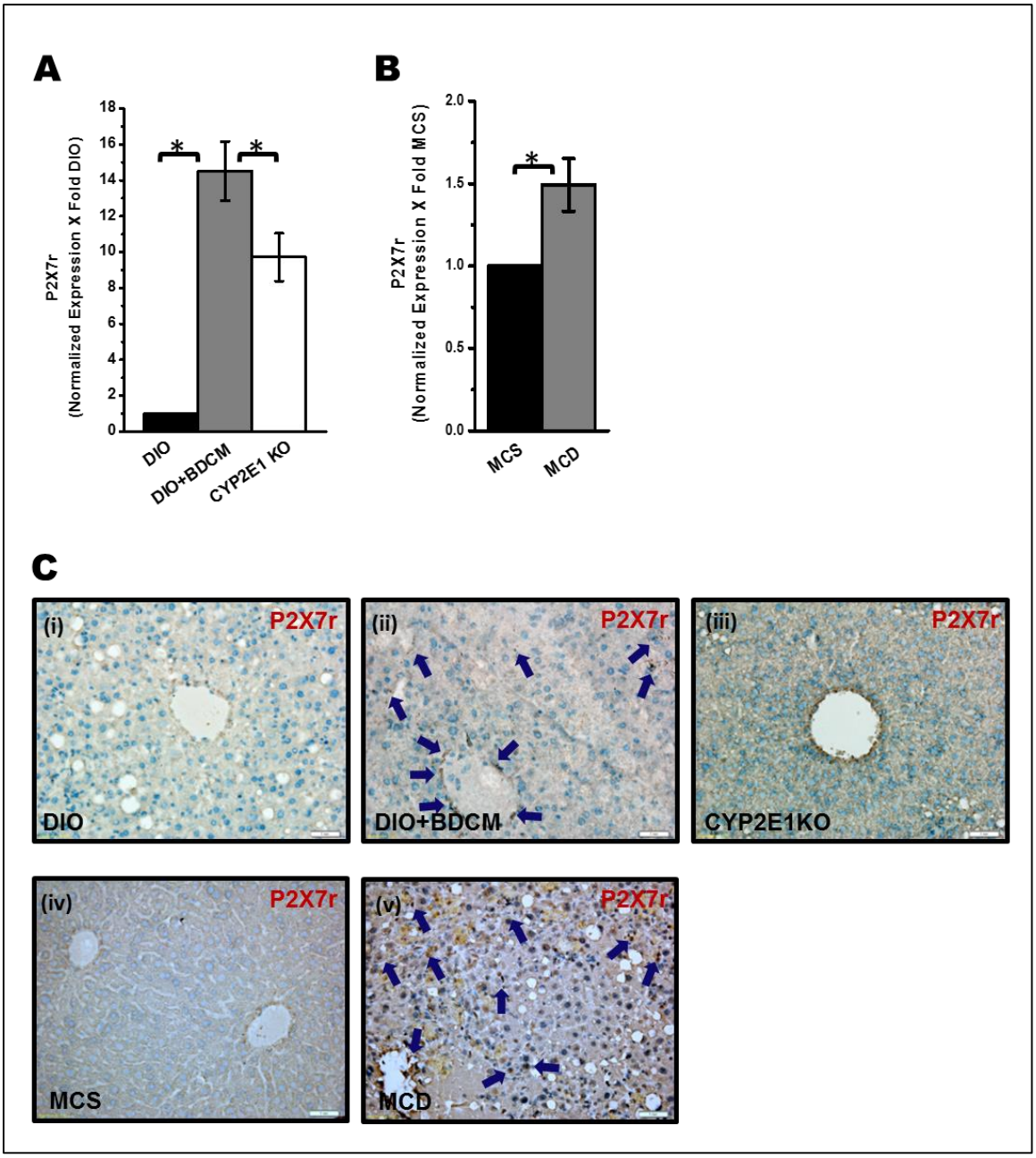

Figure 3.2 High-fat diet and BDCM co-exposure, and MCD diet increase expression of P2X7r. A and B. mRNA expression of P2X7 receptor as assessed by quantitative real time PCR, normalized against DIO and MCS groups. "CYP2E1 KO" represents liver mRNA expression from CYP2E1 gene depleted mice fed with high fat diet. (* $P<0.05$). C. Immunohistochemistry of P2X7 receptor protein from liver slices of DIO, DIO+BDCM, CYP2E1 KO, MCS and MCD groups. The localization of the receptor positive staining is shown by blue arrows.

www.manaraa.com

significant change in the expression pattern of Hsc 70 (Fig. 3.3A). LAMP2A mRNA levels were decreased in CYP2E1 deleted mice but the change was not significant (Fig. 3.3A). Immunoreactivity of early autophagy marker GABARAP (Initiator of the autophagy process), LAMP2A, an important constituent of the lysosomal translocation complex were increased in livers of steatohepatitic mice in both models of injury. (Figs. 3.3C and 3.3D; i-ii, iv-v). Absence of the CYP2E1 gene caused a decrease in the immunoreactivity of both GABARAP and LAMP2A, suggesting that metabolic oxidative stress and related oxidized proteins caused due to the involvement of CYP2E1 has led to the initiation and sustenance of the autophagy process (Figs. 3.3C iii and 3.3D iii.). Hsc 70 which is responsible for recognizing and mediating substrate targeting for chaperone-mediated autophagy, was not significantly altered in both DIO+BDCM group and MCD-diet group (Figs. 3.3E and 3.3F)($P<0.05$), however the deletion of the CYP2E1 gene had significantly decreased levels of Hsc 70 in the toxin model (Figs. 3.3E and 3.3F)($P<0.05$), suggesting a possible role of CYP2E1 in regulating the Hsc 70 expressions in this model of steatohepatitic injury.

P2X7 receptor modulates autophagy induced by metabolic oxidative stress in steatohepatitic injury. Based on our current findings that show a significant increase in P2X7 receptor gene expression upon increased metabolic oxidative stress in NASH models, we investigated its role in mediating autophagy and modulating proteins in lysosomal translocation complex. mRNA expression of early autophagy inducing genes, GABARAP, Atg2A and LC3B were significantly down regulated in P2X7 receptor gene deleted mice (a) co-administered with high fat diet+BDCM, and (b) in MCD diet fed mice when compared to DIO+BDCM and MCD diet fed groups respectively (Figs. 3.4A and 3.4B). Lysosomal translocation complex proteins Hsc 70 and LAMP2A which are

www.manaraa.com

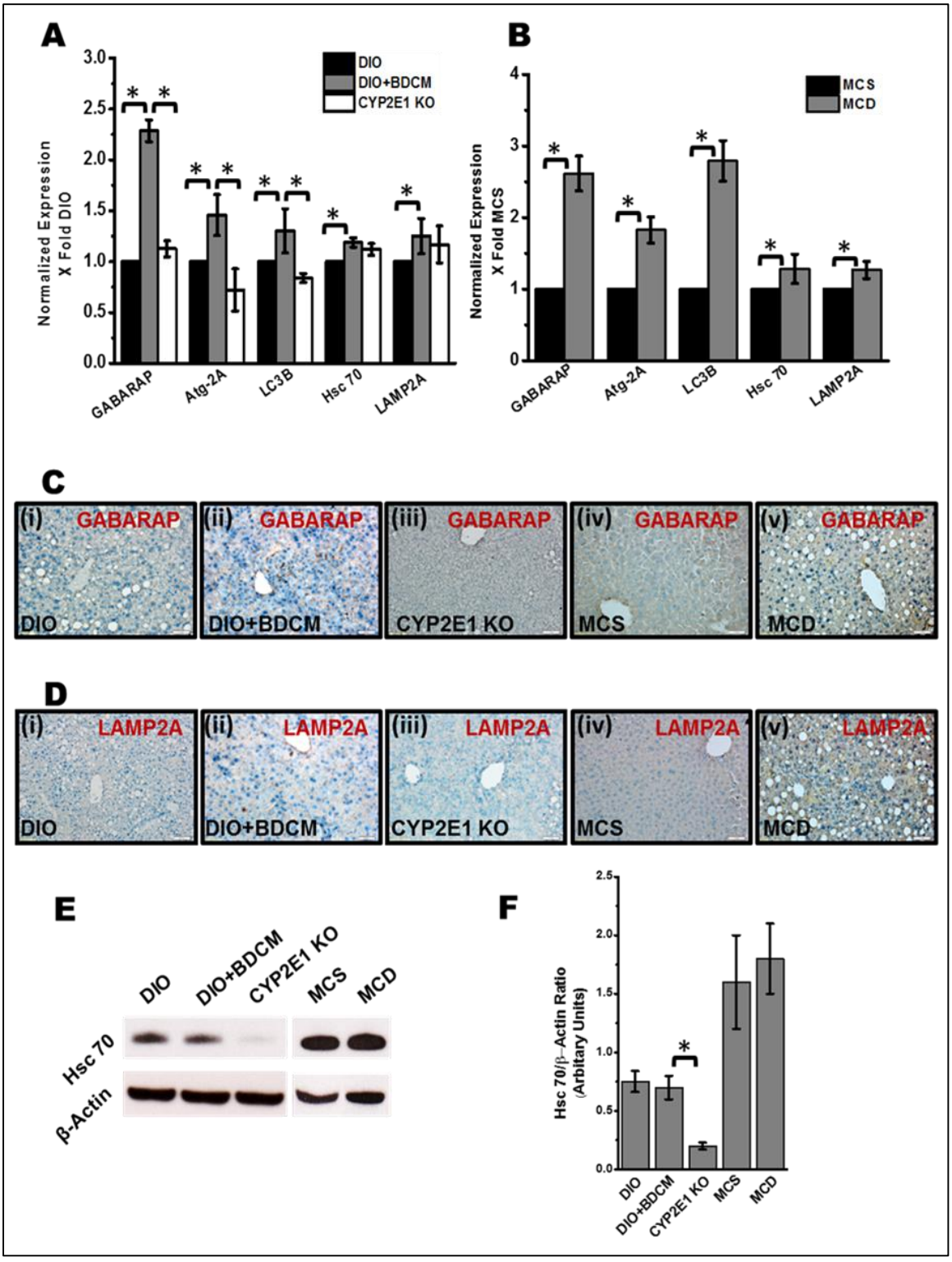

Figure 3.3 Metabolic oxidative stress influences autophagy protein profiles in NASH. A, B: mRNA expressions of early and late autophagy-related proteins in toxin and diet-models of NASH. (*P<0.05) as measured by quantitative real time PCR. Immunoreactivity of

www.manaraa.com

GABARAP (C) and LAMP2A(D) as measured by immunohistochemistry . Panels i,ii,iii,iv and v represent, DIO, DIO+BDCM, CYP2E1 KO, MCS and MCD respectively. E and F represent the western blot image for Hsc 70 and its corresponding band quantification analysis (*P<0.05). The normalization was carried out against the levels of beta-actin in the liver homogenates.

significant players in chaperone mediated autophagy were down regulated in P2X7 receptor deleted mice, either treated with toxin BDCM or fed with MCD diet, as compared to wild type counterparts (P<0.05);(Figs. 3.4A and 3.4B). Western blot analysis of GABARAP revealed a significant decrease in the band intensity, signifying a decreased GABARAP protein levels in P2X7 gene deleted mice treated with both the toxin and MCD diet as compared to the wild type counterparts (P<0.05)(Figs. 3.4C and 3.4D). Interestingly P2X7 receptor deleted mice from both DIO+BDCM and MCD-diet groups had significantly increased levels of LC3B as compared to their wild type counterparts (P<0.05)(Figs. 3.4C and 3.4D). In contrary to the P2X7 receptor gene deleted mice, protein levels of LC3B were decreased in DIO+BDCM and MCD diet fed groups as compared to DIO and MCS diet fed groups, suggesting LC3B depletion in NASH (Fig. 3.4E). Immunohistochemistry of LC3B also showed increased LC3B protein immunoreactivity in P2X7 receptor deleted liver as compared to DIO+BDCM only group (Fig. 3.4F). LAMP2A protein levels as studied by immunohistochemistry showed a decreased immunoreactivity in P2X7 receptor deleted mice, having exposed to toxin or MCD-diet as compared to the wild type counterparts (Fig. 3.5A). Since Hsc 70 plays a crucial role in recruiting peptides for the lysosomal translocation process and is a key mediator of late autophagy, western blot analysis of Hsc 70 was carried out (76, 77). Results showed that P2X7 receptor gene deleted mice had a significant decrease in Hsc 70 protein levels as compared to their wild type counter parts (P<0.05)(Fig. 3.5B and 5C). The results

www.manaraa.com

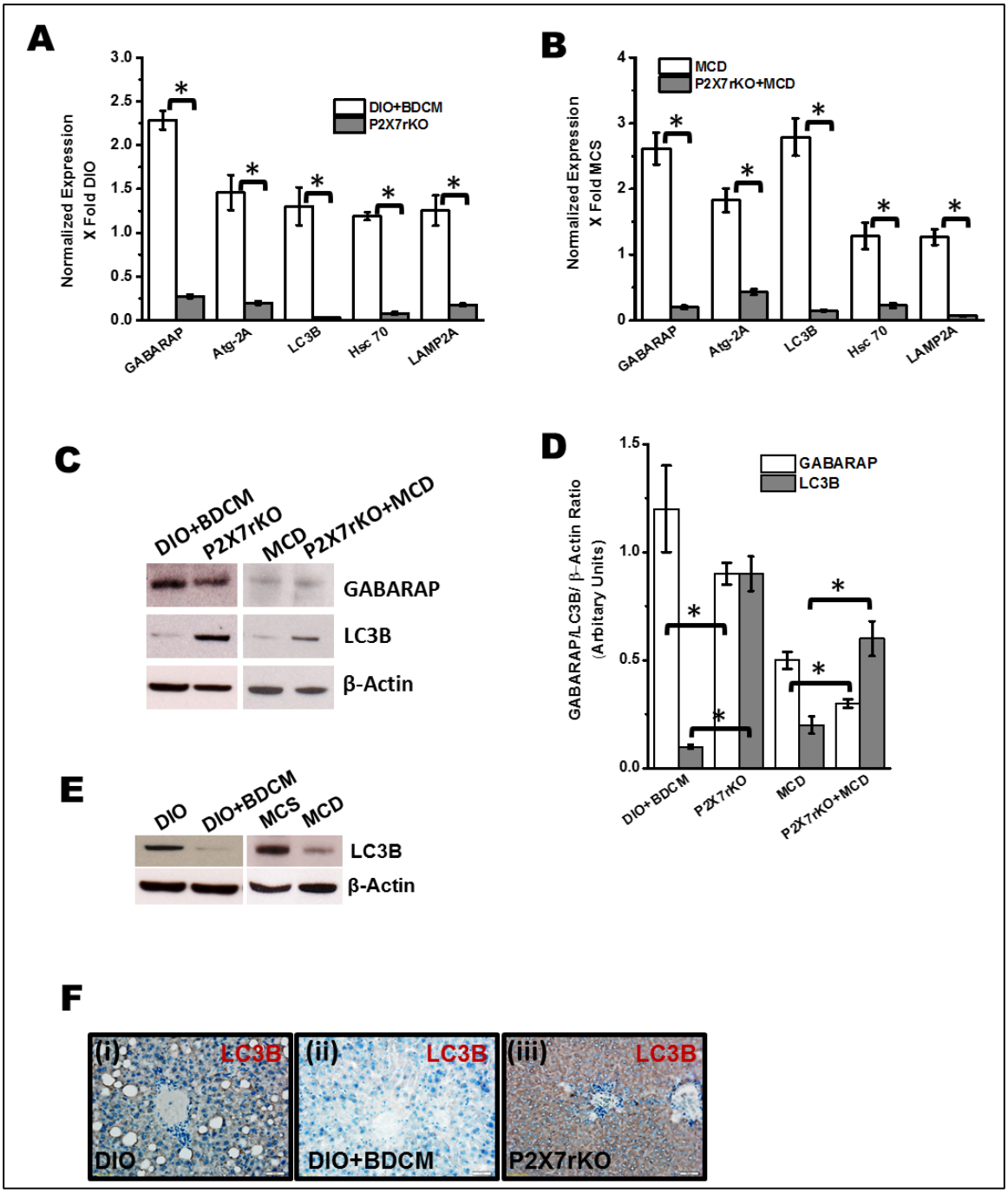

Figure 3.4 P2X7 receptor deletion modulates autophagy in NASH. A and B. mRNA expressions of early and late autophagy-related proteins in toxin and diet-models of NASH (*P<0.05) as measured by quantitative real time PCR in DIO+BDCM and P2X7 receptor gene deleted mice, co-exposed to high fat diet and toxin, MCD and P2X7 receptor gene deleted mice fed with MCD diet. C. Western blot analysis of GABARAP and LC3B and their corresponding band quantification analysis (D),(* P<0.05). E. Western blot analysis of LC3B protein in DIO, DIO+BDCM, MCS and MCD liver homogenates. Bands are

www.manaraa.com

normalized against beta-actin. F. Immunohistochemistry of LC3B protein in liver slices of DIO, DIO+BDCM and P2X7 receptor knockout mice co-exposed to high fat diet and BDCM showing perivenular areas.

demonstrate that P2X7 receptor modulates both the early autophagy and the late chaperone mediated lysosomal translocation processes in steatohepatitic injury.

P2X7 receptor is a key regulator of LAMP2A association with the lysosomal membrane during increased metabolic oxidative stress in steatohepatitic injury. To show the extent of lysosomal membrane association of LAMP2A, confocal laser scanning microscopy was performed. Results showed that there was an increase (3 fold) in the number of events of lysosomal membrane (green) associations of LAMP2A (red), as evidenced by co-localization spots (yellow) in DIO+BDCM group as compared to DIO only group (Fig 3.6A,v-viii). P2X7 receptor deleted mice that were co-administered with high fat diet and BDCM had no visible co-localizations in the same numbers of field analyzed (Fig. 3.6A, ix-xii). MCD mice liver had more LAMP-2A-membrane fusions as compared to MCS mice as evidenced by confocal microscopy (Fig. 3.6B). These results suggested that the absence of P2X7 receptor gene significantly affected LAMP2A association with the lysosomal membrane.

P2X7 receptor modulates autophagy-linked inflammation in NASH: To explore the regulation of P2X7 receptor and its downstream effectors in autophagy-linked inflammation in steatohepatitic injury, mRNA expression of caspase-1, IL-1β, TNF-α and IFN-γ were studied. Results indicated that there was a significant increase (more than 17 fold) of caspase-1, IL-1β(4 fold), TNF-α and IFN-γ in both DIO+BDCM group and MCD diet fed group, as compared to DIO or MCS diet fed group (Figs. 3.7A and 3.7B). Cleaved caspase-1 which is an indicator of active caspase-1 was significantly decreased in P2X7

www.manaraa.com

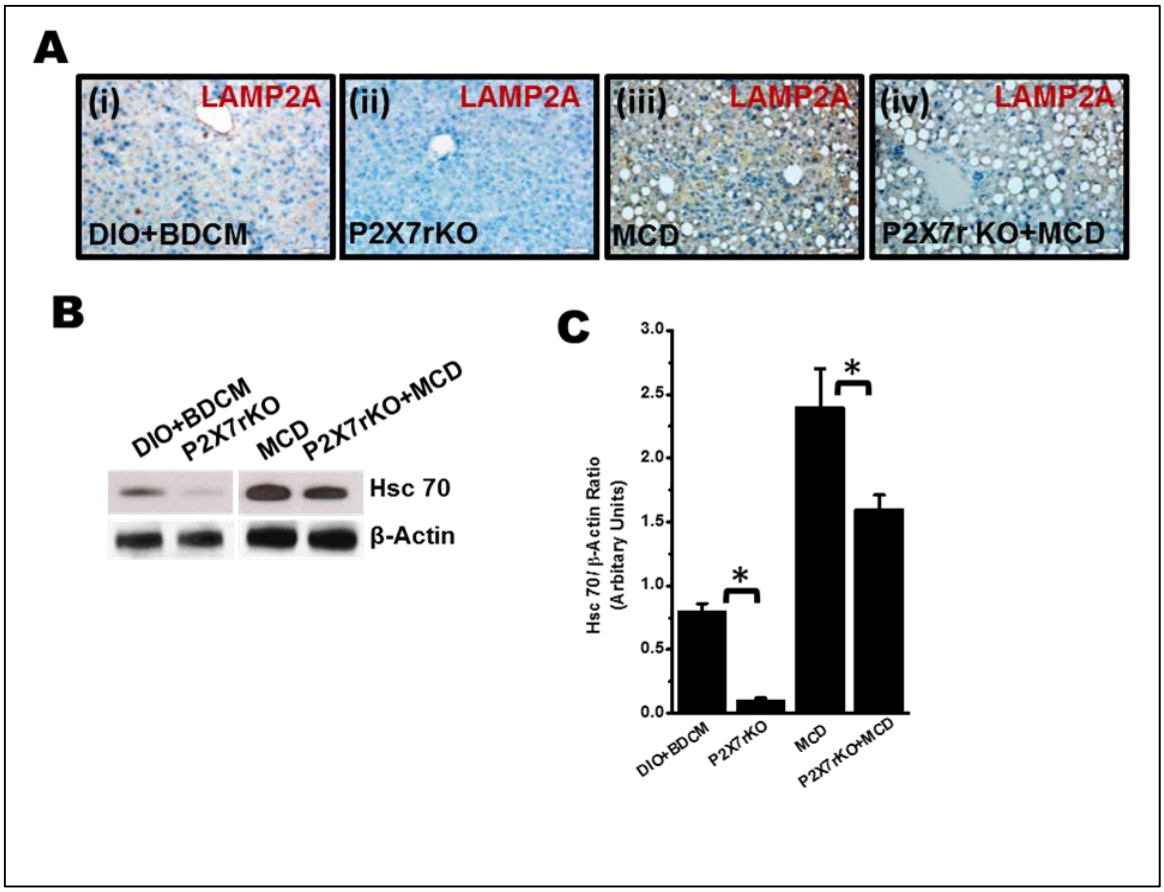

Figure 3.5 Immunodetection of late autophagic gene and chaperone protein. A. Immunoreactivity of LAMP2A as analyzed by immunohistochemistry. Panels i-iv represent, DIO+BDCM, P2X7 receptor deleted group co-exposed to high fat diet and BDCM (toxin), MCD and P2X7 receptor knockout group exposed to MCD diet respectively. B and C: Western blot analysis of Hsc70 in DIO+BDCM, P2X7 receptor deleted group co-exposed to high fat diet and BDCM (toxin), MCD and P2X7receptor deleted group (MCD) (*P<0.05). Fig. 5C represents the band quantification analysis.

Results also indicated that P2X7 gene deleted mice from both DIO+BDCM co-exposed group had decreased amounts of HMGB-1 protein, a damage associated molecular pattern linked to inflammation, as analyzed by western blot (Figs. 3.8A and 3.8B), as compared to their wild type controls (P<0.05) though the HMGB-1 protein level was not significantly different in MCD-treated group (Figs. 3.8A and 3.8B). The decreased expression of HMGB-1, IL-1β, IFN-γ and cleaved caspase-1 in P2X7 receptor deleted mice show that

www.manaraa.com

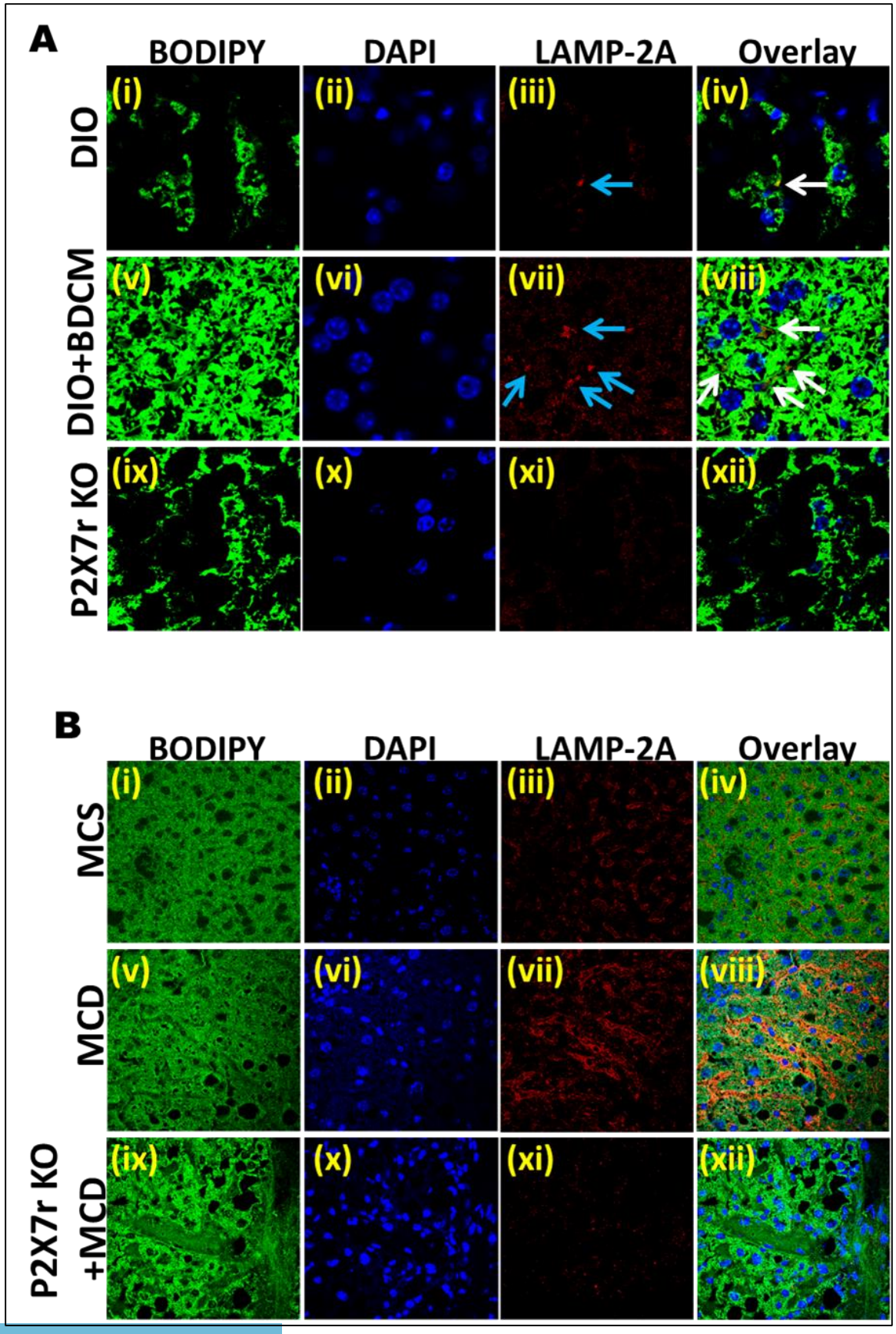

www.manaraa.com

Figure 3.6 LAMP2A and Bodipy colocalization in high-fat diet and BDCM co-exposed model and MCD model. A. LAMP2A colocalization with lysosomal membrane (60x zoom 3). Confocal laser scanning image of LAMP2A (red) and membrane lipid (Bodipy stain, green) from liver sections of DIO, DIO+BDCM and P2X7 receptor deleted group co-exposed to high fat diet and BDCM. B. LAMP2A colocalization with lysosomal membrane (60x). Confocal laser scanning image of LAMP2A (red) and membrane lipid (Bodipy stain, green) from liver sections of MCS, MCD and P2X7 receptor deleted group fed with MCD diet. Blue arrows show LAMP2A localizations, while white arrows depict colocalizations of LAMP2A with lysosomal membrane depicted by green bodipy staining. Number of colocalizing events as shown by overlay of images were counted to reveal the extent of LAMP2A attachment to the lysosomal membrane.

metabolic oxidative stress-induced autophagy and corresponding inflammation is regulated by the P2X7 receptors in steatohepatitic injury.

P2X7 receptor gene deleted mice are protected from steatohepatitic injury and fibrosis. To ensure that the genetic deletion of P2X7 receptor in mice exposed with either high fat diet+BDCM or MCD diet fed group were protected from symptoms of steatohepatitic injury, mRNA expressions of fibrotic markers α-SMA, TGF-β and Col-1-α1 were analyzed. Results showed that α-SMA, TGF-β and Col-1-α1 were significantly decreased in P2X7 receptor gene deleted mice as compared to wild type mice either fed with high fat diet and BDCM or MCD (Fig. 3.8C, $P<0.05$). Hemotoxylin and Eosin stainings of the liver slices of P2X7 receptor deleted mice administered the toxin and fed with high fat diet showed decreased hepatocyte necrosis compared to wild type mice fed with high fat diet (Fig. 3.8D).There was a decrease in Picro-Sirius red staining in livers of P2X7 receptor gene deleted mice as compared to the wild type mice fed with high fat diet and BDCM, suggesting decreased fibrosis (Fig. 3.8E). DIO+BDCM mice also had increased serum ALT, Alkaline phosphatase and albumin levels when compared to DIO and P2X7 receptor gene deleted mice.

www.manaraa.com

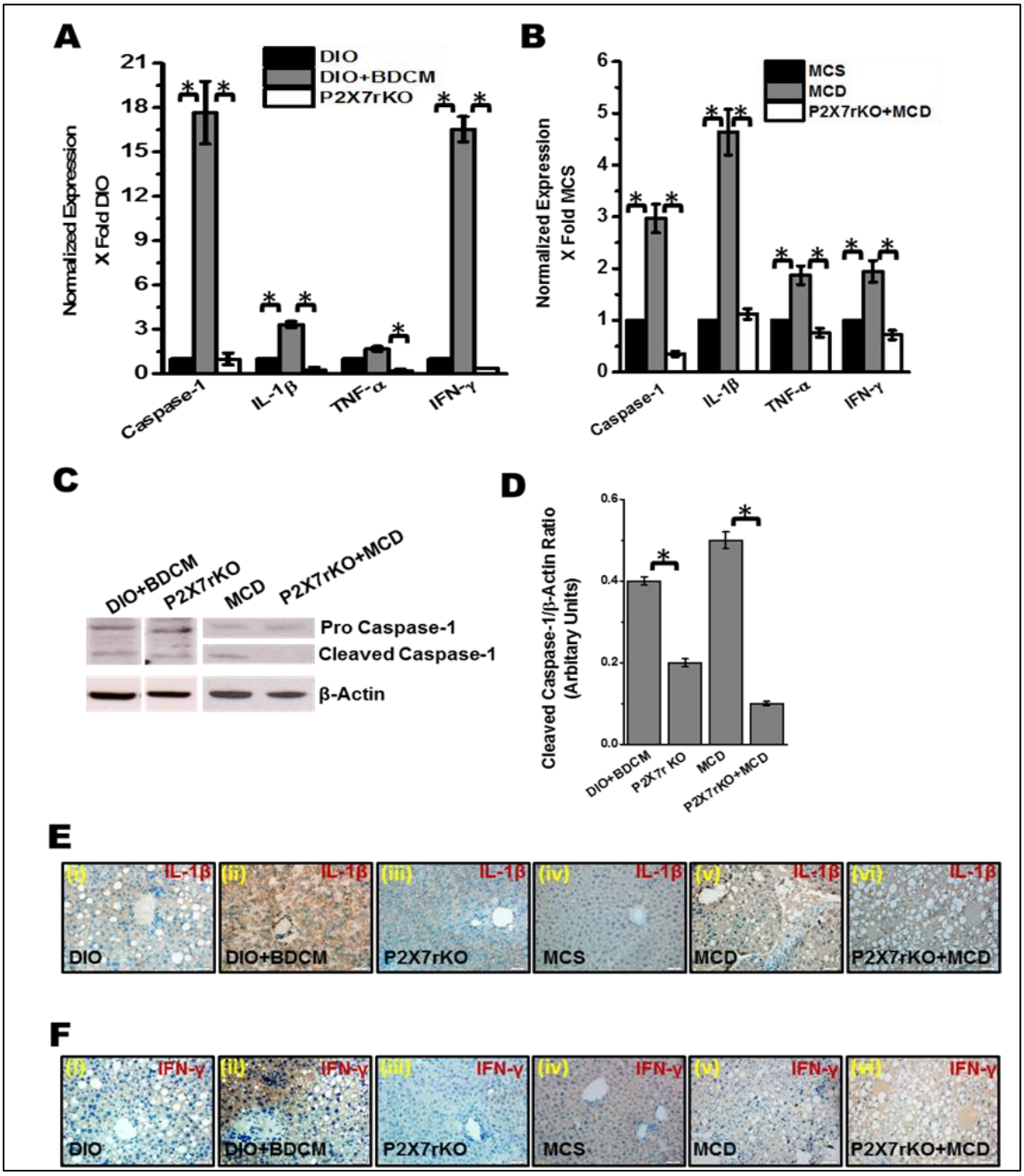

Figure 3.7 P2X7 receptor modulates inflammation in NASH. A. and B. mRNA expression of proinflammatory mediators, as measured by quantitative real time PCR in DIO, DIO+BDCM, P2X7 receptor gene deleted mice, co-exposed to high fat diet and BDCM (toxin), MCS, MCD and P2X7 receptor gene deleted mice fed with MCD diet. The expression levels were normalized against DIO in toxin model and MCS in diet model. C. Western blot analysis of cleaved caspase-1(active caspase-1) and its corresponding band quantification analysis (D), (*P<0.05).Individual lanes representing DIO+BDCM and P2X7 receptor gene deleted groups were separated from the parent blot to ensure better visibility. E and F: Immunoreactivity of IL-1β and IFN-γ as analyzed by

www.manaraa.com

immunohistochemistry. Panels i-vi represent, DIO, DIO+BDCM, P2X7 receptor deleted group co-exposed to high fat diet and BDCM (toxin), MCS, MCD and P2X7 receptor deleted group exposed to MCD diet respectively.

3.4 DISCUSSION:

Till date nonalcoholic fatty liver disease and its associated steatohepatitic injury is considered an emerging epidemic in light of the dramatic increase in obesity rates (39, 40). With the progressive nature of NASH and its rising prevalence there is a significant need for specific and targeted treatments. This is complicated by the fact that there are not many validated therapies for NAFLD other than weight loss, which is well known to have a poor long-term success rate (80). Cellular death pathways and inflammation play crucial roles in NASH pathophysiology and it is essential that we identify new mediators of NASH pathophysiology that are important regulators of autophagy and inflammatory pathways. Impairment of autophagy that is correlated with hepatic lipid accumulation and obesity has been found to have a significant impact on progression of NASH (31). There is also a perception that agents which augment autophagy can have therapeutic potential in NASH (67). However no significant research has been in place that link metabolic oxidative stress, autophagy and P2X7 receptors and their crosstalk in modulating disease progression in NASH. Targeting a key regulator of each of these components can have benefits in therapy of NASH. This study shows that P2X7 receptor, which is upregulated by metabolic oxidative stress (Fig. 3.2), serve as a key regulator in modulating the oxidative stress induced-autophagy process (Fig. 3.3). P2X7 down regulation in CYP2E1 knockout mice coupled with an earlier report by this group that showed extracellular ATP (ligand for P2X7) release from necrosed-hepatocytes (those that had higher 4-HNE staining) in a

www.manaraa.com

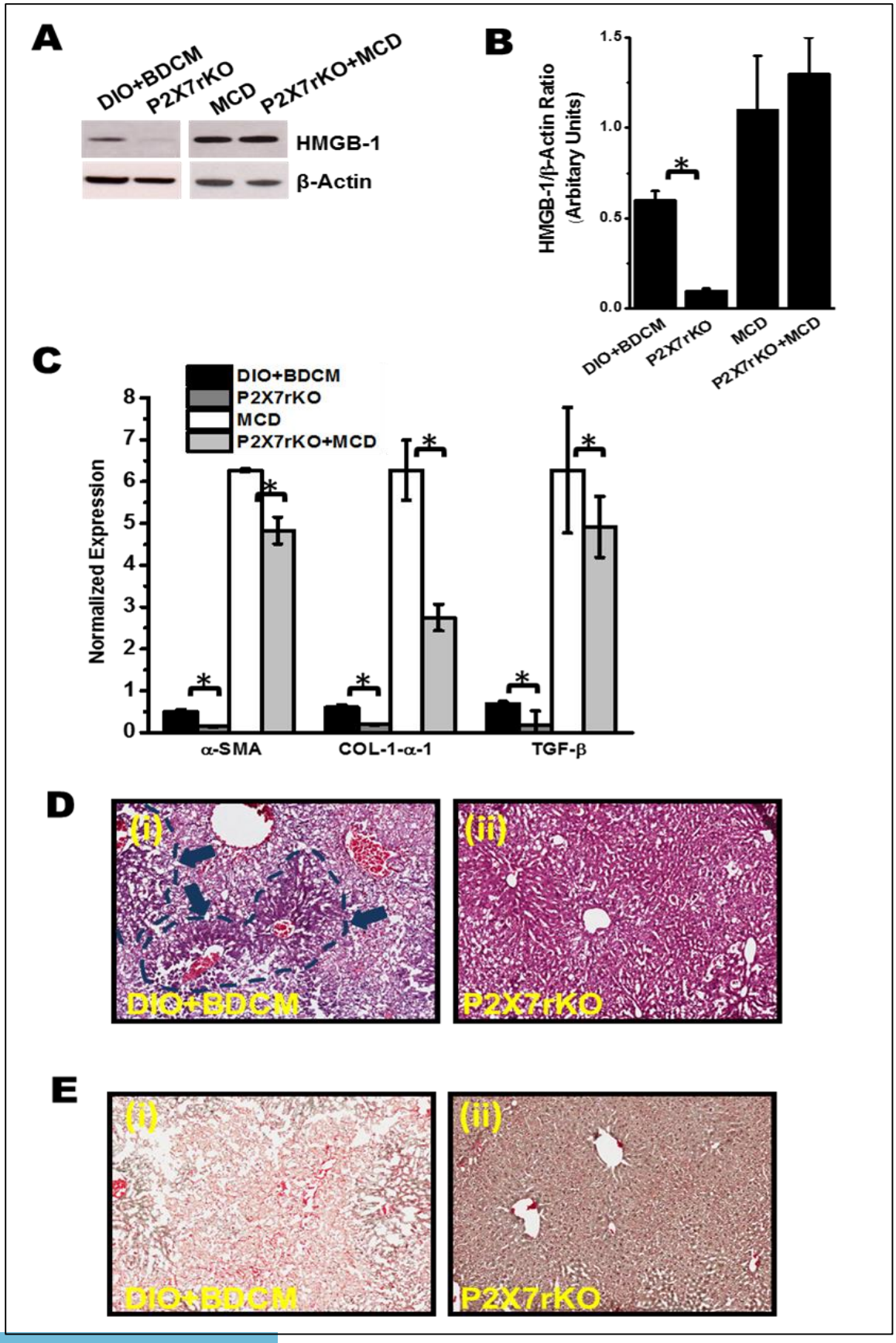

www.manaraa.com

Figure 3.8 Fibrosis and necrotic damage are mediated by P2X7r in response to DAMPs in both high-fat fed and BDCM co-exposed model and MCD model. A: Western blot analysis of HMGB-1 from liver homogenates of DIO+BDCM, P2X7 receptor deleted group co-exposed to high fat diet and BDCM (toxin), MCD and P2X7 receptor deleted group exposed to MCD diet respectively . B. represents the band quantification analysis following normalization against beta-actin (*P<0.05). C. Quantitative real time PCR analysis of the mRNA expression profiles of fibrosis markers in DIO+BDCM, P2X7 receptor deleted group co-exposed to high fat diet and BDCM (toxin), MCD and P2X7 receptor deleted group exposed to MCD diet respectively (*P<0.05). D. Hematoxylin and Eosin staining of liver sections from DIO+BDCM group and P2X7 gene deleted group co-exposed to BDCM and high fat diet. Areas of necrosis are shown in demarcated blue dotted lines and arrow heads. E. Picro-sirius red staining for fibrosis in liver sections from DIO+BDCM group and P2X7 gene deleted group co-exposed to BDCM and high fat diet.

CCl_4-mediated NASH model, correlates oxidative stress, upregulation of P2X7 receptor and its downstream events(8). The P2X7 receptor might modulate the autophagy process, by allowing depletion of LC3B, which is supposedly an early autophagy marker (Fig. 3.4E), while increasing albeit in small proportions Hsc 70 and LAMP2A mRNA levels (Figs. 3.3A and 3.3B) and allowing LAMP2A association with the lysosomal membrane, (Fig. 3.6). Interestingly, LC3B mRNA levels in NASH models showed a significant increase while the protein levels decreased (Figs. 3.3A, 3.3B and 3.4E). The contrasting result might point to a translational level regulation and can be explored further. These events can be crucial mediators of chaperone mediated autophagy in the hepatic lobe, thus increasing inflammation, in a manner perhaps similar to P2X7 receptor mediated release of autophagolysosomes/ phagolysosomes into the extracellular matrix causing increase in inflammation(81). The above mechanism of release of phagolysosomes to the extracellular matrix might be speculative for NASH at this point, but this study certainly proves the dependence of depleted LC3B, increased levels of LAMP2A and Hsc 70 on P2X7 receptor in both models of experimental NASH. A previous study by our group showed that P2X7 receptor was crucial for causing Kupffer cell activation and inflammation following release of ATP from necrosed hepatocytes in CCl_4-mediated early steatohepatitic injury (8). In the

www.manaraa.com

present study we show that metabolic oxidative stress which is associated with NASH caused an up-regulation of P2X7 receptors (Fig.3.2). Metabolic oxidative stress also, mainly characterized by oxidatively modified proteins has been known to induce chaperone-mediated autophagy, increased substrate translocation by Hsc 70 towards the lysosomal membrane and increased LAMP2A levels (82). Further, P2X7 receptors have been associated with autophagy, disruption of normal lysosomal functions and release of autophagolysosomes to the extracellular matrix in the microglial cells, causing an increase in inflammation (81). Our present study shows that there was a significant down regulation of both early and late autophagy proteins including LAMP2A in P2X7 receptor gene deleted mice. P2X7 receptor deleted mice also showed decreased release of IL-1 β, IFN-γ and HMGB-1(damage associated molecular pattern that contributes to inflammation(83), observations that were dependent on significantly less cleaved caspase-1 protein levels, implying the possible involvement of P2X7 receptors. This study however falls short on exploring the exact molecular mechanism of P2X7 receptor involvement, and to have a clear answer whether it is the increased calcium ion-mediated change in lysosomal pH, lysosomal functional impairment or expulsion of the lysophagosome to the extracellular matrix that caused an increase in the inflammation. The present study also establishes a direct correlation between the decreased numbers of LAMP2A-lysosomal membrane associations, reduced inflammation and decreased NASH pathophysiology in P2X7 receptor gene deleted mice (Figs. 3.6, 3.7 and 3.8). These observations assume significance since LAMP2A levels and its association with the lysosomal membrane is an important step for chaperone mediated autophagy, which occurs late in the autophagy process. Our studies showed a depletion of LC3B, a autophagosome protein in NASH pathophysiology

www.manaraa.com

(Fig 3.4E), but not in LAMP2A, which is contrary to a study by Fortunato et al that showed decreased LAMP2A levels linked to decreased fusion of the autophagosome with the lysosome, resulting in necrotic cell death and inflammation (84). This may be due to a different mechanism of a dysfunctional lysosomal function when compared to our model that primarily evidenced LC3B depletion. Recent studies also link P2X7 receptor to a dysfunctional lysosome and autophagy protein LC3B (81, 85). In both cases the fate of the cell and its link to immune activation remains a dysregulated lysosomal compartment and is regulated by ATP-binding P2X7 receptors in the latter study (85). Interestingly our study indicates a significantly decreased LC3B protein levels in DIO+BDCM and MCD diet fed livers as compared to DIO and MCS diet fed groups, while absence of P2X7 receptor gene elevates the LC3B protein levels (Figs. 3.4C,D and E). This result is important because it has been shown that depletion of autophagic protein LC3B enhances caspase-1 activation and increase in inflammatory microenvironment (85). We have also found higher caspase-1 activation and levels of inflammatory indicators IL-1β, TNF-α, IFN-γ and HMGB-1 in DIO+BDCM and MCD diet fed groups while a decrease in these indicators was seen in P2X7 receptor gene deleted mice (Fig. 3.7). Taken together, the present study provides first evidence that P2X7 receptor deletion results in down regulation of autophagy related proteins, inflammation and disease pathophysiology in NASH (Figs. 3.7 and 3.8). Having significant evidence that P2X7 receptor is a key regulator of autophagy in NASH, it may be presumed that targeting the P2X7 receptor or the autophagy process in NASH can emerge as a good therapeutic option for the treatment of NASH. It is increasingly becoming clear that there are series of studies that promote autophagy as a beneficial mechanism in NASH and equal number of studies that conclude autophagy is central in causing NASH,

www.manaraa.com

the present study only predicts the role of P2X7 receptor-mediated defective autophagy as a cause for inflammation in NASH(86). Translational impact of this study will be enhanced with more mechanistic studies in future involving cell specific P2X7 receptor knock downs and functional roles of different autophagy proteins in the presence or absence of the P2X7 receptor.

Acknowledgements: The authors gratefully acknowledge the technical services of Benny Davidson at the IRF, University of South Carolina, School of Medicine, Jeoffrey Hurlburt, and Ralph Wilson at NIEHS. We thank Dr. Anindya Chanda for the internal review of this manuscript. We also thank Dr. James Carson, Department of Exercise Science and the Instrumentation resource facility (IRF) at the University of South Carolina, School of Medicine for equipment usage and consulting services.

www.manaraa.com

CHAPTER 4

NADPH OXIDASE-DERIVED PEROXYNITRITE DRIVES INFLAMMATION IN MICE AND HUMAN NONALCOHOLIC STEATOHEPATITIS VIA TLR4-LIPID RAFT RECRUITMENT

Das S, Alhasson F, Dattaroy D, Pourhoseini S, Seth RK, Nagarkatti M, Nagarkatti PS, Michelotti GA, Diehl AM, Kalyanaraman B, Chatterjee S. *American Journal of Pathology*. 2015 Jul; 185(7):1944-57.

Reprinted here with permission of publisher.

www.manaraa.com

Running title: Phenylboronic acid attenuates NASH

Key words: Phenylboronic acid, ICAM-1, E-selectin, IL-1β, CD68, Stellate cell

A**uthor for correspondence:**

*Dr. Saurabh Chatterjee, Ph.D. [1]Environmental Health and Disease Laboratory, Department of Environmental Health Sciences, University of South Carolina, Columbia 29208 USA. Email: schatt@mailbox.sc.edu; Tel: 803-777-8120; Fax: 803-777-3391.

List of Abbreviations: NADPH oxidase, NOX, MD2, FeTPPS, FBA, NFkB, IL-1β, MCP-1, CD68, α-SMA

Grant Support: This work has been supported by NIH Pathway to Independence Award, R00ES019875 to Saurabh Chatterjee, R01DK053792 to Anna Mae Diehl, P01AT003961, P20GM103641, R01AT006888, R01ES019313, R01MH094755 and VA Merit Award BX001357 to Mitzi Nagarkatti and Prakash S. Nagarkatti.

Conflict of Interest: The authors declare that there is no conflict of interest.

Abstract:

The molecular events that link NADPH oxidase and induction of toll-like receptor 4 (TLR4) recruitment to hepatic lipid rafts in nonalcoholic steatohepatitis (NASH) have been unclear. We hypothesize that in the liver, NADPH oxidase activation is a key event to TLR4 recruitment to lipid rafts, that in turn upregulates NFkB translocation to the nucleus and subsequent DNA binding, leading to NASH progression. Results from confocal microscopy showed that livers from murine models of NASH and humans had NADPH

www.manaraa.com

oxidase activation. NADPH oxidase activation led to the formation of highly reactive peroxynitrite as shown by 3-nitrotyrosine formation in diseased livers. Expression and recruitment of TLR4 into the lipid rafts were observed to be significantly higher in rodent and human NASH. The described phenomenon was NADPH oxidase, p47phox and peroxynitrite dependent, since livers from p47phox deficient mice, or mice treated with peroxynitrite decomposition catalyst FeTPPS, peroxynitrite-scavenger phenyl boronic acid (FBA), had markedly lower TLR4 recruitment into lipid rafts. Mechanistically peroxynitrite-induced TLR4 recruitment was linked to increase in IL-1β, sinusoidal injury, and Kupffer cell activation while blocking peroxynitrite attenuated NASH symptoms. In conclusion, the results strongly suggest that NADPH oxidase-mediated peroxynitrite drove TLR-4 recruitment into hepatic lipid rafts and inflammation while use of peroxynitrite scavenger FBA in vivo, a novel synthetic molecule having high reactivity with peroxynitrite, attenuated inflammatory pathogenesis in NASH.

4.1 INTRODUCTION

Nonalcoholic steatohepatitis (NASH) has been studied extensively in preclinical models and humans. NASH manifestations range from an early sinusoidal endothelial dysfunction, inflammation followed by a defective tissue repair resulting in fibrosis(37-42). Inefficient tissue perfusion in the fatty tissue mostly associated with fatty liver and subsequent NASH progression can result in recruitment of other cell types including Kupffer cells, sinusoidal endothelial cells and circulating lymphocytes, making it a perfect microenvironment for forming an inflammatory foci (43).

www.manaraa.com

Recent research reports identify an emerging role of toll like receptor 4 in NASH pathogenesis(44, 45). Several endogenous mediators like gut derived endotoxin and nuclear factor HMGB-1 has been implicated to activate TLR4 signaling leading to NASH severity(46, 47). After its discovery in the 1980s, toll like receptor signaling has been in the forefront of innate immune signaling and disease pathophysiology (48). TLR4, one of the many TLRs discovered since then plays a pivotal role in cytokine release along with its adaptor molecules myeloid differentiation primary response gene 88 (MyD88) and TIR-domain-containing adapter-inducing interferon-β **(**TRIF). MyD88 was found to work as an adaptor for inflammatory signaling pathways downstream of members of the TLR and interleukin-1 (IL-1) receptor families(49). Activation of the TLR4 pathway leads to a variety of functional outputs, including the activation of nuclear factor-kappa B (NFκB), mitogen-activated protein kinases, and activator protein 1, making MyD88 a central node of inflammatory pathways(49) . Lipopolysaccharide of gram negative bacterial cell walls is a strong ligand for TLR4 on the cell membrane. MD-2 is associated with Toll-like receptor 4 (TLR4) on the cell surface and enables TLR4 to respond to LPS (50). Deficiency of MyD88 or TLR4 in mice have attenuated the development of the disease(51). Though oxidative stress via NADPH oxidase has been shown to drive NASH pathogenesis especially fibrogenesis and Kupffer cell activation, there is no direct evidence of a single mechanism where a specific oxidative species can drive the recruitment of TLR4-mediated inflammation in NASH(13, 24, 52). In this study we therefore aim to identify a single intracellular reactive nitrative species that may play a distinct role in developing the inflammatory pathogenesis in NASH via TLR4 recruitment to hepatic lipid rafts, an early yet distinct process in TLR4 activation and downstream signaling. One of the common

www.manaraa.com

sources of generation of toxic superoxide radicals may be NADPH oxidase isoforms which can be found in both phagocytic and non-phagocytic cells(53). Liver has been shown to be a rich source of various NOX isoforms, being present in phagocytic Kupffer cells, stellate cells and sinusoidal endothelial cells (39, 52, 54). Out of the various NOX isoforms NOX2 is primarily present in Kupffer cells and stellate cells whereas NOX1 and NOX4 have been found in other liver cell types(52). NOX2 is comprised of several subunits which includes the gp91, p22 (membrane subunits), p67, p47 and Rac1 (cytosolic subunits)(53). Upon receipt of proper signals, the cytosolic subunits align with their membrane counterparts to form an active NADPH oxidase complex which produce superoxide radicals to be released in the extracellular space(53). Several laboratories including us have shown the involvement of NOX2 in NASH development(13, 24, 54). NOX2 stimulation by high leptin results in peroxynitrite generation thus causing Kupffer cell activation in NASH(13). NOX2 has also been shown to facilitate recruitment of toll-like receptor 4 to lipid rafts and to help in receptor dimerization and its association with MD2 in several inflammatory diseases(55). Since there is no evidence of the molecular events that follow NADPH oxidase activation concerning the type of reactive species formation and the mechanisms that link TLR4 activation, we investigated the role of peroxynitrite in TLR4 activation in NASH. Peroxynitrite has been shown to cause cellular senescence and alter immunogenicity of proteins while many functional roles of the peroxynitrite species in protein nitration in acute and chronic liver diseases has been reviewed(53, 55, 87, 88) . Blocking peroxynitrite in vivo with newer and more specific scavengers may provide novel therapeutic strategies for NASH complications.

www.manaraa.com

In this study we aimed to investigate the molecular mechanisms of TLR4 induction by NADPH oxidase, the role of peroxynitrite followed by its effect on sinusoidal injury, inflammation, Kupffer cell activation and stellate cell proliferation, all very significant events in NASH progression from steatosis, using a high fat diet-induced obesity model where hepatotoxin bromodichloromethane was administered to generate oxidative stress, a second hit to cause steatohepatitic lesions(69). A second widely used rodent model, that is based on feeding methyl-chloine deficient diet was also used. Human NASH livers and healthy human control livers were used to corroborate the results from the murine model. We used a decomposition catalyst and a scavenger of peroxynitrite to prove the involvement of peroxynitrite(13, 53). The results of the study which uses transgenic mice and pharmacological approach, show for the first time a molecular basis of NADPH oxidase-mediated peroxynitrite-driven TLR4 activation in causing sinusoidal injury, inflammation and stellate cell proliferation in NASH.

4.2 MATERIALS AND METHODS

Obese mice:

Pathogen-free, 6 weeks old, custom high fat diet –fed adult male mice with C57BL/6J background (the Jackson Laboratory, Bar Harbor, Maine) were used as model for diet induced obesity (DIO). The animals were fed with high-fat diet (60% kcal) from 6 weeks to 16 weeks. After completion of 16 weeks, all experiments were conducted. Mice which contained disrupted p47phox gene(B6.129S2-Ncf1tm1shl N14, from Taconic, Cranbury, NJ) (annotated as **p47phox KO**), and mice with disrupted TLR4 gene (B6.B10ScN-Tlr4lps-del/JthJ, from the Jackson Laboratory, Bar Harbor, Maine) (annotated as **TLR4 KO**) were fed with high fat diet and treated identically to DIO mice. The mice were housed

www.manaraa.com

one per cage in a temperature-controlled room at 23-24 °C with a 12-h:12-h light/dark cycle with *ad libitum* access to food and water. All animals had been treated in strict accordance with the NIH guideline for Humane Care and Use of Laboratory Animals and local IACUC standards. All experiments were approved by the institutional review board at NIEHS, Duke University and the University of South Carolina.

Induction of liver injury in obese mice (Toxin Model):

Bromodichloromethane (BDCM) (1.0mM/kg, diluted in corn oil) was administered through intraperitoneal injection in 16 weeks old high fat-fed wildtype (annotated as **DIO+BDCM**) or specific gene knockout mice. Two doses of BDCM were administered per week for four weeks. DIO mice were injected with corn oil (diluent of BDCM) to use as control (annotated as **DIO**). After the treatments were complete for all mouse groups, the mice were sacrificed for liver tissue for the further experiments.

Administration of apocynin/FeTPPS/FBA in obese mice (Toxin Model)

A group of DIO mice was injected with apocynin, an NADPH oxidase inhibitor at a dose of 10mg/Kg body weight (group annotated as **Apo**). A second group of DIO mice was injected with a ferric porphyrin complex that is a decomposition catalyst of peroxynitrite, at a dose of 30mg/Kg of body weight (group annotated as **FeTPPS)**. A third group of DIO mice was injected with phenyl boronic acid, a peroxynitrite scavenger, at a dose of 50mg/Kg body weight (group annotated as **FBA**). All these injections were given1 hour prior to each BDCM injection over a period of 4 weeks.

Human tissues:

Human liver tissues both from NASH and corresponding healthy individuals were obtained from NIH repository at University of Minnesota and University of Pittsburg.

www.manaraa.com

Histopathology:

Liver sections were collected from each animal and fixed in 10% neutral buffer formalin. These formalin-fixed, paraffin embedded tissues were cut in 5μm thick sections. These sections were deparaffinized (standard protocol) and stained with Picro-Sirius red and were observed using 20x objective of light microscope. Stained liver sections were examined for stages of fibrosis using the criteria of the NIH Non Alcoholic Steatohepatitis Clinical Research Network (NIH NASH CRN) scoring system. Stages of fibrosis were determined as 1A: mild, 1C: Portal, 2: Periportal fibrosis and 3: Bridging fibrosis. Briefly, since zone 3 perisinusoidal/pericellular fibrosis develops first and is followed by portal fibrosis, we followed the fibrosis stages as described originally by Kleiner et al(89, 90). Kleiner et al. modified the fibrosis staging in the Brunt system by dividing fibrosis scores for stage 1 into delicate (1a), dense perisinusoidal fibrosis (1b), and non-bridging portal-only fibrosis (1c). Stage 2 accounts for perisinusoidal and portal/periportal fibrosis(90). The scoring pattern was found to be consistent with portal fibrosis beginning early in the disease process and playing an important role in connection with the development of portal–central fibrous bridging which is likely found in the most developed cases of fibrosis.

Immuno-fluorescence microscopy:

Formalin-fixed, paraffin embedded tissues were cut in 5μm thick sections. Each section was subjected to deparaffinization and immunostaining using standard protocol. The primary antibodies 1) anti-gp91phox, 2) anti-p47phox, 3) anti-TLR4, and 4) anti-flotillin were purchased from Santa Cruz Biotechnologies and Abcam and used at recommended dilutions. Species-specific anti-IgG secondary antibodies conjugated with Alexa Fluor 488, Alexa Fluor 633, and Alexa Fluor 568 (Invitrogen, California, USA) were used against the

www.manaraa.com

appropriate primary antibodies. The sections were mounted in a ProLong gold antifade reagent with DAPI. Images were taken under 20X/60Xoil objectives using Olympus BX73 microscope. Confocal laser scanning microscopy was performed for selected images followed by colocalization analysis using LSM software.

Immunohistochemistry:

Formalin-fixed, paraffin embedded tissues were cut in 5μm thick sections. Each section was subjected to deparaffinization and immunostaining using standard protocol. The primary antibodies were 1) anti-IL-1β 2) anti-MCP-1 3) anti-CD68, 4) anti-α-SMA. Primary antibodies were purchased from Abcam (Cambridge, MA) and used in recommended dilutions.

Vectastain Elite ABC kit (Vector Laboratories, Burlingame, CA) was used to perform antigen-specific immunohistochemistry following manufacturer's protocols. 3, 3' Diaminobenzidine (Sigma-Aldrich) was used as a chromogenic substrate. Tissue sections were counter-stained by Mayer's hematoxylin (Sigma-Aldrich).Sections were mounted in Simpo mount (GBI Laboratories, Mukilteo, WA) and observed under a 20X objective. Morphometric analysis was done using CellSens Software from Olympus America.

NF-kB transcription factor binding assay:

Nuclear fraction of each liver sample was isolated following manufacturer's standard protocol (Five photon Biochemicals). DNA binding activity of the transcription factor NF-kB present in those nuclear extracts was detected by a 96 well enzyme-linked immunosorbent assay (ELISA) method (Abcam's NF-kB p65 Transcription Factor Assay Kit) following manufacturer's standard protocol.

www.manaraa.com

Statistical Analyses:

All in vivo experiments were repeated three times with 3 mice per group (N = 3; data from each group of three mice was pooled). The statistical analysis was carried out by analysis of variance (ANOVA) followed by a post hoc test. Quantitative data from Western blots, as depicted by the relative intensity of the bands, were analyzed by performing a Student's t test. $P<0.01$ and $P<0.05$ where applicable, was considered statistically significant.

4.3 RESULTS

NASH pathogenesis is associated with NADPH oxidase activation-induced oxidative stress primarily mediated by peroxynitrite. To study the involvement of NADPH oxidase and corresponding oxidative stress in rodent and human livers with NASH, experiments were performed to prove the NADPH oxidase activation that is characterized by p47phox association with the membrane subunit gp91phox by immunostaining and immunofluroscence microscopy. Results showed that DIO+BDCM group had a significantly increased colocalization of p47phox and gp91phox in NASH livers as compared to DIO only group (Fig.4.1A,) (Fig.4.1C) ($P<0.01$). Higher magnification image of liver sections showed that colocalization was evident primarily in sinusoidal cells and occasional hepatocytes (Fig.4.1A). Gp91phox and p47 phox colocalizations were significantly increased in MCD model and human NASH livers (Suppl. fig. 4.1A and Suppl fig. 4.1C) ($P<0.05$). Increased NADPH oxidase activation was associated with increased oxidative stress as evident from the increased tyrosyl radical formation (3-nitrotyrosine immunoreactivity). Results showed that DIO+BDCM group livers had significantly increased immunoreactivity to 3-nitrotyrosine as compared to DIO only group (Fig. 4.1B)($P<0.01$). Mice that had deleted p47phox gene (p47phox KO) or

www.manaraa.com

were treated with NADPH oxidase nonspecific inhibitor apocynin inhibitor or peroxynitrite decomposition catalyst FeTPPS or peroxynitrite scavenger FBA showed significantly decreased 3-nitrotyrosine immunoreactivity as compared to DIO+BDCM group (Fig. 4.1B and Fig. 4.1D) ($P<0.01$). Livers from MCD diet-fed mice and Human NASH livers showed significantly increased immunoreactivity to 3-nitrotyrosine, an index of oxidative stress mediated tyrosyl radical formation (Suppl. fig. 4.1B and D) ($P<0.05$). The results suggested that NASH pathogenesis is associated with NADPH oxidase activation primarily via NOX2 mediation and p47phox translocation followed by peroxynitrite formation and tyrosyl radical formation. FBA scavenging of peroxynitrite also confirmed that peroxynitrite was responsible for the tyrosine nitration instead of myeloperoxidase which is also present in the injured liver.

NADPH oxidase activation mediated peroxynitrite formation and subsequent oxidative stress drives TLR4 recruitment to hepatic lipid rafts. The role of TLR4 in NASH pathogenesis has been reported lately(91, 92). However the mechanisms that drive TLR4 recruitment and subsequent signaling in NASH have been unclear. One of the primary events of TLR activation is its recruitment to the hepatic lipid rafts following which the assembly of activation complex and ligand binding occur(93, 94). Though recent studies have focused on TLR4 activation processes primarily by HMGB1, Xbox-1 or bacteria from the gut, no studies were featured that show the mechanisms that drive TLR4 to the membrane rafts(47, 95, 96). To prove that NADPH oxidase mediated peroxynitrite drives TLR4 recruitment to hepatic lipid rafts, experiments were performed in mice and

www.manaraa.com

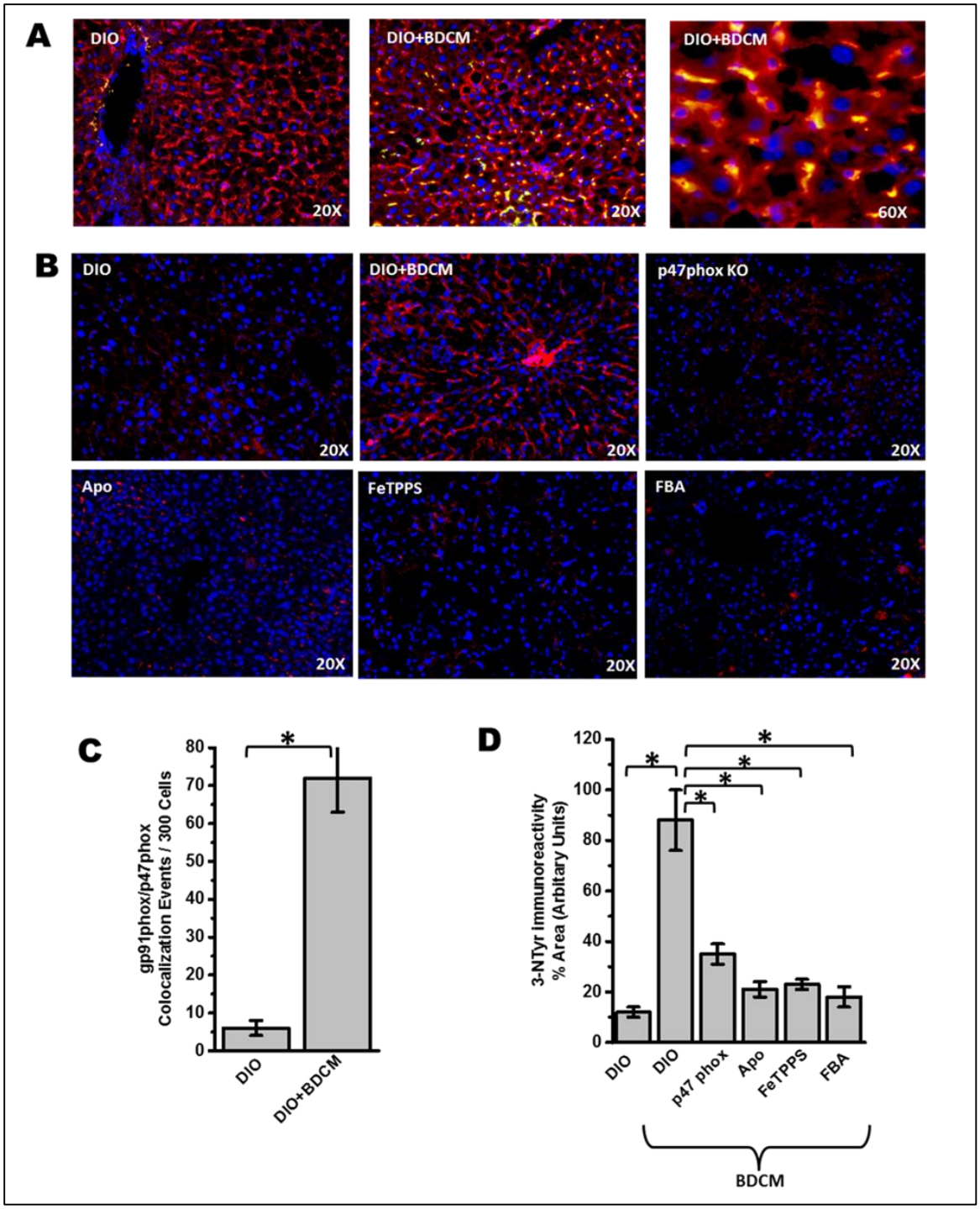

Figure 4.1 NADPH oxidase activation and peroxynitrite-mediated tyrosine nitration.
A: 20X magnification representative images of 5µm thick immunostained liver sections, imaged using immunofluorescence microscope; secondary antibodies used: alexafluor568 (red) against α-gp91phox primary antibody, alexafluor488 (green) against α-p47phox primary antibody; nuclear stain (blue) is due to prolong gold antifade reagent with DAPI; yellow spots/patches indicate alignment of cytoplasmic subunit of NADPH oxidase,

www.manaraa.com

p47phox (red), with membrane subunit gp91phox (green); samples from: high fat-fed wild-type mouse , (DIO); high fat-fed wild-type mouse exposed to BDCM (DIO+BDCM). **B**: 20X magnification representative images of 5µm thick immunostained liver sections, imaged using immunofluorescence microscope; secondary antibody used: alexafluor633 (red) against α-3-nitrotyrosine primary antibody; nuclear stain (blue) is due to prolong gold antifade reagent with DAPI; samples from: high fat-fed wild-type mouse (DIO); high fat-fed wild-type mouse exposed to BDCM (DIO+BDCM); high fat-fed p47phox gene knockout mouse exposed to BDCM (p47phox KO); high fat-fed wild-type mouse exposed to BDCM and injected with NADPH oxidase inhibitor apocynin (Apo); high fat-fed wild-type mouse exposed to BDCM and injected with peroxynitrite decomposition catalyst, a ferric porphyrin complex (FeTPPS), high fat-fed wild-type mouse exposed to BDCM and injected with peroxynitrite decomposition catalyst phenyl boronic acid (FBA). **C**: Graph depicts morphometry performed on three independent fields for each sample including representative images in **A** captured under 20X magnification lens for gp91phox/p47phox co-localization events per 300 cells. **D**: Graph depicts morphometry performed on three independent fields for each sample including representative images in **B** captured under 20X magnification lens for percent area showing positive immunoreactivity of 3-nitrotyrosine calculated in arbitrary units. $^{**}P < 0.01$.

human livers. Results showed that DIO+BDCM group livers had significant increase in TLR4-flotillin (a lipid raft protein) colocalization events as shown by immunofluorescence microscopy (6 fold increase) as compared to DIO only group (Fig. 4.2A and 4.2B)($P<0.01$). Confocal laser scanning imaging (Fig. 4.2C) and analysis (Fig. 4.2D) show colocalization of TLR4 and flotillin in sinusoidal cells of NASH livers (Fig. 4.2C). P47phox KO mice livers or mice that were treated with NADPH oxidase nonspecific inhibitor Apocynin or peroxynitrite decomposition catalyst FeTPPS or peroxynitrite scavenger FBA had significantly decreased colocalization events of TLR4 and Flotillin (Fig.4.2A and 4.2B; Suppl. Fig. 4.2A; 20x images). Livers from MCD diet-fed mice or human NASH livers showed a significant increase in TLR4-Flotillin co-localization events as compared to respective controls (Suppl fig. 4.2B)(Suppl fig. 4.2D)($P<0.05$). The results suggest that NADPH oxidase activation and subsequent peroxynitrite-mediated oxidative stress drives TLR4 recruitment in hepatic lipid rafts, a significant early event of TLR4 signaling and NASH inflammatory pathogenesis.

www.manaraa.com

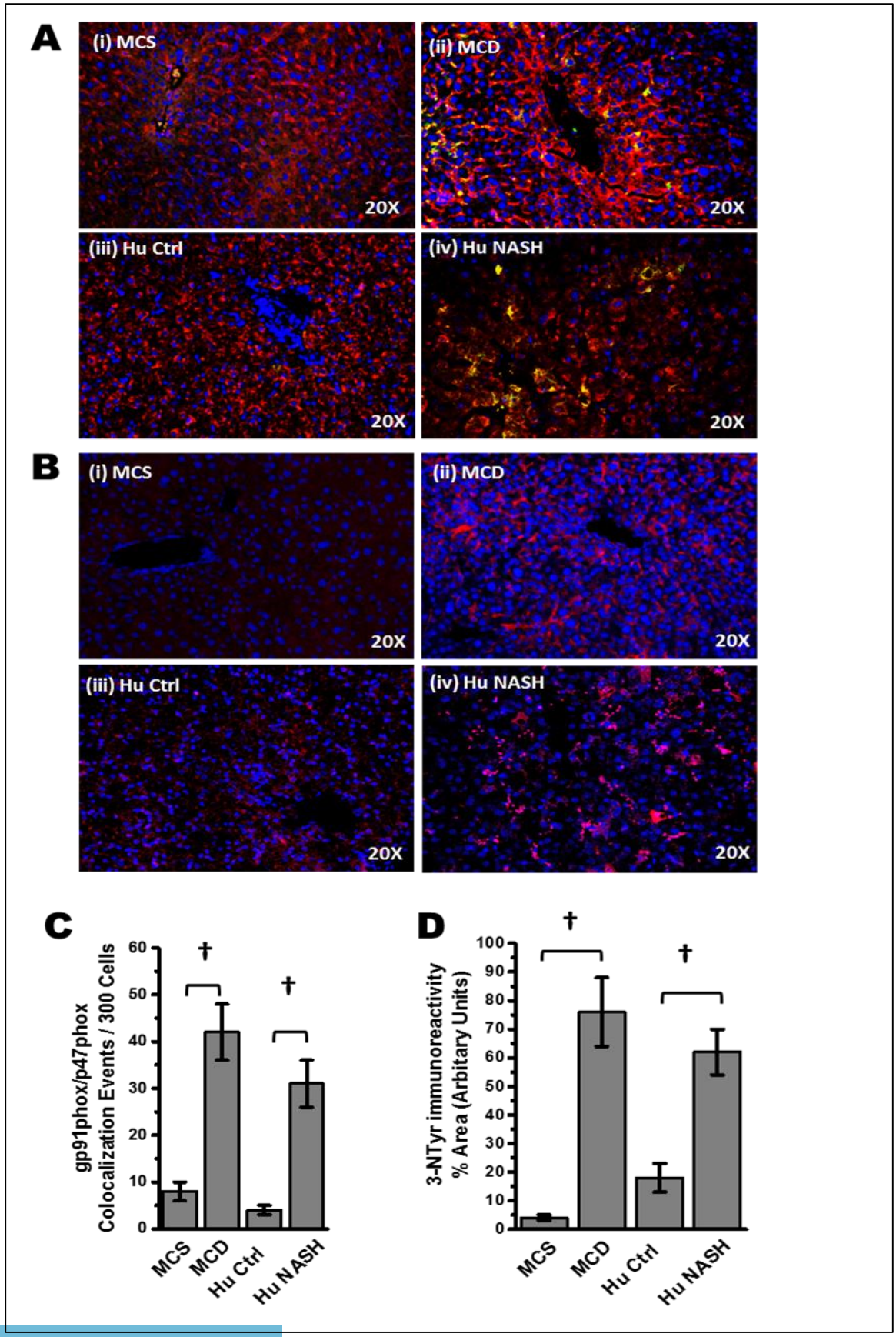

www.manaraa.com

Supplementary Figure 4.1 Immunofluorescence images for NADPH oxidase activation and 3-NT formation in MCD rodent model and human samples.
4.1A: 20X magnification representative images of 5µm thick immunostained liver sections, imaged using immunofluorescence microscope; secondary antibodies used: alexafluor568 (red) against α-gp91phox primary antibody, alexafluor488 (green) against α-p47phox primary antibody; nuclear stain (blue) is due to prolong gold antifade reagent with DAPI; yellow spots/patches indicate alignment of cytoplasmic subunit of NADPH oxidase, p47phox (red), with membrane subunit gp91phox (green); samples from: (i) methionine and choline-sufficient diet-fed mouse, annotated as MCS, (ii) methionine and choline-deficient diet-fed mouse, annotated as MCD, (iii) healthy human control, annotated as Hu Ctrl, (iv) human NASH patient, annotated as Hu NASH
4.1B: 20X magnification representative images of 5µm thick immunostained liver sections, imaged using immunofluorescence microscope; secondary antibody used: alexafluor633 (red) against α-3-nitrotyrosine primary antibody; nuclear stain (blue) is due to prolong gold antifade reagent with DAPI; samples from: (i) methionine and choline-sufficient diet-fed mouse, annotated as MCS, (ii) methionine and choline-deficient diet-fed mouse, annotated as MCD, (iii) healthy human control, annotated as Hu Ctrl, (iv) human NASH patient, annotated as Hu NASH
4.1C: graph depicting morphometry done on 3 independent fields for each sample including representative images in suppl. fig.1A captured under 20X magnification lens for gp91phox/p47phox co-localization events per 300 cells
4.1D: graph depicting morphometry done on 3 independent fields for each sample including representative images in suppl. fig.1B captured under 20X magnification lens for per cent area showing positive immunoreactivity of 3-nitrotyrosine calculated in arbitrary units. *$P<0.01$; $^{\dagger}P<0.05$

NFkB activation and DNA binding in NASH livers require NADPH oxidase mediated peroxynitrite upon TLR4 recruitment in lipid rafts. One of the key events following TLR4 recruitment from non-rafts to lipid enriched membrane rafts is the down-stream signaling leading to NFkB activation, translocation to the nucleus and subsequent DNA binding(97, 98). Following our observations that NADPH oxidase activation and peroxynitrite generation drives TLR4 recruitment to hepatic lipid rafts we probed the involvement of NADPH oxidase mediated peroxynitrite in causing NFkB activation. Results showed that DIO+BDCM group had significant increase in NFkB activation and binding to DNA as compared to DIO group alone (Fig. 4.3A)($P<0.05$). Use of p47phox KO mice or administration of NADPH oxidase nonspecific inhibitor Apocynin or

www.manaraa.com

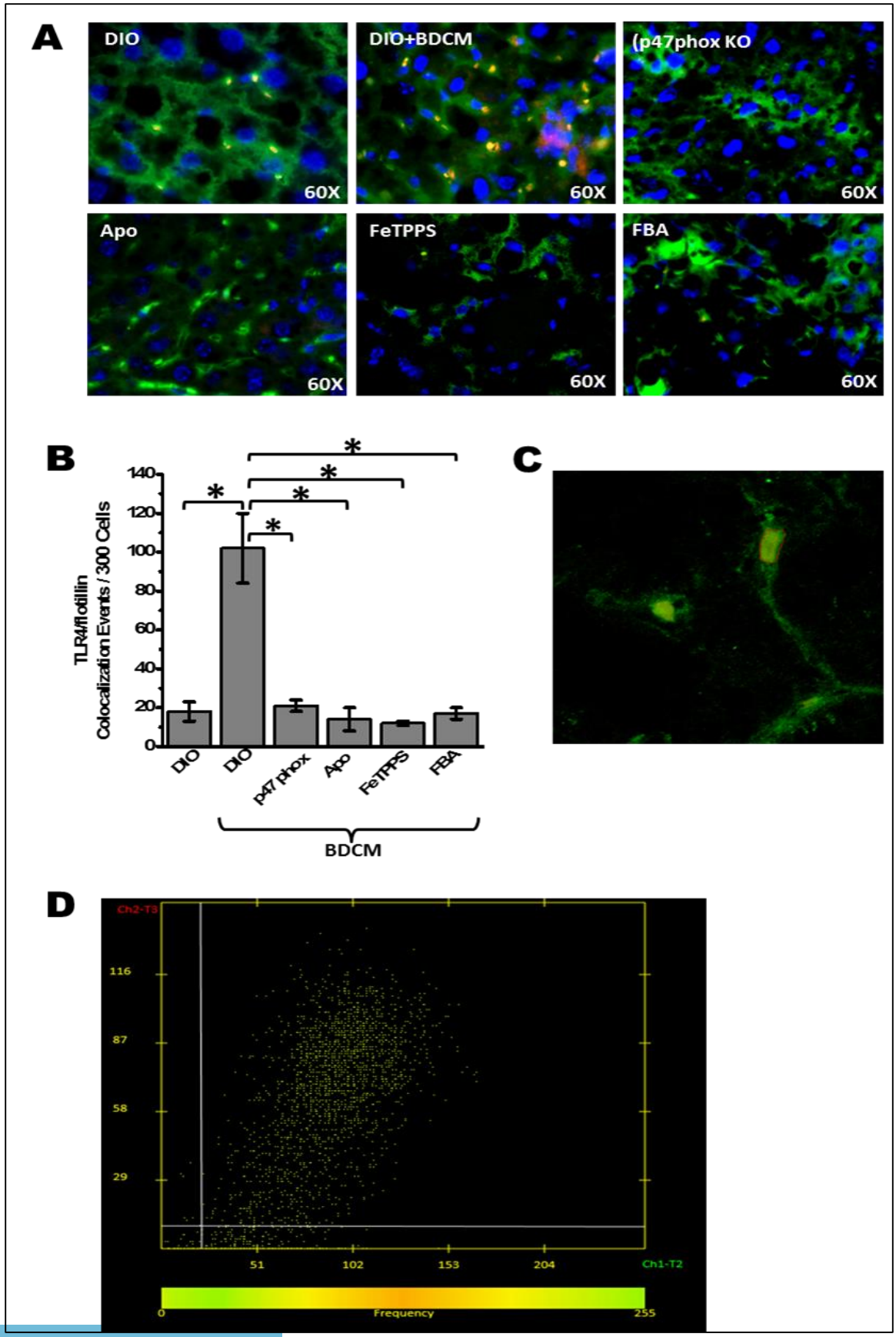

www.manaraa.com

Figure 4.2 NADPH oxidase and peroxynitrite – driven TLR4 recruitment to lipid rafts in hepatic cell-membranes
A: 60X magnification representative images of 5µm thick immunostained liver sections, imaged using immunofluorescence microscope; secondary antibodies used: alexafluor633 (red) against α-TLR4 primary antibody, alexafluor488 (green) against α-flotillin primary antibody; nuclear stain (blue) is due to prolong gold antifade reagent with DAPI; yellow spots/patches indicate alignment of TLR4 (red), with lipid raft protein flotillin (green). Samples from: high fat-fed wild-type mouse (DIO); high fat-fed wild-type mouse exposed to BDCM (DIO+BDCM); high fat-fed p47phox gene knockout mouse exposed to BDCM (p47phox KO); high fat-fed wild-type mouse exposed to BDCM and injected with NADPH oxidase inhibitor apocynin (Apo); high fat-fed wild-type mouse exposed to BDCM and injected with peroxynitrite decomposition catalyst (FeTPPS), high fat-fed wild-type mouse exposed to BDCM and injected with peroxynitrite scavenger phenyl boronic acid (FBA). **B**: Graph depicts morphometry performed on three independent fields for each sample including representative images in **A** captured using 60X magnification lens for TLR4/flotillin co-localization events per 300 cells. $^{**}P < 0.01$. **C:** Confocal laser scanning image of TLR4 and flotillin colocalization in the membranes of liver cells following NASH. **D:** Colocalization analysis using LSM software.

peroxynitrite decomposition catalyst FeTPPS or peroxynitrite scavenger FBA decreased the NFkB activation and DNA binding significantly as compared to DIO+BDCM group (Fig. 4.3A)(P<0,05). Livers from MCD dietfed mice or human NASH livers had significantly increased NFkB activation and DNA binding as compared to their respective controls (Fig. 4.3B)(P<0.05). The results suggested that upon TLR4 recruitment to hepatic lipid rafts following NADPH oxidase activation, downstream signaling is initiated that led to NFkB activation and DNA binding, a significant step towards TLR4-mediated inflammatory cytokine release and innate immune activation.

NADPH oxidase activation and formation of peroxynitrite causes sinusoidal injury primarily through their role in TLR4 recruitment. One of the primary events in NASH pathogenesis is sinusoidal injury often ascribed to insufficient perfusion and formation of inflammatory foci(42, 43, 99). Recent evidences from our laboratory and others have shown that sinusoidal injury marked by increases in ICAM-1 and E-Selectin in the liver sinusoidal endothelial cells, stellate cells and Kupffer cells form an early basis

www.manaraa.com

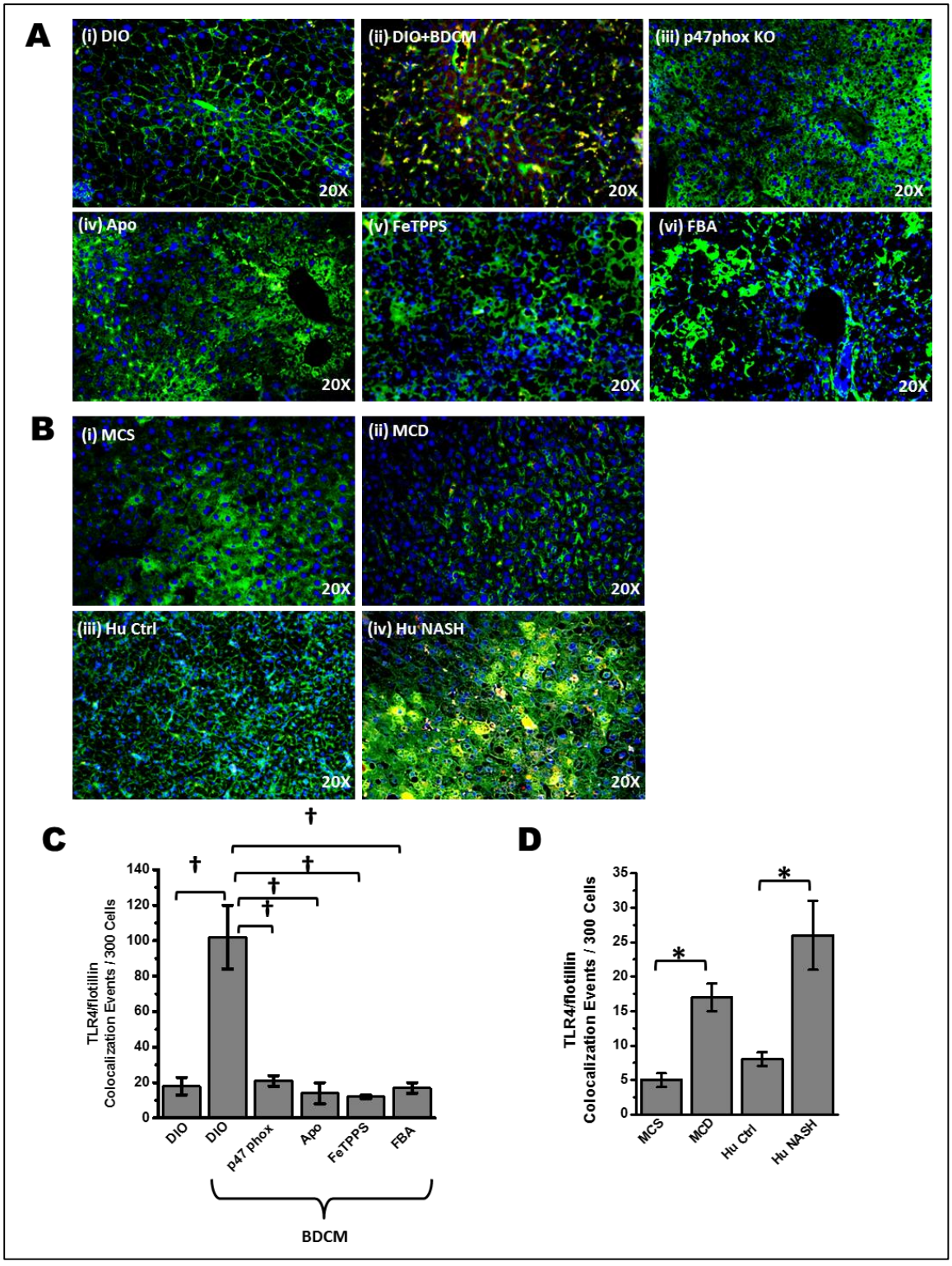

Supplementary Figure 4.2 NADPH oxidase and peroxynitrite – driven TLR4 recruitment to lipid rafts in hepatic cell-membranes including MCD rodent model and human samples

www.manaraa.com

4.2A: 20X magnification representative images of 5µm thick immunostained liver sections, imaged using immunofluorescence microscope; secondary antibodies used: alexafluor633 (red) against α-TLR4 primary antibody, alexafluor488 (green) against α-flotillin primary antibody; nuclear stain (blue) is due to prolong gold antifade reagent with DAPI; yellow spots/patches indicate alignment of TLR4 (red), with lipid raft protein flotillin (green); samples from: (i) high fat-fed wildtype mouse, annotated as DIO; (ii) high fat-fed wildtype mouse exposed to BDCM, annotated as DIO+BDCM; (iii) high fat-fed p47phox gene knockout mouse exposed to BDCM, annotated as p47phox KO; (iv) high fat-fed wildtype mouse exposed to BDCM and injected with NADPH oxidase inhibitor, apocynin, annotated as Apo; (v) high fat-fed wildtype mouse exposed to BDCM and injected with peroxynitrite decomposition catalyst, a ferric porphyrin complex, annotated as FeTPPS, (vi) high fat-fed wildtype mouse exposed to BDCM and injected with peroxynitrite scavenger, phenyl boronic acid, annotated as FBA
4.2B: 20X magnification representative images of 5µm thick immunostained liver sections, imaged using immunofluorescence microscope; secondary antibodies used: alexafluor633 (red) against α-TLR4 primary antibody, alexafluor488 (green) against α-flotillin primary antibody; nuclear stain (blue) is due to prolong gold antifade reagent with DAPI; yellow spots/patches indicate alignment of TLR4 (red), with lipid raft protein flotillin (green); samples from: (i) methionine and choline-sufficient diet-fed mouse, annotated as MCS, (ii) methionine and choline-deficient diet-fed mouse, annotated as MCD, (iii) healthy human control, annotated as Hu Ctrl, (iv) human NASH patient, annotated as Hu NASH
4.2C: graph depicting morphometry done on 3 independent fields for each sample including representative images in suppl. fig.2A captured under 20X magnification lens for TLR4/flotillin co-localization events per 300 cells
4.2D: graph depicting morphometry done on 3 independent fields for each sample including representative images in suppl. fig.2B captured under 20X magnification lens for TLR4/flotillin co-localization events per 300 cells
*P<0.01; † P<0.05

for inflammatory pathogenesis in NASH. Following such observations it was essential that the role of NADPH oxidase mediated formation of peroxynitrite and TLR4 recruitment into lipid rafts be shown to initiate sinusoidal injury in the NASH liver. Results showed that DIO+BDCM group livers had a significant increase in immunoreactivity to ICAM-1 and E-selectin as compared to DIO only group (Fig. 4.4A, Fig. 4.4C)(4B, Fig. 4.4D)($P<0.01$). Use of p47phox KO mice or administration of Apocynin significantly decreased the immunoreactivity of ICAM-1 and E-selectin as compared to DIO+BDCM group, showing the involvement of NADPH oxidase activation (Fig. 4.4A , 4.4B and 4.4C)($P<0.01$). Use

www.manaraa.com

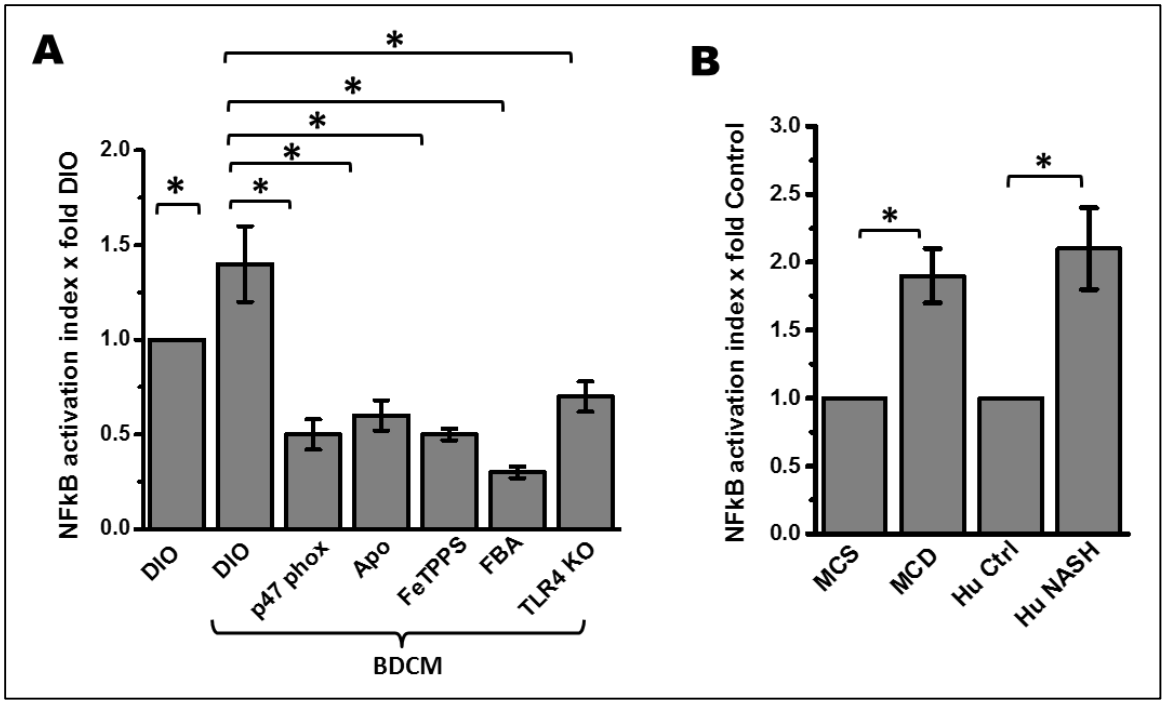

Figure 4.3 NADPH oxidase and peroxynitrite–driven NFkB translocation and DNA-binding via TLR4 signaling. **A**: Graph depicts results of NFkB activation assay in murine samples of toxin-induced NASH model; NFkB activation index (assessed from nuclear translocation and DNA-binding of p65 subunit) is normalized against DIO sample. **B**: Graph depicts results of NFkB activation assay in murine samples of diet-induced NASH model and human samples; NFkB activation index is normalized against appropriate and respective control samples. *$P < 0.05$.

of either peroxynitrite decomposition catalyst FeTPPS or peroxynitrite scavenger FBA further decreased the levels of ICAM-1 and E-Selectin in livers as compared to DIO+BDCM group (Fig. 4.4A and 4.4B)(P<0.01). Use of mice that are deficient in TLR4 gene showed significantly decreased levels of ICAM-1 and E-Selectin thus showing a strong correlation between NADPH oxidase activation and presence of TLR4 with sinusoidal injury as depicted by the increased levels of ICAM-1 and E-Selectin (Fig. 4.4A , 4.4B)(P<0.01). MCD diet-fed mouse livers and Human NASH livers showed a significant increase in immunoreactivity to ICAM-1 and E-Selectin as compared to their respective controls (Suppl. fig. 4.3A-4.3D)(P<0.05). Apart from the immunohistochemistry data,

www.manaraa.com

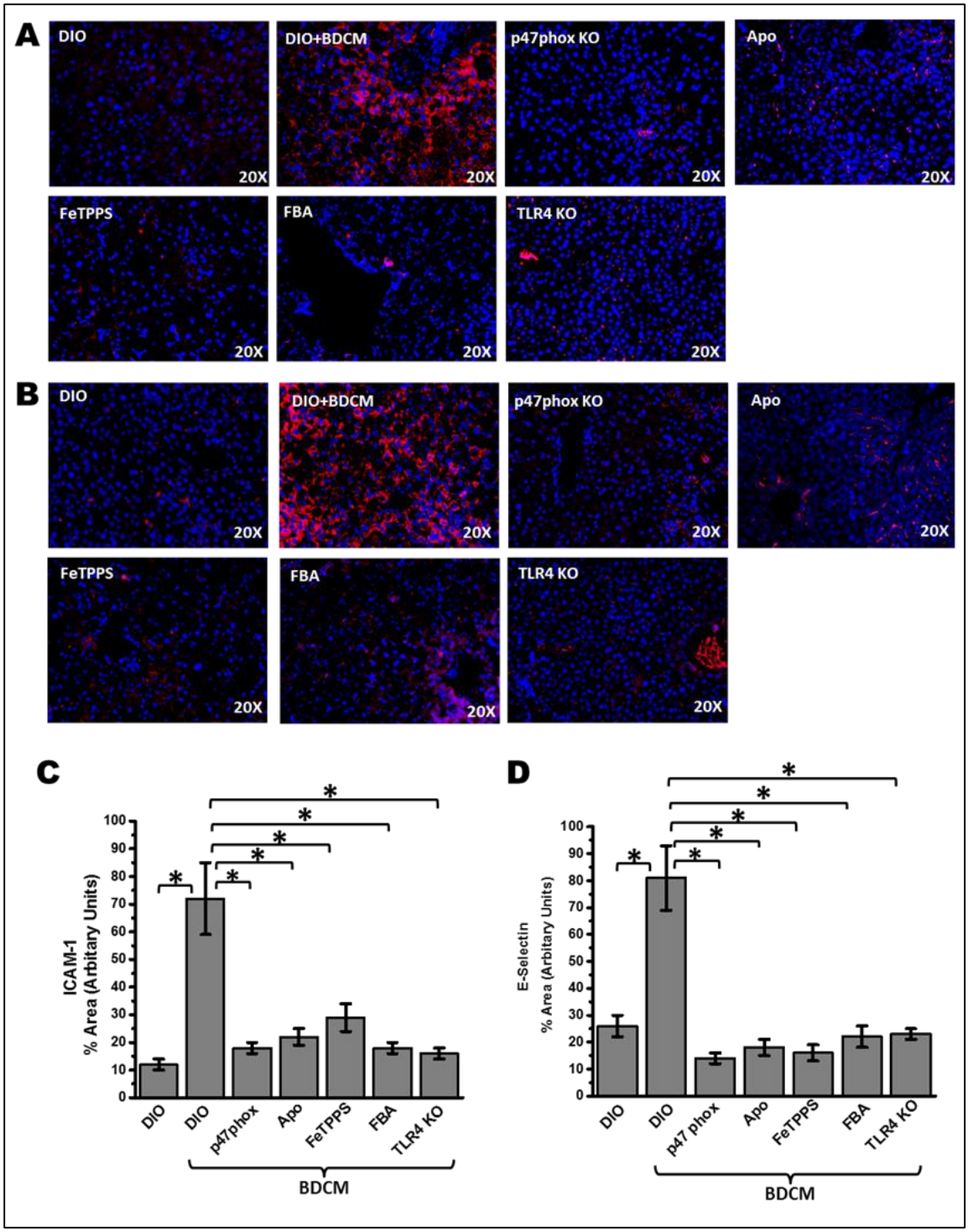

Figure 4.4 NADPH oxidase and peroxynitrite–driven hepatic sinusoidal injury via TLR4 signaling. 20X magnification representative images of 5µm thick immunostained liver sections, imaged using immunofluorescence microscope; secondary antibody used: alexafluor568 (red) against α-ICAM-1 primary antibody (**A**), and alexafluor568 (red) against α-E-selectin primary antibody (**B**); both ICAM-1 and E-selectin are sinusoidal injury markers. **A** and **B**: Nuclear stain (blue) is due to prolong gold antifade reagent with

www.manaraa.com

DAPI; samples from: high fat-fed wild-type mouse (DIO); high fat-fed wild-type mouse exposed to BDCM (DIO+BDCM); high fat-fed p47phox gene knockout mouse exposed to BDCM (p47phox KO); high fat-fed wild-type mouse exposed to BDCM and injected with NADPH oxidase inhibitor apocynin (Apo); high fat-fed wild-type mouse exposed to BDCM and injected with peroxynitrite decomposition catalyst, a ferric porphyrin complex (FeTPPS), high fat-fed wild-type mouse exposed to BDCM and injected with peroxynitrite decomposition catalyst phenyl boronic acid (FBA); high fat-fed TLR4 gene knockout mouse exposed to BDCM (TLR4 KO). **C**: Graph depicts morphometry performed on three independent fields for each sample including representative images in **A** captured under 20X magnification lens for percent area showing positive immunoreactivity of ICAM-1, calculated in arbitrary units. **D**: Graph depicts morphometry performed on three independent fields for each sample including representative images in B captured under 20X magnification lens for percent area showing positive immunoreactivity of E-selectin, calculated in arbitrary units. $^{**}P < 0.01$.

mRNA expression profiles of ICAM-1 and E-Selectin showed a significant increase in murine NASH tissues and human NASH tissues while use of gene deficient mice for p47phox, TLR4 or administration of peroxynitrite scavengers had significantly decreased levels of these sinusoidal injury markers ($P<0.05$) (Suppl. Figs. 4.4 and 4.5) The results suggested that NADPH oxidase activation and subsequent formation of peroxynitrite caused increased sinusoidal injury in NASH and were strongly associated to the presence of TLR4.

NADPH Oxidase mediated peroxynitrite generation drives TLR4 signaling induced IL-1β, chemokine release and Kupffer cell activation in NASH.

Previous experiments showed the strong association of NADPH oxidase mediated peroxynitrite formation and TLR4 recruitment followed by NFkB activation, crucial processes for downstream TLR4 signaling. It is essential that TLR4-mediated IL-1β release and Kupffer cell activation that have been shown to be mediated by TLR4 signaling be proven to establish the significance of NADPH oxidase driven TLR4 recruitment. Results showed that immunoreactivity of IL-1 β in mice liver slices in DIO+BDCM group

www.manaraa.com

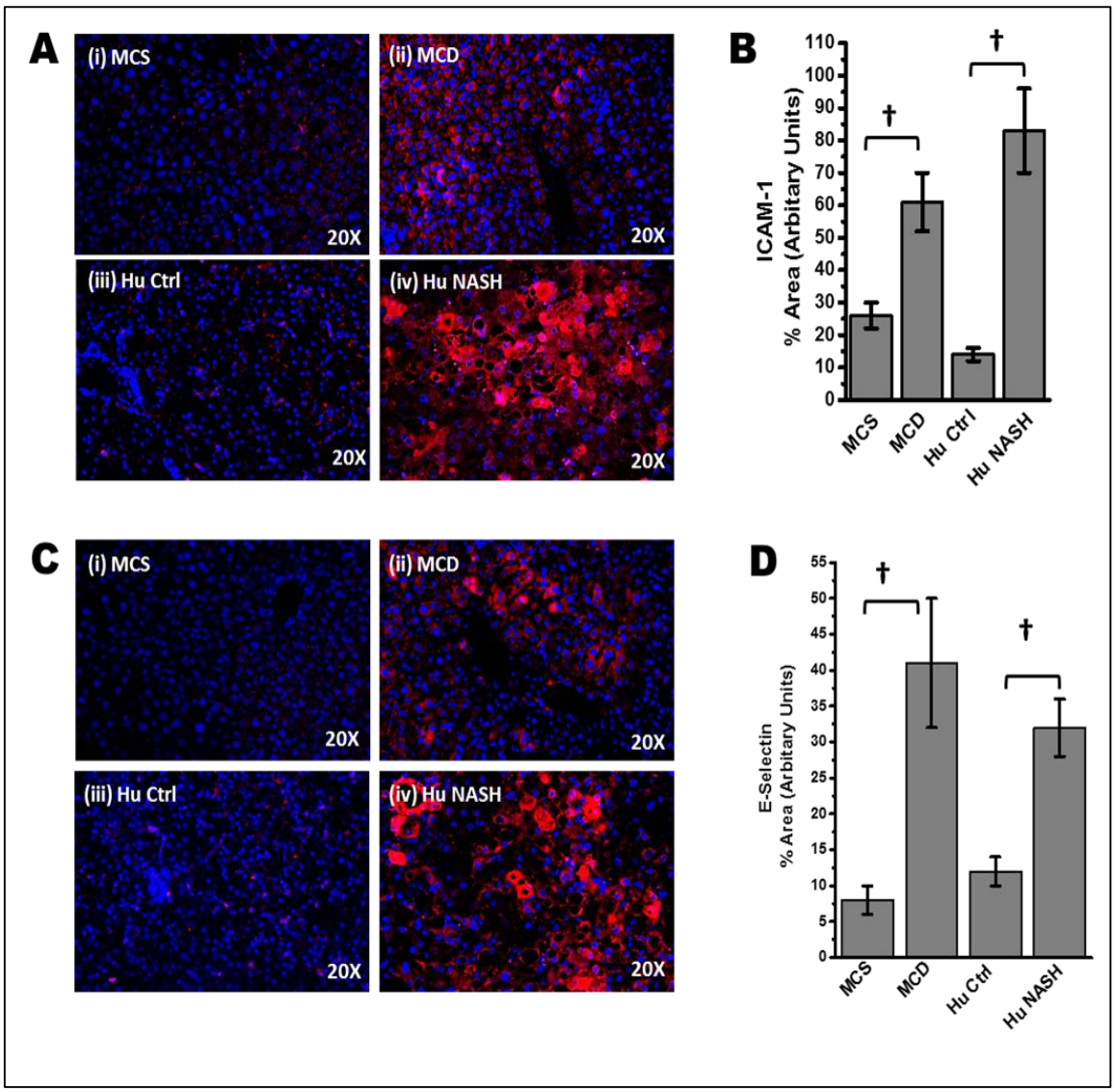

Supplementary Figure 4.3 Hepatic sinusoidal injury in MCD rodent model and human samples. 20X magnification representative images of 5µm thick immunostained liver sections, imaged using immunofluorescence microscope; secondary antibody used: alexafluor568 (red) against α-ICAM-1 primary antibody (**suppl. Fig. 4.3A**), and alexafluor568 (red) against α-E-selectin primary antibody (**suppl. Fig. 4.3C**); both ICAM-1 and E-selectin are sinusoidal injury markers; **suppl. Figs. 4.3A & 4.3C**: nuclear stain (blue) is due to prolong gold antifade reagent with DAPI; samples from (i) methionine and choline-sufficient diet-fed mouse, annotated as MCS, (ii) methionine and choline-deficient diet-fed mouse, annotated as MCD, (iii) healthy human control, annotated as Hu Ctrl, (iv) human NASH patient, annotated as Hu NASH

4.3B: graph depicting morphometry done on 3 independent fields for each sample including representative images in suppl. fig.3A captured under 20X magnification lens

www.manaraa.com

for per cent area showing positive immunoreactivity of ICAM-1, calculated in arbitrary units

4.3D: graph depicting morphometry done on 3 independent fields for each sample including representative images in suppl. fig.3C captured under 20X magnification lens for per cent area showing positive immunoreactivity of E-selectin, calculated in arbitrary units. *P<0.01; † P<0.05

is significantly higher as compared to DIO only group (Fig. 4.5A, Fig. 4.5D)(P<0.01). P47phox KO mice or mice that were treated with peroxynitrite decomposition catalyst FeTPPS showed significant decrease in IL-1β immunoreactivity as compared to DIO+BDCM group (Fig. 4.5A , Fig. 4.5D)(P<0.01). TLR4 KO mice showed significant decrease in IL-1β immunoreactivity as compared to DIO+BDCM group suggesting the strong involvement of TLR4 signaling (Fig. 4.5A , Fig. 4.5D). MCP-1 release is considered a hallmark of Kupffer cell activation and it plays a huge role in liver inflammation to attract circulating leucocytes to the inflamed liver in NASH. Results showed that DIO+BDCM group had significantly increased MCP-1 immunoreactivity as compared to DIO only group (Fig. 4.5B)(P<0.01). P47phox KO mice or mice treated with peroxynitrite decomposition catalyst FeTPPS had significantly decreased MCP-1 immunoreactivity as compared to DIO+BDCM group (Fig. 4.5B Fig. 4.5E)(P<0.01). TLR4 KO mice also had significant decrease in MCP-1 immunoreactivity as compared to DIO+BDCM group (Fig. 4.5B and Fig. 4.5E)(P<0.01). The above inflammatory cytokines were also verified for their mRNA expression. Results showed that the mRNA expressions of TNF-α, IL-6, Lipocalin-2 (Lcn2), serum amyloid A1 (SAA1), IL-1β and MCP-1 were significantly increased in rodent and human NASH livers while use of p47 phox KO mice, TLR4 KO mice or administration of FeTPPS showed a significant decrease in the expression levels (P<0.05)(Suppl. Figs. 4.6, 4.7 and 4.8). Next we explored the role of NADPH oxidase

www.manaraa.com

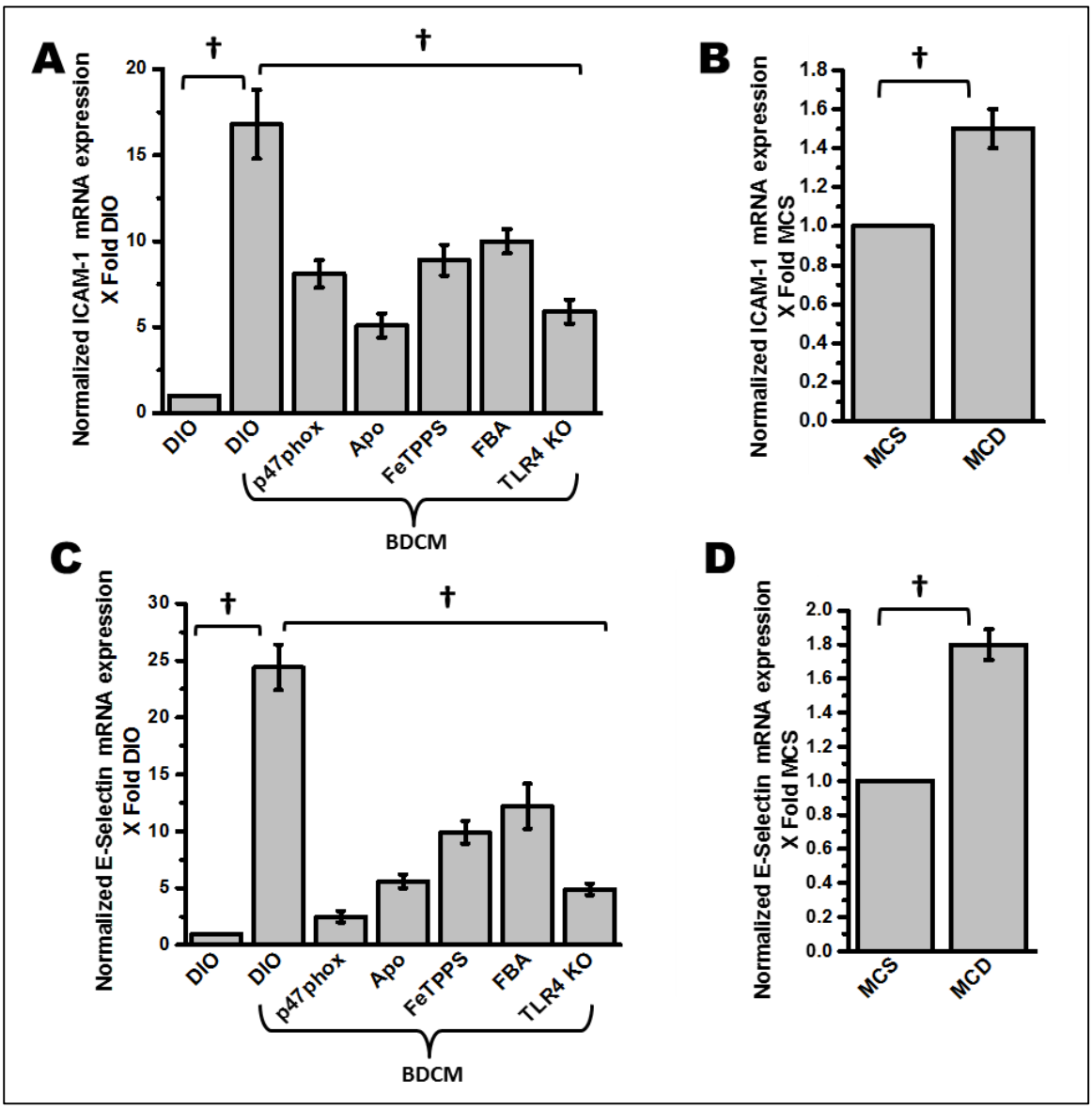

Supplementary Figure 4.4 quantitative real time PCR analyses of mRNA levels of ICAM-1 and E-Selectin in NASH models. **4.4A**: ICAM-1 in toxin model of NASH, **4.4B**: ICAM-1 in MCS and MCD model. **4.4C**: E-Selectin in toxin model of NASH. **4.4D**: E-Selectin in MCS and MCD model of NASH.
† $P<0.05$

mediated TLR recruitment in Kupffer cell activation by studying the immunoreactivity of CD68 (a Kupffer cell activation marker). Results showed that DIO+BDCM group livers had significantly increased CD68 immunoreactivity as compared to DIO only group (Fig.

www.manaraa.com

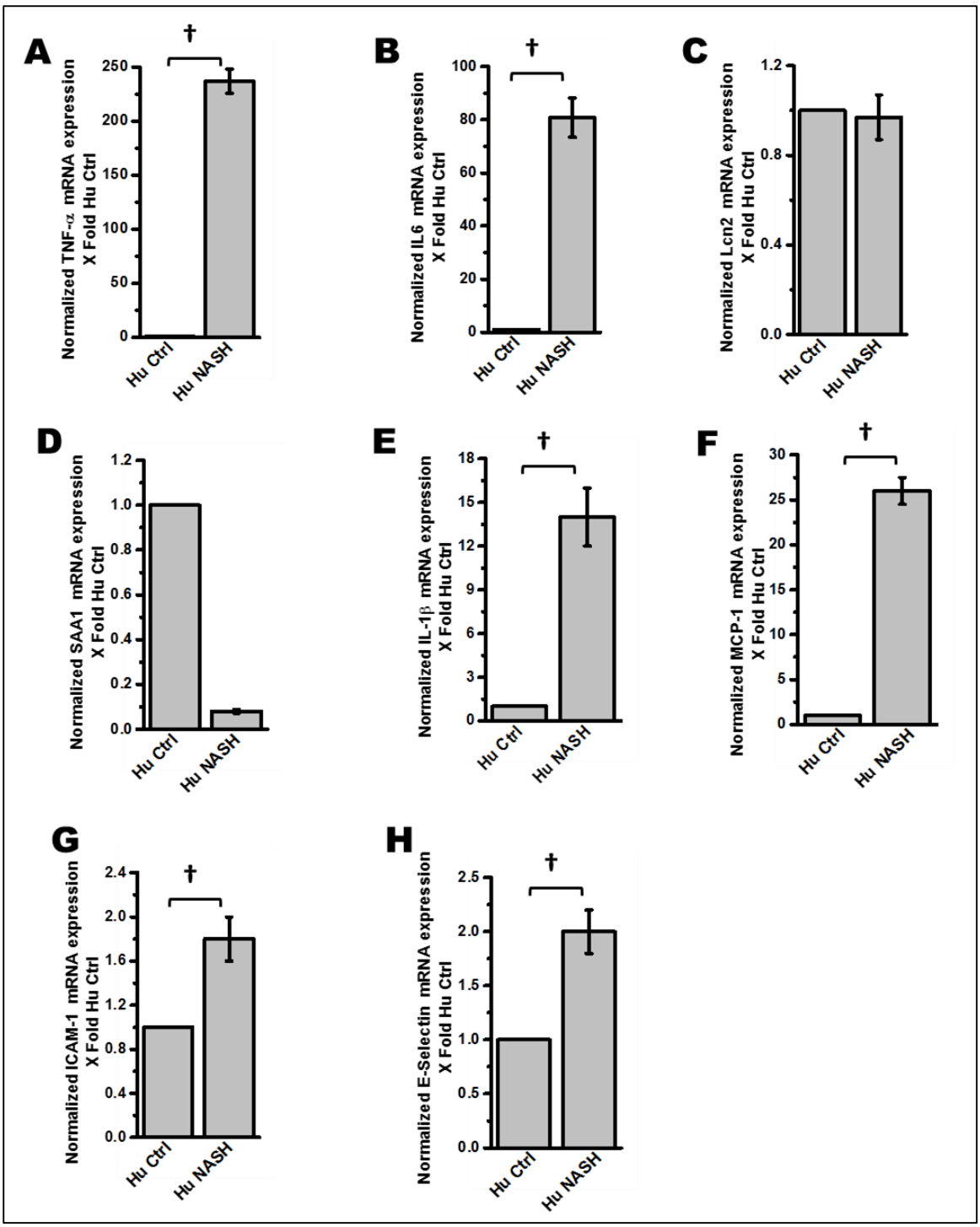

Supplementary Figure 4.5 quantitative real time PCR analyses of mRNA levels of proinflammatory mediators in Human control and Human NASH livers. TNF-α (**4.5A**), IL-6 (**4.5B**), Lcn2 (**4.5C**), SAA1 (**4.5D**), IL-1β (**4.5E**), MCP1 (**4.5F**), ICAM-1 (**4.5G**), E-Selectin (**4.5H**) † P<0.05

www.manaraa.com

4.5C, Fig. 4.5F)(P<0.01) whereas using p47phox KO mice or attenuating formation of peroxynitrite significantly decreased CD68 immunoreactivity (Fig. 4.5C Fig. 4.5F)(P<0.01). TLR4 KO mice had significantly decreased CD68 immunoreactivity in the liver as compared to the DIO+BDCM group suggesting a strong role of TLR4 signaling in Kupffer cell activation (Fig.4.5C and 4.5F)(P<0.01). The results strongly suggested that NADPH oxidase mediated peroxynitrite that drove TLR4 recruitment was also correlated with TLR4 signaling indicated by a significant attenuation of IL-1β release, MCP-1 and CD68 protein levels when administered agents that block NADPH oxidase mediated peroxynitrite. The results of decreased IL-1β release and Kupffer cell activation in TLR4 KO mice further confirmed the role of TLR4 involvement in NASH inflammatory pathogenesis. MCD diet-fed mouse livers and Human NASH livers showed significantly decreased IL-1β (Suppl fig. 4.4A and 4.4D)(P<0.05), decreased MCP-1 levels (Suppl. fig. 4.4B and 4.4E)(P<0.05) and decreased CD68 immunoreactivity (Suppl. fig. 4.4C and Fig. 4.4F)(P<0.05) compared to their respective controls thus suggesting that NADPH oxidase driven TLR4 recruitment and subsequent NASH inflammatory pathogenesis is prevalent across different mouse models and in human form of the disease.

Recent reports suggest that the strong involvement of TLR4/NFkB pathway in migration and activation of hepatic stellate cells is, known to be a hallmark of NASH pathogenesis(100) . To associate the phenomenon of NADPH oxidase driven recruitment of TLR4 into hepatic lipid rafts in activating hepatic stellate cells, α -SMA immunoreactivity in liver slices were studied by immunohistochemistry. Results showed that DIO+BDCM group showed a significant increase in α -SMA immunoreactivity as compared to DIO only group (Fig. 4.6A , Fig. 4.6D)(P<0.01). Use of p47phox KO mice or

www.manaraa.com

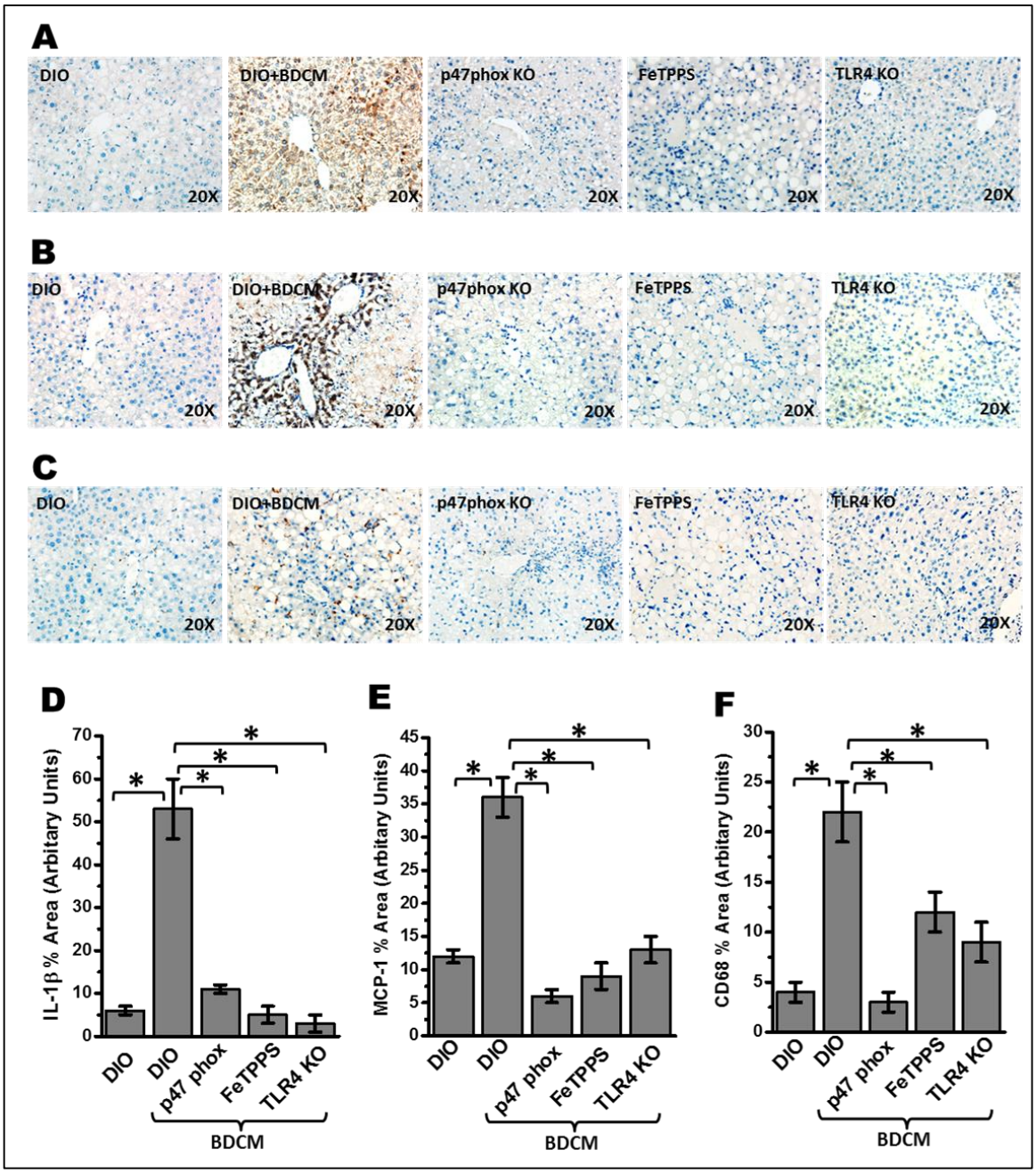

Figure 4.5 TLR4 signaling-mediated cytokine release and Kupffer cell activation. 20X magnification representative images of 5µm thick immunostained liver sections, imaged using brightfield microscope; positive immunoreactivities (brown) are due to DAB binding to respective biotinylated secondary antibodies via streptavidin-HRP; nuclei (blue) counterstained with Mayer's hematoxylin solution; immunoreactivities detected are for proinflammatory cytokines: IL-1β(**A**), MCP-1(**B**), and Kupffer cell activation marker, CD68 (**C**), respectively. **A**-**C**: Samples from: high fat-fed wild-type mouse (DIO); high fat-fed wild-type mouse exposed to BDCM (DIO+BDCM); high fat-fed p47phox gene knockout mouse exposed to BDCM (p47phox KO); high fat-fed wild-type mouse exposed

www.manaraa.com

to BDCM and injected with peroxynitrite decomposition catalyst, a ferric porphyrin complex (FeTPPS), high fat-fed TLR4 gene knockout mouse exposed to BDCM (TLR4 KO). **D**: Graph depicts morphometry performed on three independent fields for each sample including representative images in **A** captured under 20X magnification lens for percent area showing positive immunoreactivity of IL-1β, calculated in arbitrary units. **E**: Graph depicting morphometry performed on three independent fields for each sample including representative images in **B** captured under 20X magnification lens for percent area showing positive immunoreactivity of MCP-1, calculated in arbitrary units. **F**: Graph depicts morphometry performed on three independent fields for each sample including representative images in **C** captured under 20X magnification lens for percent area showing positive immunoreactivity of CD68, calculated in arbitrary units. $^{**}P < 0.01$

scavenging peroxynitrite or use of TLR4 KO mice showed significant decrease in α -SMA immunoreactivity as compared to DIO+BDCM group (Fig. 4.6A)(Fig. 4.6D)($P<0.01$). MCD diet-fed mice showed significant increase in α -SMA immunoreactivity as compared to MCS group (Fig. 4.6B, Fig. 4.6E)($P<0.05$). Human NASH livers had significantly increased α -SMA levels as shown by immunohistochemistry when compared with control livers from healthy subjects (Fig. 4.6C, 4.6F)($P<0.05$). The immunohistochemistry data was also verified using western blot analysis of liver tissue homogenates (Suppl. Fig. 4.9).The data strongly suggested that hepatic stellate cell proliferation depended on the NADPH oxidase mediated peroxynitrite formation and its induction of TLR4 recruitment into hepatic lipid rafts. NADPH oxidase mediated TLR4 recruitment was also strongly correlated with histological assessment of NASH, inflammation, and fibrosis as shown by NAS scores (Table 4.1)

4.4 DISCUSSION

In this report related to molecular mechanisms of inflammatory pathogenesis in NASH, we show that NADPH oxidase-derived peroxynitrite drives TLR 4 recruitment in hepatic lipid rafts. Further, we use a novel synthetic peroxynitrite scavenger boronic acid (FBA) to

www.manaraa.com

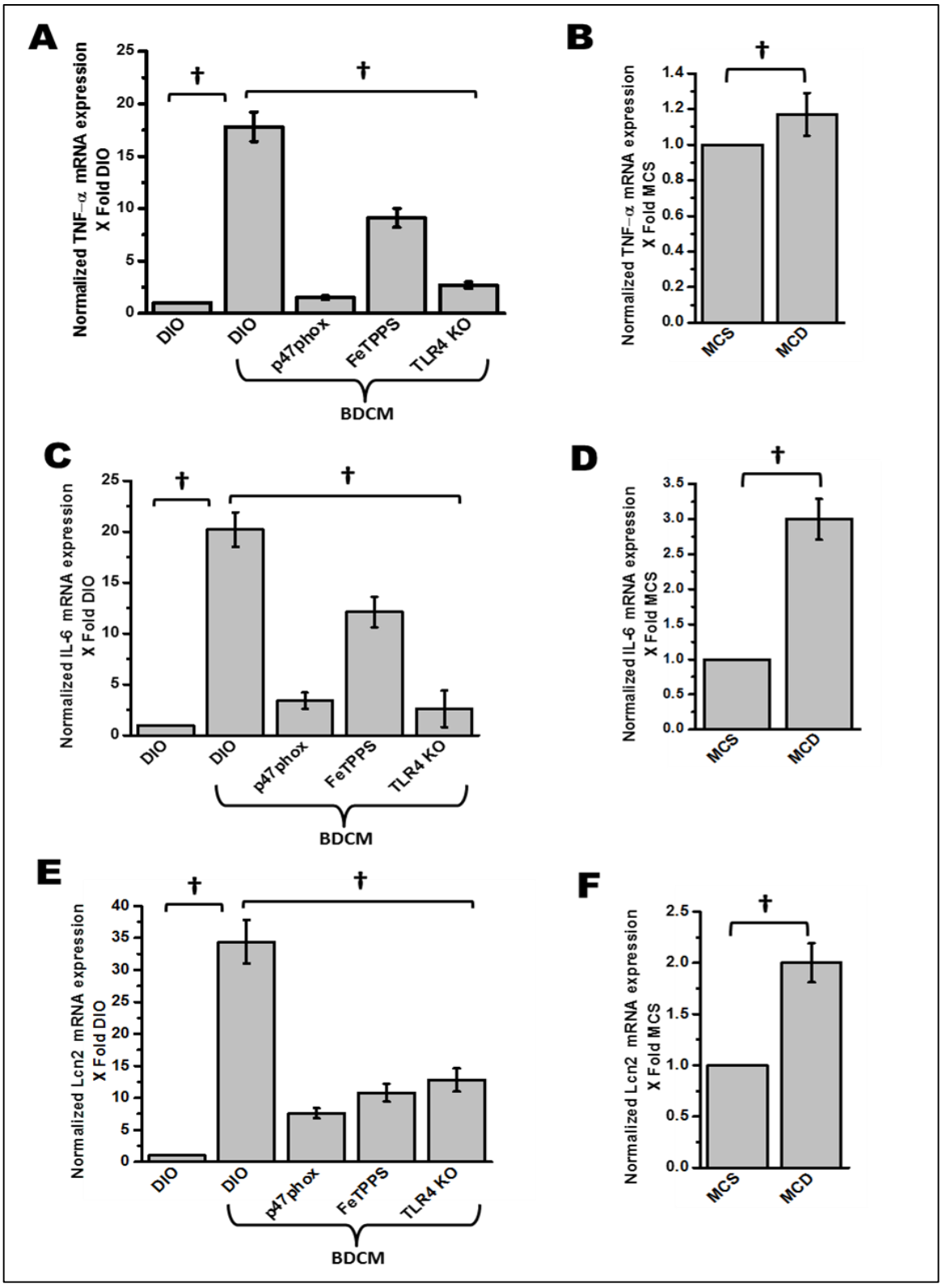

Supplementary Figure 4.6 quantitative real time PCR analyses of mRNA levels of TNF-α, IL-6 and Lcn2 in NASH models. TNF- α in the toxin model of NASH (**6A**) and MCS/MCD model of NASH (**6B**). IL-6 in the toxin model of NASH (**6C**) and MCS/MCD model of

www.manaraa.com

NASH (**6D**). Lcn2 in the toxin model of NASH (**6E**) and MCS/MCD model of NASH (**6F**). † P<0.05

abrogate the peroxynitrite formation and attenuate IL-1β production, sinusoidal injury, Kupffer cell activation and stellate cell proliferation. NASH is clinically silent and is presented late in clinics, making it difficult to treat(101, 102). The multiple phases of NASH pathogenesis that include an initial lipotoxicity, macrophage activation leading to inflammation and a late stage fibrosis, makes devising a therapeutic strategy challenging. Thus identification of early molecular signatures of injury initiation in the fatty liver is of paramount importance. The recent literature reports of the involvement of TLR4-mediated pathways in NASH have identified the molecular basis of inflammation that often precedes a late stage fibrosis(102). Since TLR4-mediated inflammation is a sufficiently early event in NASH pathophysiology, understanding the molecular basis of its synthesis, recruitment to lipid rafts and downstream signaling becomes essential for resolving the disease itself(103). Our results, of the strong involvement of NADPH oxidase activation in driving TLR4 into the lipid rafts show a novel mechanism of TLR4 activation and NFkB translocation in NASH. The results also identify peroxynitrite-mediated TLR4 recruitment to lipid rafts as an early molecular event in NASH. The pharmacological approach of using a NADPH oxidase inhibitor and use of transgenic mice that lacks the p47phox subunit of NADPH oxidase confirm the role of this vital enzyme in lipid raft recruitment of TLR4. We have reported previously that NADPH oxidase release of superoxide radicals leads to peroxynitrite formation that in turn was instrumental in causing Kupffer cell activation in steatohepatitic injury(13). In the present study we used a dual approach to study the formation of peroxynitrite via NADPH oxidase, firstly by using a general decomposition catalyst FeTPPS and secondly by helping peroxynitrite react with a novel boronic

www.manaraa.com

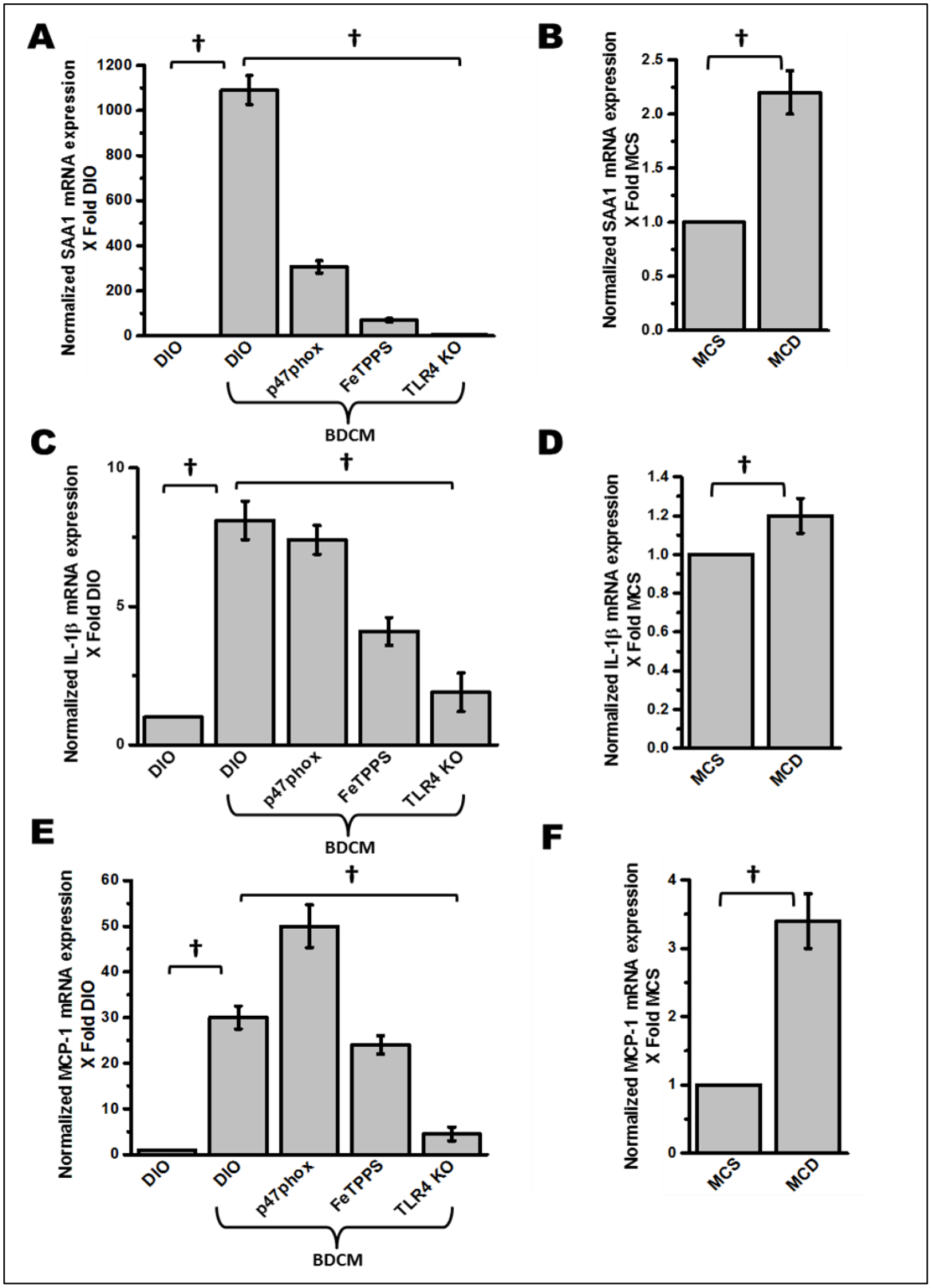

www.manaraa.com

Supplementary Figure 4.7 quantitative real time PCR analyses of mRNA levels of SAA1, IL-1β and MCP-1 in NASH models. SAA1 in the toxin model of NASH (4.**7A**) and MCS/MCD model of NASH (4.**7B**). IL-1β in the toxin model of NASH (4.**7C**) and MCS/MCD model of NASH (4.**7D**). MCP-1 in the toxin model of NASH(**4.7E**) and (**4.7F**). MCS/MCD model of NASH. † $P<0.05$.

compound FBA in vivo (104). Modelling human NASH using rodent models remain a challenge to the researchers. There is no single model that illustrates the symptoms of human NASH in a clear and decisive way(105). Several concepts involving "dual hits" and multiple hit paradigms have been proposed but this has been the focus of debate(6, 106). The lipotoxicity based model that includes generation of oxidative stress following administration of hepatotoxins, a second hit, was previously described by us and others, recognizing the fact that it does not reflect the true developmental stages of human NASH but represents an underlying condition of steatosis, insulin and leptin resistance that is found in human NASH patients(69, 106). Since oxidative stress is undoubtedly a major player in human NASH, our model exemplifies a logical approach to study oxidative stress mechanisms in the progression of NASH and can be used to test compounds that attenuate oxidative stress-mediated inflammation in this disease. On the other hand, use of MCD diet model is used widely to depict steatohepatitic lesions coupled with fibrosis, symptoms that are found in more progressive stages of human NASH(105, 107, 108). The symptoms found in this model represent lesions of human NASH but in a non-insulin resistant state though some studies have found hepatic insulin resistance in this model. The results thus obtained from these studies reported here may be the beginning of many future studies involving NADPH oxidase activation induced TLR4 trafficking and could be validated using other models of NASH.

www.manaraa.com

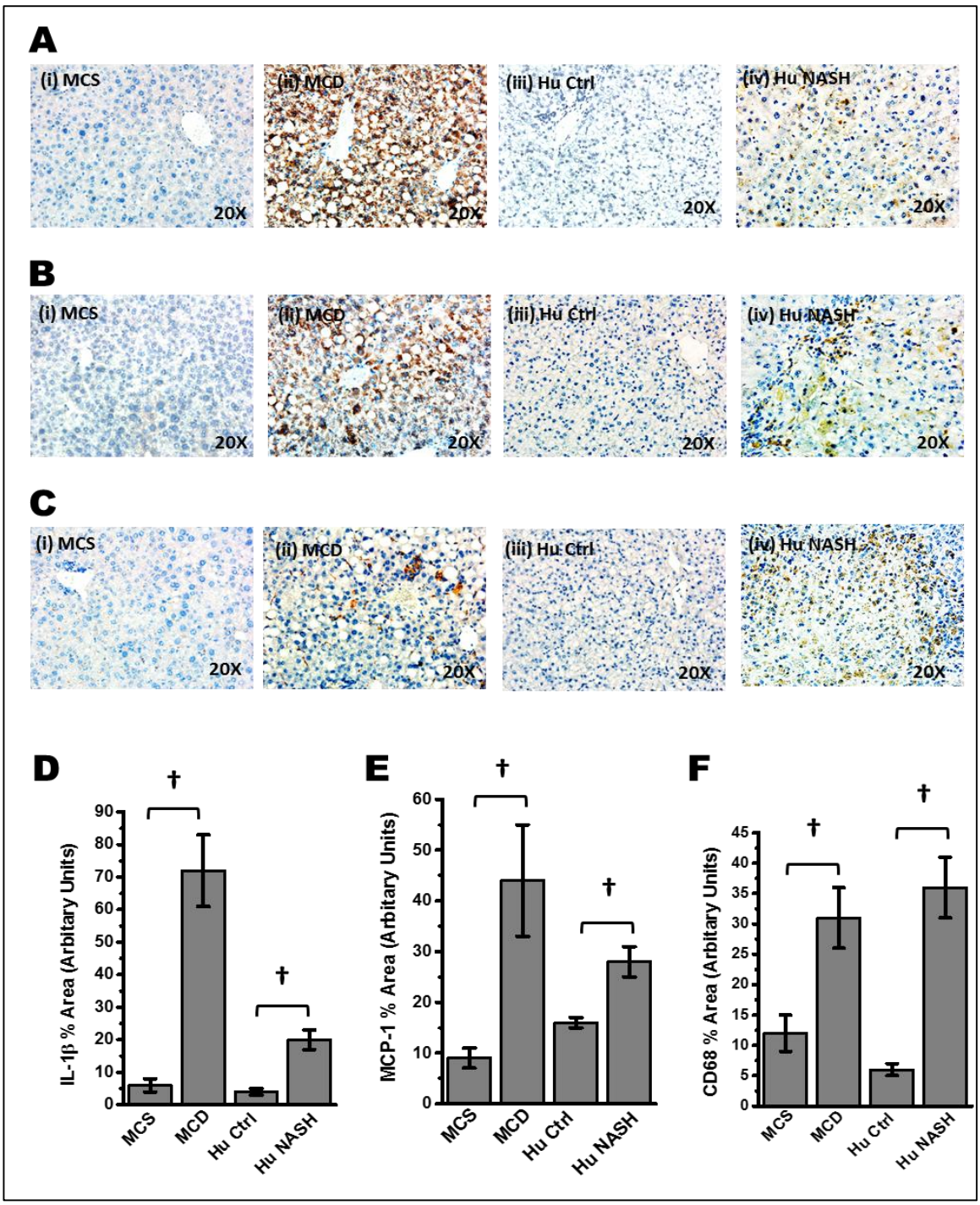

Supplementary Figure 4.8 Immunodetection of IL-1β, MCP-1 AND CD68 in MCD rodent models and human samples. 20X magnification representative images of 5µm thick immunostained liver sections, imaged using brightfield microscope; positive immunoreactivities (brown) are due to DAB binding to respective biotinylated secondary antibodies via streptavidin-HRP; nuclei (blue) counterstained with Mayer's hematoxylin solution; immunoreactivities detected are for proinflammatory cytokines: IL-1β(4.8**A**), MCP-1(**4.8B**), and Kupffer cell activation marker, CD68 (**4.8C**) respectively; **4.8A, 4.8B**

www.manaraa.com

&4.8C: samples are from (i) methionine and choline-sufficient diet-fed mouse, annotated as MCS, (ii) methionine and choline-deficient diet-fed mouse, annotated as MCD, (iii) healthy human control, annotated as Hu Ctrl, (iv) human NASH patient, annotated as Hu NASH
4.8D: graph depicting morphometry done on 3 independent fields for each sample including representative images in suppl. fig.5A captured under 20X magnification lens for per cent area showing positive immunoreactivity of IL-1β, calculated in arbitrary units
4.8E: graph depicting morphometry done on 3 independent fields for each sample including representative images in suppl. fig.4B captured under 20X magnification lens for per cent area showing positive immunoreactivity of MCP-1, calculated in arbitrary units
4.8F: graph depicting morphometry done on 3 independent fields for each sample including representative images in suppl. Fig.4C captured under 20X magnification lens for per cent area showing positive immunoreactivity of CD68, calculated in arbitrary units . *P<0.01; † P<0.05

The dual approach of using two different peroxynitrite blockers was significant since FeTPPS and other metaloporphyrins have been used in various rodent models of inflammatory diseases but has low oral bioavailability and lacked specificity(53). FBA, an aromatic boronate was shown to react specifically with peroxynitrite to yield tyrosine as a major product and the probability of formation of nitrotyrosine following a reaction with peroxynitrite is negligible because of the stoichiometry of the chemical reaction(109). This reaction kinetics made FBA to be a specific scavenger and blocking agent for peroxynitrite(109). FBA reacts with peroxynitrite at a rapid rate and stoichiometrically to form phenol ($k=1.6x10^6$ $M^{-1}s^{-1}$)(110). FBA is also highly specific to react with peroxynitrite and can be used to infer the source of tyrosine nitration since it does not inhibit myeloperoxidase-dependent tyrosine nitration. We utilized the effectiveness of FBA as a candidate drug to attenuate peroxynitrite mediated recruitment of TLR4 into hepatic lipid rafts. Our results of a significant attenuation of TLR4 recruitment to lipid rafts as shown by the colocalization of TLR4 and the lipid raft protein, flotillin in NASH livers of mice might provide a rationale for using FBA as a future small molecule to attenuate TLR4 mediated inflammation in NASH. However caution should be exercised before

www.manaraa.com

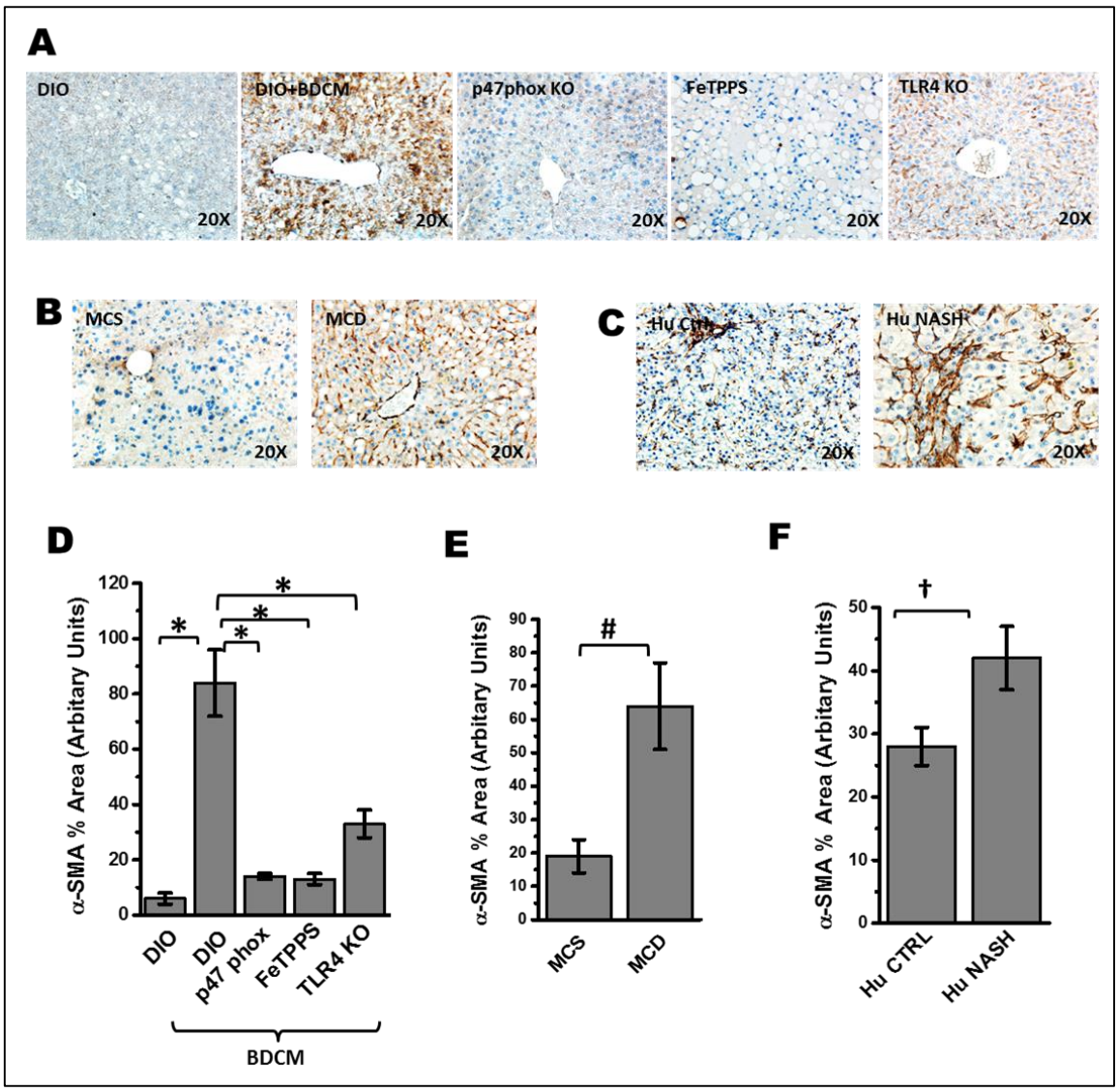

Figure 4.6 **A-C**: Immunohistochemistry images for α-SMA in rodent NASH models and human samples. 20X magnification representative images of 5µm thick immunostained liver sections, imaged using brightfield microscope; positive immunoreactivities (brown) are due to DAB binding to respective biotinylated secondary antibodies via streptavidin-HRP; nuclei (blue) counterstained with Mayer's hematoxylin solution; immunoreactivities detected are for stellate cell proliferation marker, α-SMA. **4.6 A**: Samples are from high fat-fed wild-type mouse (DIO); high fat-fed wild-type mouse exposed to BDCM (DIO+BDCM); high fat-fed p47phox gene knockout mouse exposed to BDCM (p47phox KO); high fat-fed wild-type mouse exposed to BDCM and injected with peroxynitrite decomposition catalyst, a ferric porphyrin complex (FeTPPS), high fat-fed TLR4 gene knockout mouse exposed to BDCM (TLR4 KO). **4.6 B:** Samples are from: methionine and choline-sufficient diet-fed mouse (MCS), methionine and choline-deficient diet-fed mouse (MCD). **4.6 C**: Samples are from: healthy human control (Hu Ctrl), human NASH patient (Hu NASH). **4.6 D-F**: Graphs depict morphometries performed on three independent fields for each sample including representative images in **4.6 A** (**D**), **B** (**E**), and **C** (**F**), captured

www.manaraa.com

under 20X magnification lens for percent area showing positive immunoreactivity of α-SMA, calculated in arbitrary units. $^{**}P < 0.01$ and $^{*}P < 0.05$.

interpreting the findings reported here since FBA has not been used previously in other inflammatory disease models. Further FBA treatment also abrogated TLR4-induced NFkB translocation and DNA binding, increased levels of sinusoidal injury markers ICAM-1 and E-selectin, Kupffer cell activation marker CD68 and stellate cell proliferation. FBA treated NASH livers had significantly less fibrosis as assessed by NAS scores.

Our results further underline an alternate mechanism of lipid raft recruitment of TLR4 via an oxidative and nitrative stress pathway, unique in NASH pathophysiology. The recruitment of TLR4 might happen as a result of Nrf2 depletion which has a direct effect on glutathione synthesizing enzymes and lower levels of glutathione seen in NASH, though this remains speculative at this point(111, 112). The results reported here support the role of highly reactive peroxynitrite in causing TLR4 trafficking rather than oxyradicals generated as a result of TLR4 activation, a concept that has been reported before and is widely prevalent in inflammatory diseases(113). Our data supports the peroxynitrite mechanism owing to the faster rate kinetics of formation reported for peroxynitrite (10^{10} $M^{-1}S^{-1}$) but the TLR4-induced NADPH oxidase activation in NASH cannot be ruled out owing to the complex innate immune regulations associated in the pathophysiology of the disease itself(110).

In summary we showed that TLR-recruitment in lipid rafts is an early event in both rodent and human NASH pathogenesis. TLR4-recruitment was initiated by NADPH oxidase and the molecular basis of this early event was dependent on the formation of peroxynitrite. The use of FBA as a novel compound to attenuate peroxynitrite in vivo might

www.manaraa.com

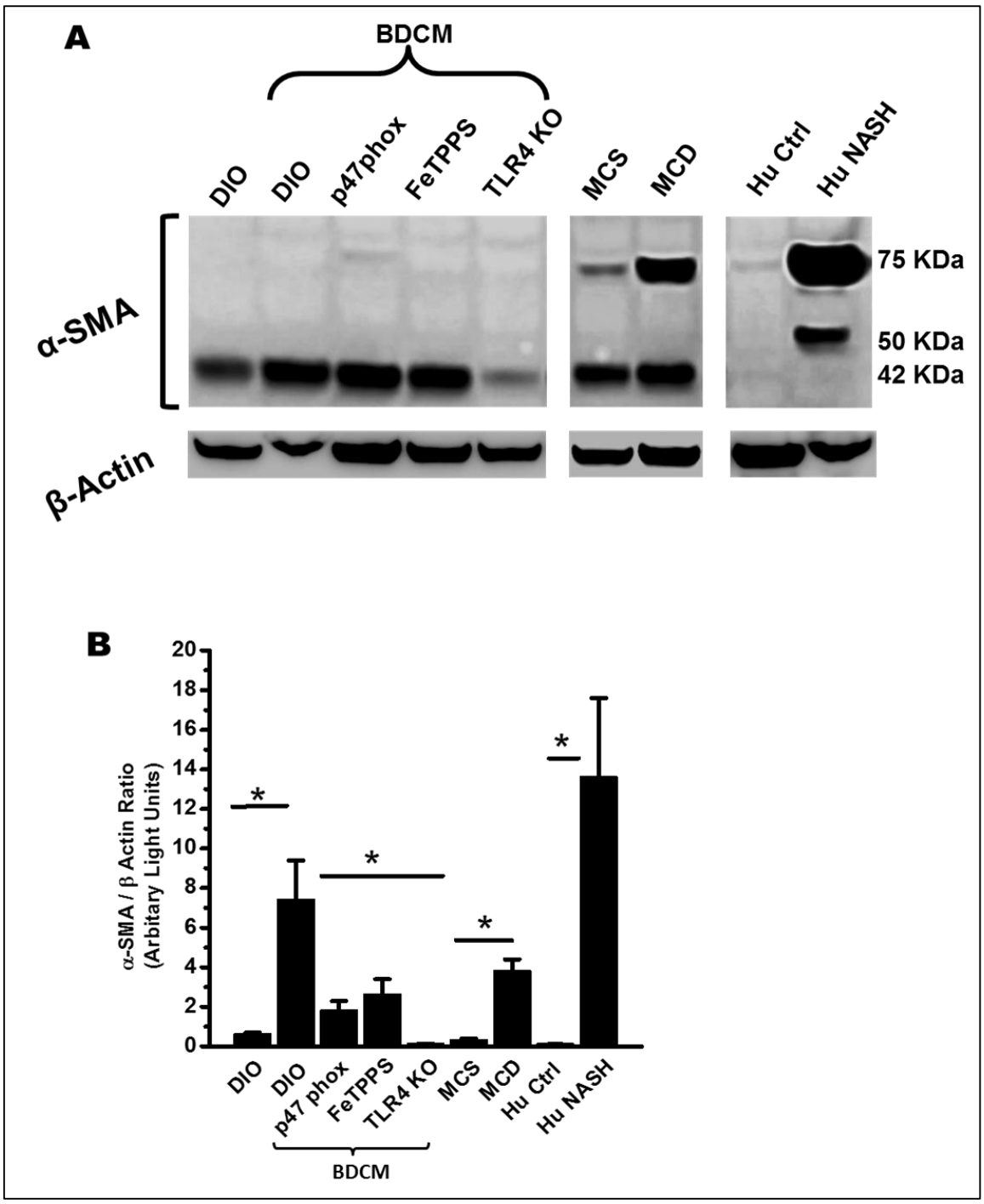

Supplementary Figure 4.9 Western blot analysis of alpha smooth muscle actin (α-SMA) in liver homogenates from rodent models of NASH and human NASH livers. (**9A**). Immunoblot images for the immunoreactive bands of α-SMA and β-actin. (**9B**) Band analysis after normalizing against β-actin

www.manaraa.com

Table 4.1: NASH CRN Scores For NASH Model

	DIO	DIO+ BDCM	p47 phox	FeTPPS	FBA	TLR4 KO
Steatosis	**2**	**3**	**2**	**2**	**2**	**1**
Lobular Inflammation	**1**	**3**	**1**	**2**	**0**	**0**
Heaptocyte Ballooning	**1**	**2**	**2**	**1**	**1**	**0**
Stage of Fibrosis	**1C**	**3**	**1C**	**1B**	**1A**	**1A**

Index 1A:Mild; 1C: Portal, Periportal Fibrosis, 3: Bridging Fibrosis

Table 4.1 NAS Scores for rodent model of NASH. The scores were calculated following analysis of histological features of NASH as described by Kleinter et. al and the guidelines laid down by the NASH clinical research network. DIO+BDCM group represent the NASH model with P47 phox, TLR4 KO mice being the NASH group where the mcie are deficient in P47 Phox and TLR4 genes. FBA and FeTPPS represent the mice groups where the peroxynitrite scavengers are co-administered with BDCM.

serve as a new approach to initiate further studies involving relevant rodent models of NASH and inflammatory pathogenesis in this disease. This might have significant relevance for research in drug development concerning the attenuation of NASH. The study is highly significant since we used two different models of NASH, elucidated the formation of peroxynitrite and TLR4 lipid raft recruitment in human NASH and avoided in vitro cellular experimentation to prove the involvement of peroxynitrite in TLR4 lipid raft recruitment, primarily because of the advanced tools to detect peroxynitrite. However, caution should be exercised in interpreting some of the results noted in this report since we are not aware of the oral bioavailability of this compound and future rodent based studies need to focus more on the pharmacokinetics of FBA.

www.manaraa.com

Acknowledgements: The authors gratefully acknowledge the technical services of Benny Davidson at the IRF, University of South Carolina School of Medicine. We also thank Dr. Gary Schools, Department of Drug Discovery and Biomedical Sciences and the Instrumentation resource facility (IRF) at the University of South Carolina for equipment usage (Confocal microscopy and analysis) and consulting services.

www.manaraa.com

CHAPTER 5

CONCLUSION

Acute bromodichloromethane (BDCM) exposure in mice that were high fat fed led to increased oxidative stress, increased expression of leptin, liver inflammation through Kupffer cell activation, NADPH oxidase membrane assembly, cytokine release and non-programmed cell death following the reductive metabolism of this water disinfection byproduct. These events following BDCM exposure are hallmarks of early steatohepatitic injury in the liver and showed adherence to the two hit hypothesis and the multi hit paradigm (6, 7). The observations showed for the first time that an underlying condition of obesity can potentiate the risk of developing steatohepatitis following drinking water disinfection byproduct exposure. Assuming that more than 34% of the US population is obese, the results underline a serious public health problem not only in this country but in developed and developing nations where use of chlorine as a disinfectant is largely used.

Findings from Chapter 2 showed that BDCM formed 4HNE adducts, a lipid peroxidation product at 6 hours followed by protein free radical formation and stable nitrotyrosine adducts in the hepatocytes and Kupffer cells (Fig. 2.1A). Interestingly, following free radical generation, BDCM exposure also significantly increased leptin mRNA expression in both adipose tissue and liver of high fat fed mice (DIO) (Fig. 2.2A). This data was important to finding a strong correlation between obesity, BDCM-induced oxidative stress

www.manaraa.com

and altered histopathology in the liver. Increased leptin in DIO mice coupled with higher release of this adipokine following CCl_4 induced NASH caused immune cell activation and necrosis in the liver (Chatterjee S et al, Journal of Hepatology). Similarly our finding that BDCM caused an increase of leptin mRNA in liver of obese mice, over and above the high leptin levels found in obesity, was crucial to find a causal effect in BDCM induced early steatohepatic lesions.

Our results of increased release of leptin following BDCM exposure allowed us to probe the significance of leptin in BDCM exposed early steatohepatitic lesions. Results showed that both whole liver homogenates and isolated Kupffer cells produced protein free radicals as measured by the immune-spin trapping technique (Fig. 2.3). The radicals further stabilized to form nitrotyrosine adducts, which are formed from either peroxynitrite metabolism or in a direct reaction of peroxidases in presence of nitric oxide (65). Nitrotyrosine formation is correlated with immune pathogenesis of many diseases. The significant formation of 3-nitrotyrosine indicated a prominent role of BDCM-Leptin interplay in the steatohepatitic lesions in DIO mice. Isolated Kupffer cells that were incubated with leptin and BDCM, showed increased oxidative stress but oxidative stress was significantly decreased in the presence of apocynin, an NADPH oxidase inhibitor or Tempol, an SOD mimetic compound or excess DMPO (Fig. 2.3C). Kupffer cells that lacked the leptin receptor isoforms had significant decrease in oxidative stress, suggesting that the presence of leptin, leptin receptor signaling coupled with BDCM was strongly associated with the Kupffer cell reactive oxygen species generation (Fig. 2.3C and D). Published literature indicates that oxidative stress in Kupffer cells leads to release of proinflammatory cytokines and chemokines that are central to inflammatory disease

www.manaraa.com

pathogenesis in fatty liver disease (24, 40). We and others have shown that Kupffer cell activation by leptin results in a poor outcome in fatty liver disease, leading to NASH like symptoms (23, 58) (13) . The release of proinflammatory cytokines and chemotactic proteins like TNF-α and MCP-1 from Kupffer cells lead to activation of inflammatory pathways that mediate disease progression in the liver(40). Our results showed that BDCM-leptin synchrony *in vivo* and *in vitro* led to TNF-α and MCP-1 release (Fig. 2.4). Further there was a significant increase in the CD68 protein in liver homogenates following BDCM exposure suggesting activation of Kupffer cells (Fig. 2.4). Kupffer cell activation was also confirmed by the use of Gdcl3-induced depletion of resident macrophages. $GdCl_3$-treated group showed significant decrease in CD68 expression as compared to DIO+BDCM group (Fig. 2.4B). Kupffer cell activation in liver disease to either alcohol treatment or NASH pathophysiology is crucial for disease progression. It has been presumed that inflammatory events in the Kupffer cells primarily trigger the increased antigen presentation, T cell proliferation and amplification of the inflammatory cascade (8, 23). Our results of increased oxidative stress, TNF-α and MCP-1 release and increased CD68 in liver confirm the Kupffer cell activation in BDCM exposure and show that it is leptin dependent.

Kupffer cell activation and the resultant inflammatory events that follow in liver injury lead to cell death. There is evidence where damage associated molecular patterns have resulted in hepatocyte necrosis in CCl_4 mediated early steatohepatitis (8). Leptin, which is found in higher concentrations in obesity due to suspected central leptin resistance may contribute to the cell death patterns in the liver. NASH histopathology shows that hepatocyte necrosis is a key event in the pathogenesis of disease progression (8, 40, 66). We argued that BDCM-induced early steatohepatitic injury will cause hepatic cell death

www.manaraa.com

and is regulated by leptin and involves its receptor. We also hypothesized that absence of leptin would prevent non programmed cell death in hepatic microenvironment. Results showed that there was a significant increase in apoptotic nuclei in DIO group whereas DIO+BDCM group or the group that had absence of leptin or its receptor showed decreased apoptosis in the liver (Fig. 2.5C). Interestingly the levels of Isocitrate Dehydrogenase, a hepatocyte marker of necrosis increased significantly in DIO+BDCM group as compared to DIO alone or in groups that were devoid of leptin or leptin receptor (Fig. 2.5A and 2.5B). These results assumed significance since apoptosis and other programmed cell death patterns like autophagy are increasingly being recognized as cell survival mechanisms (60). Necrosis, as seen in DIO+BDCM group is a significant event in steatohepatitis of obesity and can also be perceived as leptin dependent in BDCM exposed early steatohepatitic lesions.

In my next project recorded in Chapter 3, I have considered the fact that cellular death pathways and inflammation play crucial roles in NASH pathophysiology. Thus it is essential that I identify new mediators of NASH pathophysiology that are important regulators of autophagy and inflammatory pathways. Impairment of autophagy that is correlated with hepatic lipid accumulation and obesity has been found to have a significant impact on progression of NASH (31). This study shows that P2X7 receptor, which is upregulated by metabolic oxidative stress (Fig. 3.2), serve as a key regulator in modulating the oxidative stress induced-autophagy process (Fig. 3.3). P2X7 down regulation in CYP2E1 knockout mice coupled with an earlier report by this group that showed extracellular ATP (ligand for P2X7) release from necrosed-hepatocytes (those that had higher 4-HNE staining) in a CCl_4-mediated NASH model, correlates oxidative stress,

www.manaraa.com

upregulation of P2X7 receptor and its downstream events (8). The P2X7 receptor might modulate the autophagy process, by allowing depletion of LC3B, which is supposedly an early autophagy marker (Fig. 3.4E), while increasing albeit in small proportions Hsc 70 and LAMP2A mRNA levels (Figs. 3.3A and 3.3B) and allowing LAMP2A association with the lysosomal membrane, (Fig. 3.6). Interestingly, LC3B mRNA levels in NASH models showed a significant increase while the protein levels decreased (Figs. 3.3A, 3.3B and 3.4E). The contrasting result might point to a translational level regulation and can be explored further. These events can be crucial mediators of chaperone mediated autophagy in the hepatic lobe, thus increasing inflammation, in a manner perhaps similar to P2X7 receptor mediated release of autophagolysosomes/ phagolysosomes into the extracellular matrix causing increase in inflammation (81). The above mechanism of release of phagolysosomes to the extracellular matrix might be speculative for NASH at this point, but this study certainly proves the dependence of depleted LC3B, increased levels of LAMP2A and Hsc 70 on P2X7 receptor in both models of experimental NASH.

A previous study by our group showed that P2X7 receptor was crucial for causing Kupffer cell activation and inflammation following release of ATP from necrosed hepatocytes in CCl_4-mediated early steatohepatitic injury (8). In the present study I show that metabolic oxidative stress which is associated with NASH caused an up-regulation of P2X7 receptors (Fig.3.2). Metabolic oxidative stress also, mainly characterized by oxidatively modified proteins has been known to induce chaperone-mediated autophagy, increased substrate translocation by Hsc 70 towards the lysosomal membrane and increased LAMP2A levels (82). Further, P2X7 receptors have been associated with autophagy, disruption of normal lysosomal functions and release of autophagolysosomes to the

www.manaraa.com

extracellular matrix in the microglial cells, causing an increase in inflammation (81). My present study shows that there is a significant down regulation of both early and late autophagy proteins including LAMP2A in P2X7 receptor gene deleted mice. P2X7 receptor deleted mice also show decreased release of IL-1 β, IFN-γ and HMGB-1(damage associated molecular pattern that contributes to inflammation (83), observations that were dependent on significantly less cleaved caspase-1 protein levels, implying the possible involvement of P2X7 receptors. This study however falls short on exploring the exact molecular mechanism of P2X7 receptor involvement, and to have a clear answer whether it is the increased calcium ion-mediated change in lysosomal pH, lysosomal functional impairment or expulsion of the lysophagosome to the extracellular matrix that caused an increase in the inflammation. The present study also establishes a direct correlation between the decreased numbers of LAMP2A-lysosomal membrane associations, reduced inflammation and decreased NASH pathophysiology in P2X7 receptor gene deleted mice (Figs. 3.6, 3.7 and 3.8). These observations assume significance since LAMP2A levels and its association with the lysosomal membrane is an important step for chaperone mediated autophagy, which occurs late in the autophagy process. My studies show a depletion of LC3B, a autophagosome protein in NASH pathophysiology (Fig 3.4E), but not in LAMP2A, which is contrary to a study by Fortunato et al that showed decreased LAMP2A levels linked to decreased fusion of the autophagosome with the lysosome, resulting in necrotic cell death and inflammation (84). This may be due to a different mechanism of a dysfunctional lysosomal function when compared to our model that primarily evidenced LC3B depletion. Recent studies also link P2X7 receptor to a dysfunctional lysosome and autophagy protein LC3B (81, 85). In both cases the fate of the cell and its link to immune

www.manaraa.com

activation remains a dysregulated lysosomal compartment and is regulated by ATP-binding P2X7 receptors in the latter study (85). Interestingly my study indicates significantly decreased LC3B protein levels in DIO+BDCM and MCD diet fed livers as compared to DIO and MCS diet fed groups, while absence of P2X7 receptor gene elevates the LC3B protein levels (Figs. 3.4C,D and E). This result is important because it has been shown that depletion of autophagic protein LC3B enhances caspase-1 activation and increase in inflammatory microenvironment (85). I have also found higher caspase-1 activation and levels of inflammatory indicators IL-1β, TNF-α, IFN-γ and HMGB-1 in DIO+BDCM and MCD diet fed groups while a decrease in these indicators is seen in P2X7 receptor gene deleted mice (Fig. 3.7). Taken together, the present study provides first evidence that P2X7 receptor deletion results in down regulation of autophagy related proteins, inflammation and disease pathophysiology in NASH (Figs. 3.7 and 3.8). Having significant evidence that P2X7 receptor is a key regulator of autophagy in NASH, it may be presumed that targeting the P2X7 receptor or the autophagy process in NASH can emerge as a good therapeutic option for the treatment of NASH. It is increasingly becoming clear that there are series of studies that promote autophagy as a beneficial mechanism in NASH and equal number of studies that conclude autophagy is central in causing NASH, the present study only predicts the role of P2X7 receptor-mediated defective autophagy as a cause for inflammation in NASH (86). Translational impact of this study will be enhanced with more mechanistic studies in future involving cell specific P2X7 receptor knock downs and functional roles of different autophagy proteins in the presence or absence of the P2X7 receptor.

In the report recorded in Chapter 3, related to molecular mechanisms of inflammatory pathogenesis in NASH, I show that NADPH oxidase-derived peroxynitrite

www.manaraa.com

drives TLR 4 recruitment in hepatic lipid rafts. Further, I use a novel synthetic peroxynitrite scavenger phenyl boronic acid (FBA) to abrogate the peroxynitrite formation and attenuate IL-1β production, sinusoidal injury, Kupffer cell activation and stellate cell proliferation. NASH is clinically silent and is presented late in clinics, making it difficult to treat (101, 102). The multiple phases of NASH pathogenesis that include an initial lipotoxicity, macrophage activation leading to inflammation and a late stage fibrosis, makes devising a therapeutic strategy challenging. Thus identification of early molecular signatures of injury initiation in the fatty liver is of paramount importance. The recent literature reports of the involvement of TLR4-mediated pathways in NASH have identified the molecular basis of inflammation that often precedes a late stage fibrosis (102). Since TLR4-mediated inflammation is a sufficiently early event in NASH pathophysiology, understanding the molecular basis of its synthesis, recruitment to lipid rafts and downstream signaling becomes essential for resolving the disease itself (103). Our results, of the strong involvement of NADPH oxidase activation in driving TLR4 into the lipid rafts show a novel mechanism of TLR4 activation and NFkB translocation in NASH. The results also identify peroxynitrite-mediated TLR4 recruitment to lipid rafts as an early molecular event in NASH. The pharmacological approach of using a NADPH oxidase inhibitor and use of transgenic mice that lacks the p47phox subunit of NADPH oxidase confirm the role of this vital enzyme in lipid raft recruitment of TLR4. Our lab has reported previously that NADPH oxidase release of superoxide radicals leads to peroxynitrite formation that in turn was instrumental in causing Kupffer cell activation in steatohepatitic injury (13). In the present study I use a dual approach to study the formation of peroxynitrite via NADPH oxidase, firstly by using a general decomposition catalyst FeTPPS and secondly by helping

www.manaraa.com

peroxynitrite react with a novel boronic compound FBA in vivo (104). Modelling human NASH using rodent models remain a challenge to the researchers. There is no single model that illustrates the symptoms of human NASH in a clear and decisive way (105). Several concepts involving "dual hits" and multiple hit paradigms have been proposed but this has been the focus of debate (6, 106). The lipotoxicity based model that includes generation of oxidative stress following administration of hepatotoxins, a second hit, was previously described by us and others, recognizing the fact that it does not reflect the true developmental stages of human NASH but represents an underlying condition of steatosis, insulin and leptin resistance that is found in human NASH patients (69, 106). Since oxidative stress is undoubtedly a major player in human NASH, our model exemplifies a logical approach to study oxidative stress mechanisms in the progression of NASH and can be used to test compounds that attenuate oxidative stress-mediated inflammation in this disease. On the other hand, use of MCD diet model is used widely to depict steatohepatitic lesions coupled with fibrosis, symptoms that are found in more progressive stages of human NASH (105, 107, 108). The symptoms found in this model represent lesions of human NASH but in a non-insulin resistant state though some studies have found hepatic insulin resistance in this model. The results thus obtained from these studies reported here may be the beginning of many future studies involving NADPH oxidase activation induced TLR4 trafficking and could be validated using other models of NASH.

The dual approach of using two different peroxynitrite blockers was significant since FeTPPS and other metaloporphyrins have been used in various rodent models of inflammatory diseases but has low oral bioavailability and lacked specificity (53). FBA, an aromatic boronate has been shown to react specifically with peroxynitrite to yield

www.manaraa.com

tyrosine as a major product and the probability of formation of nitrotyrosine following a reaction with peroxynitrite is negligible because of the stoichiometry of the chemical reaction (109). This reaction kinetics made FBA to be a specific scavenger and blocking agent for peroxynitrite (109). FBA reacts with peroxynitrite at a rapid rate and stoichiometrically to form phenol ($k=1.6x10^6$ $M^{-1}s^{-1}$)(110). FBA is also highly specific to react with peroxynitrite and can be used to infer the source of tyrosine nitration since it does not inhibit myeloperoxidase-dependent tyrosine nitration. We utilized the effectiveness of FBA as a candidate drug to attenuate peroxynitrite mediated recruitment of TLR4 into hepatic lipid rafts. My results of a significant attenuation of TLR4 recruitment to lipid rafts as shown by the colocalization of TLR4 and the lipid raft protein, flotillin in NASH livers of mice might provide a rationale for using FBA as a future small molecule to attenuate TLR4 mediated inflammation in NASH. However caution should be exercised before interpreting the findings reported here since FBA has not been used previously in other inflammatory disease models. Further FBA treatment also abrogated TLR4-induced NFkB translocation and DNA binding, increased levels of sinusoidal injury markers ICAM-1 and E-selectin, Kupffer cell activation marker CD68 and stellate cell proliferation. FBA treated NASH livers had significantly less fibrosis as assessed by NAS scores.

The results further underline an alternate mechanism of lipid raft recruitment of TLR4 via an oxidative and nitrative stress pathway, unique in NASH pathophysiology. The recruitment of TLR4 might happen as a result of Nrf2 depletion which has a direct effect on glutathione synthesizing enzymes and lower levels of glutathione seen in NASH, though this remains speculative at this point (111, 112). The results reported here support the role

www.manaraa.com

of highly reactive peroxynitrite in causing TLR4 trafficking rather than oxyradicals generated as a result of TLR4 activation, a concept that has been reported before and is widely prevalent in inflammatory diseases (113). My data supports the peroxynitrite mechanism owing to the faster rate kinetics of formation reported for peroxynitrite (10^{10} $M^{-1}S^{-1}$) but the TLR4-induced NADPH oxidase activation in NASH cannot be ruled out owing to the complex innate immune regulations associated in the pathophysiology of the disease itself (110).

In summary I show that TLR-recruitment in lipid rafts is an early event in both rodent and human NASH pathogenesis. TLR4-recruitment is initiated by NADPH oxidase and the molecular basis of this early event is dependent on the formation of peroxynitrite. The use of FBA as a novel compound to attenuate peroxynitrite in vivo might serve as a new approach to initiate further studies involving relevant rodent models of NASH and inflammatory pathogenesis in this disease. This might have significant relevance for research in drug development concerning the attenuation of NASH. The study is highly significant since I used two different models of NASH, elucidated the formation of peroxynitrite and TLR4 lipid raft recruitment in human NASH and avoided in vitro cellular experimentation to prove the involvement of peroxynitrite in TLR4 lipid raft recruitment, primarily because of the advanced tools to detect peroxynitrite. However, caution should be exercised in interpreting some of the results noted in this report since we are not aware of the oral bioavailability of this compound and future rodent based studies need to focus more on the pharmacokinetics of FBA

www.manaraa.com

REFERENCES

1. Farooqi IS. Genetic, molecular and physiological insights into human obesity. European journal of clinical investigation. 2011;41(4):451-5. Epub 2011/03/12. doi: 10.1111/j.1365-2362.2010.02468.x. PubMed PMID: 21391993.
2. Rius B, Lopez-Vicario C, Gonzalez-Periz A, Moran-Salvador E, Garcia-Alonso V, Claria J, et al. Resolution of inflammation in obesity-induced liver disease. Frontiers in immunology. 2012;3:257. Epub 2012/08/31. doi: 10.3389/fimmu.2012.00257. PubMed PMID: 22934096; PubMed Central PMCID: PMCPMC3422856.
3. Johnson AR, Milner JJ, Makowski L. The inflammation highway: metabolism accelerates inflammatory traffic in obesity. Immunological reviews. 2012;249(1):218-38. Epub 2012/08/15. doi: 10.1111/j.1600-065X.2012.01151.x. PubMed PMID: 22889225; PubMed Central PMCID: PMCPMC3422768.
4. Ikejima K, Honda H, Yoshikawa M, Hirose M, Kitamura T, Takei Y, et al. Leptin augments inflammatory and profibrogenic responses in the murine liver induced by hepatotoxic chemicals. Hepatology. 2001;34(2):288-97. Epub 2001/08/02. doi: 10.1053/jhep.2001.26518. PubMed PMID: 11481614.
5. Shen C, Zhao CY, Zhang R, Qiao L. Obesity-related hepatocellular carcinoma: roles of risk factors altered in obesity. Frontiers in bioscience : a journal and virtual library. 2012;17:2356-70. Epub 2012/06/02. PubMed PMID: 22652784.
6. Day CP, James OF. Steatohepatitis: a tale of two "hits"? Gastroenterology. 1998;114(4):842-5. Epub 1998/04/18. PubMed PMID: 9547102.
7. Tilg H, Moschen AR. Evolution of inflammation in nonalcoholic fatty liver disease: the multiple parallel hits hypothesis. Hepatology. 2010;52(5):1836-46. Epub 2010/11/03. doi: 10.1002/hep.24001. PubMed PMID: 21038418.
8. Chatterjee S, Rana R, Corbett J, Kadiiska MB, Goldstein J, Mason RP. P2X7 receptor-NADPH oxidase axis mediates protein radical formation and Kupffer cell activation in carbon tetrachloride-mediated steatohepatitis in obese mice. Free Radic Biol Med. 2012;52(9):1666-79. Epub 2012/02/22. doi: 10.1016/j.freeradbiomed.2012.02.010. PubMed PMID: 22343416; PubMed Central PMCID: PMCPMC3341527.
9. Cave M, Appana S, Patel M, Falkner KC, McClain CJ, Brock G. Polychlorinated biphenyls, lead, and mercury are associated with liver disease in American adults: NHANES 2003-2004. Environmental health perspectives. 2010;118(12):1735-42. Epub 2010/12/04. doi: 10.1289/ehp.1002720. PubMed PMID: 21126940; PubMed Central PMCID: PMCPMC3002193.
10. Abdelmegeed MA, Banerjee A, Yoo SH, Jang S, Gonzalez FJ, Song BJ. Critical role of cytochrome P450 2E1 (CYP2E1) in the development of high fat-induced non-alcoholic steatohepatitis. J Hepatol. 2012;57(4):860-6. Epub 2012/06/07. doi:

www.manaraa.com

10.1016/j.jhep.2012.05.019. PubMed PMID: 22668639; PubMed Central PMCID: PMCPMC3445664.
11. Leung TM, Nieto N. CYP2E1 and oxidant stress in alcoholic and non-alcoholic fatty liver disease. J Hepatol. 2012. Epub 2012/09/04. doi: 10.1016/j.jhep.2012.08.018. PubMed PMID: 22940046.
12. Parola M, Marra F. Adipokines and redox signaling: impact on fatty liver disease. Antioxid Redox Signal. 2011;15(2):461-83. Epub 2011/01/05. doi: 10.1089/ars.2010.3848. PubMed PMID: 21194387.
13. Chatterjee S, Ganini D, Tokar EJ, Kumar A, Das S, Corbett J, et al. Leptin is key to peroxynitrite-mediated oxidative stress and Kupffer cell activation in experimental nonalcoholic steatohepatitis. J Hepatol. 2012. Epub 2012/12/05. doi: 10.1016/j.jhep.2012.11.035. PubMed PMID: 23207144.
14. Mezyk SP, Helgeson T, Cole SK, Cooper WJ, Fox RV, Gardinali PR, et al. Free radical chemistry of disinfection-byproducts. 1. Kinetics of hydrated electron and hydroxyl radical reactions with halonitromethanes in water. The journal of physical chemistry A. 2006;110(6):2176-80. Epub 2006/02/10. doi: 10.1021/jp054962+. PubMed PMID: 16466253.
15. Tomasi A, Albano E, Biasi F, Slater TF, Vannini V, Dianzani MU. Activation of chloroform and related trihalomethanes to free radical intermediates in isolated hepatocytes and in the rat in vivo as detected by the ESR-spin trapping technique. Chemico-biological interactions. 1985;55(3):303-16. Epub 1985/11/01. PubMed PMID: 3000632.
16. Lilly PD, Andersen ME, Ross TM, Pegram RA. Physiologically based estimation of in vivo rates of bromodichloromethane metabolism. Toxicology. 1997;124(2):141-52. PubMed PMID: 9458004.
17. Keegan TE, Simmons JE, Pegram RA. NOAEL and LOAEL determinations of acute hepatotoxicity for chloroform and bromodichloromethane delivered in an aqueous vehicle to F344 rats. Journal of toxicology and environmental health Part A. 1998;55(1):65-75. Epub 1998/09/25. PubMed PMID: 9747604.
18. Bromodichloromethane. Report on carcinogens : carcinogen profiles / US Dept of Health and Human Services, Public Health Service, National Toxicology Program. 2011;12:73-5. Epub 2011/08/19. PubMed PMID: 21850115.
19. Kamada Y, Takehara T, Hayashi N. Adipocytokines and liver disease. Journal of gastroenterology. 2008;43(11):811-22. Epub 2008/11/18. doi: 10.1007/s00535-008-2213-6. PubMed PMID: 19012034.
20. Konner AC, Bruning JC. Selective insulin and leptin resistance in metabolic disorders. Cell metabolism. 2012;16(2):144-52. Epub 2012/08/14. doi: 10.1016/j.cmet.2012.07.004. PubMed PMID: 22883229.
21. Krawczyk K, Szczesniak P, Kumor A, Jasinska A, Omulecka A, Pietruczuk M, et al. Adipohormones as prognostric markers in patients with nonalcoholic steatohepatitis (NASH). J Physiol Pharmacol. 2009;60 Suppl 3:71-5. Epub 2010/01/09. PubMed PMID: 19996485.
22. Li Z, Lin H, Yang S, Diehl AM. Murine leptin deficiency alters Kupffer cell production of cytokines that regulate the innate immune system. Gastroenterology. 2002;123(4):1304-10. Epub 2002/10/03. PubMed PMID: 12360490.
23. Wang J, Leclercq I, Brymora JM, Xu N, Ramezani-Moghadam M, London RM, et al. Kupffer cells mediate leptin-induced liver fibrosis. Gastroenterology. 2009;137(2):713-

www.manaraa.com

23. Epub 2009/04/21. doi: 10.1053/j.gastro.2009.04.011. PubMed PMID: 19375424; PubMed Central PMCID: PMC2757122.
24. De Minicis S, Seki E, Oesterreicher C, Schnabl B, Schwabe RF, Brenner DA. Reduced nicotinamide adenine dinucleotide phosphate oxidase mediates fibrotic and inflammatory effects of leptin on hepatic stellate cells. Hepatology. 2008;48(6):2016-26. Epub 2008/11/26. doi: 10.1002/hep.22560. PubMed PMID: 19025999.
25. Handy JA, Fu PP, Kumar P, Mells JE, Sharma S, Saxena NK, et al. Adiponectin inhibits leptin signalling via multiple mechanisms to exert protective effects against hepatic fibrosis. The Biochemical journal. 2011;440(3):385-95. Epub 2011/08/19. doi: 10.1042/bj20102148. PubMed PMID: 21846328; PubMed Central PMCID: PMCPMC3226855.
26. Sanyal AJ, Campbell-Sargent C, Mirshahi F, Rizzo WB, Contos MJ, Sterling RK, et al. Nonalcoholic steatohepatitis: association of insulin resistance and mitochondrial abnormalities. Gastroenterology. 2001;120(5):1183-92. Epub 2001/03/27. doi: 10.1053/gast.2001.23256. PubMed PMID: 11266382.
27. Seki S, Kitada T, Yamada T, Sakaguchi H, Nakatani K, Wakasa K. In situ detection of lipid peroxidation and oxidative DNA damage in non-alcoholic fatty liver diseases. J Hepatol. 2002;37(1):56-62. Epub 2002/06/22. PubMed PMID: 12076862.
28. Mendelson KG, Contois LR, Tevosian SG, Davis RJ, Paulson KE. Independent regulation of JNK/p38 mitogen-activated protein kinases by metabolic oxidative stress in the liver. Proceedings of the National Academy of Sciences of the United States of America. 1996;93(23):12908-13. Epub 1996/11/12. PubMed PMID: 8917518; PubMed Central PMCID: PMCPMC24019.
29. Wang Y, Qin ZH. Coordination of autophagy with other cellular activities. Acta pharmacologica Sinica. 2013. Epub 2013/03/12. doi: 10.1038/aps.2012.194. PubMed PMID: 23474706.
30. Deretic V. Autophagy: an emerging immunological paradigm. J Immunol. 2012;189(1):15-20. Epub 2012/06/23. doi: 10.4049/jimmunol.1102108. PubMed PMID: 22723639; PubMed Central PMCID: PMCPMC3382968.
31. Amir M, Czaja MJ. Autophagy in nonalcoholic steatohepatitis. Expert review of gastroenterology & hepatology. 2011;5(2):159-66. Epub 2011/04/12. doi: 10.1586/egh.11.4. PubMed PMID: 21476911; PubMed Central PMCID: PMCPMC3104297.
32. Mehrpour M, Esclatine A, Beau I, Codogno P. Autophagy in health and disease. 1. Regulation and significance of autophagy: an overview. American journal of physiology Cell physiology. 2010;298(4):C776-85. Epub 2010/01/22. doi: 10.1152/ajpcell.00507.2009. PubMed PMID: 20089931.
33. Orenstein SJ, Cuervo AM. Chaperone-mediated autophagy: molecular mechanisms and physiological relevance. Seminars in cell & developmental biology. 2010;21(7):719-26. Epub 2010/02/24. doi: 10.1016/j.semcdb.2010.02.005. PubMed PMID: 20176123; PubMed Central PMCID: PMCPMC2914824.
34. Kaushik S, Cuervo AM. Chaperone-mediated autophagy: a unique way to enter the lysosome world. Trends in cell biology. 2012;22(8):407-17. Epub 2012/07/04. doi: 10.1016/j.tcb.2012.05.006. PubMed PMID: 22748206; PubMed Central PMCID: PMCPMC3408550.

www.manaraa.com

35. Qu Y, Dubyak GR. P2X7 receptors regulate multiple types of membrane trafficking responses and non-classical secretion pathways. Purinergic signalling. 2009;5(2):163-73. Epub 2009/02/04. doi: 10.1007/s11302-009-9132-8. PubMed PMID: 19189228; PubMed Central PMCID: PMCPMC2686822.
36. Arulkumaran N, Unwin RJ, Tam FW. A potential therapeutic role for P2X7 receptor (P2X7R) antagonists in the treatment of inflammatory diseases. Expert opinion on investigational drugs. 2011;20(7):897-915. Epub 2011/04/23. doi: 10.1517/13543784.2011.578068. PubMed PMID: 21510825; PubMed Central PMCID: PMCPMC3114873.
37. Bohinc BN, Diehl AM. Mechanisms of disease progression in NASH: new paradigms. Clinics in liver disease. 2012;16(3):549-65. Epub 2012/07/25. doi: 10.1016/j.cld.2012.05.002. PubMed PMID: 22824480.
38. Bosch J, Abraldes JG, Fernandez M, Garcia-Pagan JC. Hepatic endothelial dysfunction and abnormal angiogenesis: new targets in the treatment of portal hypertension. J Hepatol. 2010;53(3):558-67. Epub 2010/06/22. doi: 10.1016/j.jhep.2010.03.021. PubMed PMID: 20561700.
39. Diehl AM. Nonalcoholic steatohepatitis. Seminars in liver disease. 1999;19(2):221-9. Epub 1999/07/28. doi: 10.1055/s-2007-1007111. PubMed PMID: 10422202.
40. Farrell GC, van Rooyen D, Gan L, Chitturi S. NASH is an Inflammatory Disorder: Pathogenic, Prognostic and Therapeutic Implications. Gut and liver. 2012;6(2):149-71. Epub 2012/05/10. doi: 10.5009/gnl.2012.6.2.149. PubMed PMID: 22570745; PubMed Central PMCID: PMCPMC3343154.
41. Marra F, Aleffi S, Bertolani C, Petrai I, Vizzutti F. Adipokines and liver fibrosis. European review for medical and pharmacological sciences. 2005;9(5):279-84. Epub 2005/10/20. PubMed PMID: 16231590.
42. Pasarin M, La Mura V, Gracia-Sancho J, Garcia-Caldero H, Rodriguez-Vilarrupla A, Garcia-Pagan JC, et al. Sinusoidal endothelial dysfunction precedes inflammation and fibrosis in a model of NAFLD. PloS one. 2012;7(4):e32785. Epub 2012/04/18. doi: 10.1371/journal.pone.0032785. PubMed PMID: 22509248; PubMed Central PMCID: PMCPMC3317918.
43. Tilg H, Diehl AM. Cytokines in alcoholic and nonalcoholic steatohepatitis. The New England journal of medicine. 2000;343(20):1467-76. Epub 2000/11/18. doi: 10.1056/nejm200011163432007. PubMed PMID: 11078773.
44. Clark JM, Brancati FL, Diehl AM. Nonalcoholic fatty liver disease. Gastroenterology. 2002;122(6):1649-57. Epub 2002/05/23. PubMed PMID: 12016429.
45. Li Z, Clark J, Diehl AM. The liver in obesity and type 2 diabetes mellitus. Clinics in liver disease. 2002;6(4):867-77. Epub 2003/01/09. PubMed PMID: 12516196.
46. Diehl AM, Li ZP, Lin HZ, Yang SQ. Cytokines and the pathogenesis of non-alcoholic steatohepatitis. Gut. 2005;54(2):303-6. Epub 2005/01/14. doi: 10.1136/gut.2003.024935. PubMed PMID: 15647199; PubMed Central PMCID: PMCPMC1774847.
47. Abdelmalek MF, Diehl AM. Nonalcoholic fatty liver disease as a complication of insulin resistance. The Medical clinics of North America. 2007;91(6):1125-49, ix. Epub 2007/10/30. doi: 10.1016/j.mcna.2007.06.001. PubMed PMID: 17964913.

www.manaraa.com

48. Gay NJ, Symmons MF, Gangloff M, Bryant CE. Assembly and localization of Toll-like receptor signalling complexes. Nature reviews Immunology. 2014;14(8):546-58. Epub 2014/07/26. doi: 10.1038/nri3713. PubMed PMID: 25060580.
49. Deguine J, Barton GM. MyD88: a central player in innate immune signaling. F1000prime reports. 2014;6:97. Epub 2015/01/13. doi: 10.12703/p6-97. PubMed PMID: 25580251; PubMed Central PMCID: PMCPMC4229726.
50. Dziarski R, Wang Q, Miyake K, Kirschning CJ, Gupta D. MD-2 enables Toll-like receptor 2 (TLR2)-mediated responses to lipopolysaccharide and enhances TLR2-mediated responses to Gram-positive and Gram-negative bacteria and their cell wall components. J Immunol. 2001;166(3):1938-44. Epub 2001/02/13. PubMed PMID: 11160242.
51. Choi S, Diehl AM. Role of inflammation in nonalcoholic steatohepatitis. Current opinion in gastroenterology. 2005;21(6):702-7. Epub 2005/10/13. PubMed PMID: 16220049.
52. Paik YH, Kim J, Aoyama T, De Minicis S, Bataller R, Brenner DA. Role of NADPH oxidases in liver fibrosis. Antioxid Redox Signal. 2014;20(17):2854-72. Epub 2013/09/18. doi: 10.1089/ars.2013.5619. PubMed PMID: 24040957; PubMed Central PMCID: PMCPMC4026397.
53. Yang L, Li P, Fu S, Calay ES, Hotamisligil GS. Defective hepatic autophagy in obesity promotes ER stress and causes insulin resistance. Cell metabolism. 2010;11(6):467-78. Epub 2010/06/04. doi: 10.1016/j.cmet.2010.04.005. PubMed PMID: 20519119; PubMed Central PMCID: PMCPMC2881480.
54. Yang SQ, Lin HZ, Lane MD, Clemens M, Diehl AM. Obesity increases sensitivity to endotoxin liver injury: implications for the pathogenesis of steatohepatitis. Proceedings of the National Academy of Sciences of the United States of America. 1997;94(6):2557-62. Epub 1997/03/18. PubMed PMID: 9122234; PubMed Central PMCID: PMCPMC20127.
55. Hotamisligil GS, Shargill NS, Spiegelman BM. Adipose expression of tumor necrosis factor-alpha: direct role in obesity-linked insulin resistance. Science (New York, NY). 1993;259(5091):87-91. Epub 1993/01/01. PubMed PMID: 7678183.
56. Chatterjee S, Ehrenshaft M, Bhattacharjee S, Deterding LJ, Bonini MG, Corbett J, et al. Immuno-spin trapping of a post-translational carboxypeptidase B1 radical formed by a dual role of xanthine oxidase and endothelial nitric oxide synthase in acute septic mice. Free Radic Biol Med. 2009;46(4):454-61. Epub 2008/12/04. doi: 10.1016/j.freeradbiomed.2008.10.046. PubMed PMID: 19049863; PubMed Central PMCID: PMC2661569.
57. Munzberg H. Leptin-signaling pathways and leptin resistance. Forum of nutrition. 2010;63:123-32. Epub 2009/12/04. doi: 10.1159/000264400. PubMed PMID: 19955780.
58. Tosello-Trampont AC, Landes SG, Nguyen V, Novobrantseva TI, Hahn YS. Kuppfer cells trigger nonalcoholic steatohepatitis development in diet-induced mouse model through TNFalpha production. J Biol Chem. 2012. Epub 2012/10/16. doi: 10.1074/jbc.M112.417014. PubMed PMID: 23066023.
59. Miura K, Yang L, van Rooijen N, Ohnishi H, Seki E. Hepatic recruitment of macrophages promotes nonalcoholic steatohepatitis through CCR2. American journal of physiology Gastrointestinal and liver physiology. 2012;302(11):G1310-21. Epub

www.manaraa.com

2012/03/24. doi: 10.1152/ajpgi.00365.2011. PubMed PMID: 22442158; PubMed Central PMCID: PMCPMC3378163.
60. Tang D, Kang R, Coyne CB, Zeh HJ, Lotze MT. PAMPs and DAMPs: signal 0s that spur autophagy and immunity. Immunological reviews. 2012;249(1):158-75. Epub 2012/08/15. doi: 10.1111/j.1600-065X.2012.01146.x. PubMed PMID: 22889221.
61. Torti VR, Cobb AJ, Everitt JI, Marshall MW, Boorman GA, Butterworth BE. Nephrotoxicity and hepatotoxicity induced by inhaled bromodichloromethane in wild-type and p53-heterozygous mice. Toxicological sciences : an official journal of the Society of Toxicology. 2001;64(2):269-80. Epub 2001/11/24. PubMed PMID: 11719710.
62. Gorska E, Popko K, Stelmaszczyk-Emmel A, Ciepiela O, Kucharska A, Wasik M. Leptin receptors. Eur J Med Res. 2010;15 Suppl 2:50-4. Epub 2010/12/22. PubMed PMID: 21147620.
63. Lafrance V, Inoue W, Kan B, Luheshi GN. Leptin modulates cell morphology and cytokine release in microglia. Brain Behav Immun. 2010;24(3):358-65. Epub 2009/11/20. doi: 10.1016/j.bbi.2009.11.003. PubMed PMID: 19922787.
64. Shen J, Sakaida I, Uchida K, Terai S, Okita K. Leptin enhances TNF-alpha production via p38 and JNK MAPK in LPS-stimulated Kupffer cells. Life Sci. 2005;77(13):1502-15. Epub 2005/06/28. doi: 10.1016/j.lfs.2005.04.004. PubMed PMID: 15979653.
65. Souza JM, Peluffo G, Radi R. Protein tyrosine nitration--functional alteration or just a biomarker? Free Radic Biol Med. 2008;45(4):357-66. Epub 2008/05/08. doi: 10.1016/j.freeradbiomed.2008.04.010. PubMed PMID: 18460345.
66. Kim CH, Younossi ZM. Nonalcoholic fatty liver disease: a manifestation of the metabolic syndrome. Cleveland Clinic journal of medicine. 2008;75(10):721-8. Epub 2008/10/23. PubMed PMID: 18939388.
67. Lin CW, Zhang H, Li M, Xiong X, Chen X, Chen X, et al. Pharmacological promotion of autophagy alleviates steatosis and injury in alcoholic and non-alcoholic fatty liver conditions in mice. J Hepatol. 2013;58(5):993-9. Epub 2013/01/24. doi: 10.1016/j.jhep.2013.01.011. PubMed PMID: 23339953; PubMed Central PMCID: PMCPMC3634371.
68. Das S, Kumar A, Seth RK, Tokar EJ, Kadiiska MB, Waalkes MP, et al. Proinflammatory adipokine leptin mediates disinfection byproduct bromodichloromethane-induced early steatohepatitic injury in obesity. Toxicology and applied pharmacology. 2013. Epub 2013/02/27. doi: 10.1016/j.taap.2013.02.003. PubMed PMID: 23438451.
69. Seth RK, Kumar A, Das S, Kadiiska MB, Michelotti G, Diehl AM, et al. Environmental toxin-linked nonalcoholic steatohepatitis and hepatic metabolic reprogramming in obese mice. Toxicological sciences : an official journal of the Society of Toxicology. 2013. Epub 2013/05/04. doi: 10.1093/toxsci/kft104. PubMed PMID: 23640861.
70. Witek RP, Stone WC, Karaca FG, Syn WK, Pereira TA, Agboola KM, et al. Pan-caspase inhibitor VX-166 reduces fibrosis in an animal model of nonalcoholic steatohepatitis. Hepatology. 2009;50(5):1421-30. Epub 2009/08/14. doi: 10.1002/hep.23167. PubMed PMID: 19676126.
71. Yamaguchi K, Yang L, McCall S, Huang J, Yu XX, Pandey SK, et al. Inhibiting triglyceride synthesis improves hepatic steatosis but exacerbates liver damage and fibrosis

www.manaraa.com

in obese mice with nonalcoholic steatohepatitis. Hepatology. 2007;45(6):1366-74. Epub 2007/05/04. doi: 10.1002/hep.21655. PubMed PMID: 17476695.
72. Eccleston HB, Andringa KK, Betancourt AM, King AL, Mantena SK, Swain TM, et al. Chronic exposure to a high-fat diet induces hepatic steatosis, impairs nitric oxide bioavailability, and modifies the mitochondrial proteome in mice. Antioxid Redox Signal. 2011;15(2):447-59. Epub 2010/10/06. doi: 10.1089/ars.2010.3395. PubMed PMID: 20919931; PubMed Central PMCID: PMCPMC3118652.
73. Mantena SK, Vaughn DP, Andringa KK, Eccleston HB, King AL, Abrams GA, et al. High fat diet induces dysregulation of hepatic oxygen gradients and mitochondrial function in vivo. The Biochemical journal. 2009;417(1):183-93. Epub 2008/08/30. doi: 10.1042/bj20080868. PubMed PMID: 18752470; PubMed Central PMCID: PMCPMC2637578.
74. Shertzer HG, Kendig EL, Nasrallah HA, Johansson E, Genter MB. Protection from olanzapine-induced metabolic toxicity in mice by acetaminophen and tetrahydroindenoindole. International journal of obesity (2005). 2010;34(6):970-9. Epub 2010/01/13. doi: 10.1038/ijo.2009.291. PubMed PMID: 20065957; PubMed Central PMCID: PMCPMC2885476.
75. Pacana T, Sanyal AJ. Vitamin E and nonalcoholic fatty liver disease. Current opinion in clinical nutrition and metabolic care. 2012;15(6):641-8. Epub 2012/10/19. doi: 10.1097/MCO.0b013e328357f747. PubMed PMID: 23075940.
76. Chiang HL, Terlecky SR, Plant CP, Dice JF. A role for a 70-kilodalton heat shock protein in lysosomal degradation of intracellular proteins. Science (New York, NY). 1989;246(4928):382-5. Epub 1989/10/20. PubMed PMID: 2799391.
77. Li W, Yang Q, Mao Z. Chaperone-mediated autophagy: machinery, regulation and biological consequences. Cellular and molecular life sciences : CMLS. 2011;68(5):749-63. Epub 2010/10/27. doi: 10.1007/s00018-010-0565-6. PubMed PMID: 20976518.
78. Li G, Liang X, Lotze MT. HMGB1: The Central Cytokine for All Lymphoid Cells. Frontiers in immunology. 2013;4:68. Epub 2013/03/23. doi: 10.3389/fimmu.2013.00068. PubMed PMID: 23519706; PubMed Central PMCID: PMCPMC3602962.
79. Kawano A, Tsukimoto M, Mori D, Noguchi T, Harada H, Takenouchi T, et al. Regulation of P2X7-dependent inflammatory functions by P2X4 receptor in mouse macrophages. Biochem Biophys Res Commun. 2012;420(1):102-7. Epub 2012/03/13. doi: 10.1016/j.bbrc.2012.02.122. PubMed PMID: 22405772.
80. Durazzo M, Belci P, Collo A, Grisoglio E, Bo S. Focus on therapeutic strategies of nonalcoholic Fatty liver disease. International journal of hepatology. 2012;2012:464706. Epub 2012/12/05. doi: 10.1155/2012/464706. PubMed PMID: 23209914; PubMed Central PMCID: PMCPMC3502854.
81. Takenouchi T, Nakai M, Iwamaru Y, Sugama S, Tsukimoto M, Fujita M, et al. The activation of P2X7 receptor impairs lysosomal functions and stimulates the release of autophagolysosomes in microglial cells. J Immunol. 2009;182(4):2051-62. Epub 2009/02/10. doi: 10.4049/jimmunol.0802577. PubMed PMID: 19201858.
82. Kiffin R, Christian C, Knecht E, Cuervo AM. Activation of chaperone-mediated autophagy during oxidative stress. Molecular biology of the cell. 2004;15(11):4829-40. Epub 2004/08/28. doi: 10.1091/mbc.E04-06-0477. PubMed PMID: 15331765; PubMed Central PMCID: PMCPMC524731.

www.manaraa.com

83. Venereau E, Casalgrandi M, Schiraldi M, Antoine DJ, Cattaneo A, De Marchis F, et al. Mutually exclusive redox forms of HMGB1 promote cell recruitment or proinflammatory cytokine release. The Journal of experimental medicine. 2012;209(9):1519-28. Epub 2012/08/08. doi: 10.1084/jem.20120189. PubMed PMID: 22869893; PubMed Central PMCID: PMCPMC3428943.
84. Fortunato F, Burgers H, Bergmann F, Rieger P, Buchler MW, Kroemer G, et al. Impaired autolysosome formation correlates with Lamp-2 depletion: role of apoptosis, autophagy, and necrosis in pancreatitis. Gastroenterology. 2009;137(1):350-60, 60 e1-5. Epub 2009/04/14. doi: 10.1053/j.gastro.2009.04.003. PubMed PMID: 19362087.
85. Nakahira K, Haspel JA, Rathinam VA, Lee SJ, Dolinay T, Lam HC, et al. Autophagy proteins regulate innate immune responses by inhibiting the release of mitochondrial DNA mediated by the NALP3 inflammasome. Nature immunology. 2011;12(3):222-30. Epub 2010/12/15. doi: 10.1038/ni.1980. PubMed PMID: 21151103; PubMed Central PMCID: PMCPMC3079381.
86. Friedman SL. Focus. J Hepatol. 2013;58(5):845-6. Epub 2013/02/05. doi: 10.1016/j.jhep.2013.01.031. PubMed PMID: 23376365.
87. Reaven G. Metabolic syndrome: pathophysiology and implications for management of cardiovascular disease. Circulation. 2002;106(3):286-8. Epub 2002/07/18. PubMed PMID: 12119239.
88. Gallagher EJ, Leroith D, Karnieli E. Insulin resistance in obesity as the underlying cause for the metabolic syndrome. The Mount Sinai journal of medicine, New York. 2010;77(5):511-23. Epub 2010/10/21. doi: 10.1002/msj.20212. PubMed PMID: 20960553.
89. Brunt EM, Janney CG, Di Bisceglie AM, Neuschwander-Tetri BA, Bacon BR. Nonalcoholic steatohepatitis: a proposal for grading and staging the histological lesions. The American journal of gastroenterology. 1999;94(9):2467-74. Epub 1999/09/14. doi: 10.1111/j.1572-0241.1999.01377.x. PubMed PMID: 10484010.
90. Kleiner DE, Brunt EM, Van Natta M, Behling C, Contos MJ, Cummings OW, et al. Design and validation of a histological scoring system for nonalcoholic fatty liver disease. Hepatology. 2005;41(6):1313-21. Epub 2005/05/26. doi: 10.1002/hep.20701. PubMed PMID: 15915461.
91. Chen SH, He F, Zhou HL, Wu HR, Xia C, Li YM. Relationship between nonalcoholic fatty liver disease and metabolic syndrome. Journal of digestive diseases. 2011;12(2):125-30. Epub 2011/03/16. doi: 10.1111/j.1751-2980.2011.00487.x. PubMed PMID: 21401898.
92. Kelley CE, Brown AJ, Diehl AM, Setji TL. Review of nonalcoholic fatty liver disease in women with polycystic ovary syndrome. World journal of gastroenterology : WJG. 2014;20(39):14172-84. Epub 2014/10/24. doi: 10.3748/wjg.v20.i39.14172. PubMed PMID: 25339805; PubMed Central PMCID: PMCPMC4202347.
93. Angulo P. Treatment of nonalcoholic fatty liver disease. Annals of hepatology. 2002;1(1):12-9. Epub 2004/04/29. PubMed PMID: 15114291.
94. Chalasani N, Younossi Z, Lavine JE, Diehl AM, Brunt EM, Cusi K, et al. The diagnosis and management of non-alcoholic fatty liver disease: practice Guideline by the American Association for the Study of Liver Diseases, American College of Gastroenterology, and the American Gastroenterological Association. Hepatology. 2012;55(6):2005-23. Epub 2012/04/11. doi: 10.1002/hep.25762. PubMed PMID: 22488764.

www.manaraa.com

95. Rosso N, Chavez-Tapia NC, Tiribelli C, Bellentani S. Translational approaches: from fatty liver to non-alcoholic steatohepatitis. World journal of gastroenterology : WJG. 2014;20(27):9038-49. Epub 2014/08/02. doi: 10.3748/wjg.v20.i27.9038. PubMed PMID: 25083077; PubMed Central PMCID: PMCPMC4112858.
96. Vernon G, Baranova A, Younossi ZM. Systematic review: the epidemiology and natural history of non-alcoholic fatty liver disease and non-alcoholic steatohepatitis in adults. Alimentary pharmacology & therapeutics. 2011;34(3):274-85. Epub 2011/06/01. doi: 10.1111/j.1365-2036.2011.04724.x. PubMed PMID: 21623852.
97. Bugianesi E, Moscatiello S, Ciaravella MF, Marchesini G. Insulin resistance in nonalcoholic fatty liver disease. Current pharmaceutical design. 2010;16(17):1941-51. Epub 2010/04/08. PubMed PMID: 20370677.
98. Lu YC, Yeh WC, Ohashi PS. LPS/TLR4 signal transduction pathway. Cytokine. 2008;42(2):145-51. Epub 2008/02/29. doi: 10.1016/j.cyto.2008.01.006. PubMed PMID: 18304834.
99. Farrell GC, Teoh NC, McCuskey RS. Hepatic microcirculation in fatty liver disease. Anatomical record (Hoboken, NJ : 2007). 2008;291(6):684-92. Epub 2008/05/20. doi: 10.1002/ar.20715. PubMed PMID: 18484615.
100. Sumida Y, Niki E, Naito Y, Yoshikawa T. Involvement of free radicals and oxidative stress in NAFLD/NASH. Free radical research. 2013;47(11):869-80. Epub 2013/09/06. doi: 10.3109/10715762.2013.837577. PubMed PMID: 24004441.
101. Ramesh S, Sanyal AJ. Evaluation and management of non-alcoholic steatohepatitis. J Hepatol. 2005;42 Suppl(1):S2-12. Epub 2005/03/22. doi: 10.1016/j.jhep.2004.11.022. PubMed PMID: 15777569.
102. Michelotti GA, Machado MV, Diehl AM. NAFLD, NASH and liver cancer. Nature reviews Gastroenterology & hepatology. 2013;10(11):656-65. Epub 2013/10/02. doi: 10.1038/nrgastro.2013.183. PubMed PMID: 24080776.
103. Petrasek J, Csak T, Szabo G. Toll-like receptors in liver disease. Advances in clinical chemistry. 2013;59:155-201. Epub 2013/03/07. PubMed PMID: 23461136.
104. Aubert J, Begriche K, Knockaert L, Robin MA, Fromenty B. Increased expression of cytochrome P450 2E1 in nonalcoholic fatty liver disease: mechanisms and pathophysiological role. Clinics and research in hepatology and gastroenterology. 2011;35(10):630-7. Epub 2011/06/15. doi: 10.1016/j.clinre.2011.04.015. PubMed PMID: 21664213.
105. Nakamura A, Terauchi Y. Lessons from mouse models of high-fat diet-induced NAFLD. International journal of molecular sciences. 2013;14(11):21240-57. Epub 2013/11/29. doi: 10.3390/ijms141121240. PubMed PMID: 24284392; PubMed Central PMCID: PMCPMC3856002.
106. Takaki A, Kawai D, Yamamoto K. Multiple hits, including oxidative stress, as pathogenesis and treatment target in non-alcoholic steatohepatitis (NASH). International journal of molecular sciences. 2013;14(10):20704-28. Epub 2013/10/18. doi: 10.3390/ijms141020704. PubMed PMID: 24132155; PubMed Central PMCID: PMCPMC3821639.
107. Koppe SW, Sahai A, Malladi P, Whitington PF, Green RM. Pentoxifylline attenuates steatohepatitis induced by the methionine choline deficient diet. J Hepatol. 2004;41(4):592-8. Epub 2004/10/07. doi: 10.1016/j.jhep.2004.06.030. PubMed PMID: 15464239.

www.manaraa.com

108. Oz HS, Chen TS, Neuman M. Methionine deficiency and hepatic injury in a dietary steatohepatitis model. Digestive diseases and sciences. 2008;53(3):767-76. Epub 2007/08/22. doi: 10.1007/s10620-007-9900-7. PubMed PMID: 17710550; PubMed Central PMCID: PMCPMC2271115.
109. Gawrieh S, Opara EC, Koch TR. Oxidative stress in nonalcoholic fatty liver disease: pathogenesis and antioxidant therapies. J Investig Med. 2004;52(8):506-14. Epub 2005/02/03. PubMed PMID: 15682682.
110. Sikora A, Zielonka J, Lopez M, Joseph J, Kalyanaraman B. Direct oxidation of boronates by peroxynitrite: mechanism and implications in fluorescence imaging of peroxynitrite. Free radical biology & medicine. 2009;47(10):1401-7. Epub 2009/08/19. doi: 10.1016/j.freeradbiomed.2009.08.006. PubMed PMID: 19686842; PubMed Central PMCID: PMCPMC3375817.
111. Skamarauskas JT, Oakley F, Smith FE, Bawn C, Dunn M, Vidler DS, et al. Noninvasive in vivo magnetic resonance measures of glutathione synthesis in human and rat liver as an oxidative stress biomarker. Hepatology (Baltimore, Md). 2014;59(6):2321-30. Epub 2013/11/19. doi: 10.1002/hep.26925. PubMed PMID: 24242936; PubMed Central PMCID: PMCPMC4160151.
112. Kong X, Thimmulappa R, Kombairaju P, Biswal S. NADPH oxidase-dependent reactive oxygen species mediate amplified TLR4 signaling and sepsis-induced mortality in Nrf2-deficient mice. Journal of immunology (Baltimore, Md : 1950). 2010;185(1):569-77. Epub 2010/06/01. doi: 10.4049/jimmunol.0902315. PubMed PMID: 20511556; PubMed Central PMCID: PMCPMC2913313.
113. Park HS, Jung HY, Park EY, Kim J, Lee WJ, Bae YS. Cutting edge: direct interaction of TLR4 with NAD(P)H oxidase 4 isozyme is essential for lipopolysaccharide-induced production of reactive oxygen species and activation of NF-kappa B. Journal of immunology (Baltimore, Md : 1950). 2004;173(6):3589-93. Epub 2004/09/10. PubMed PMID: 15356101.

www.manaraa.com

APPENDIX A: LICENSE AGREEMENT FOR CHAPTER 2

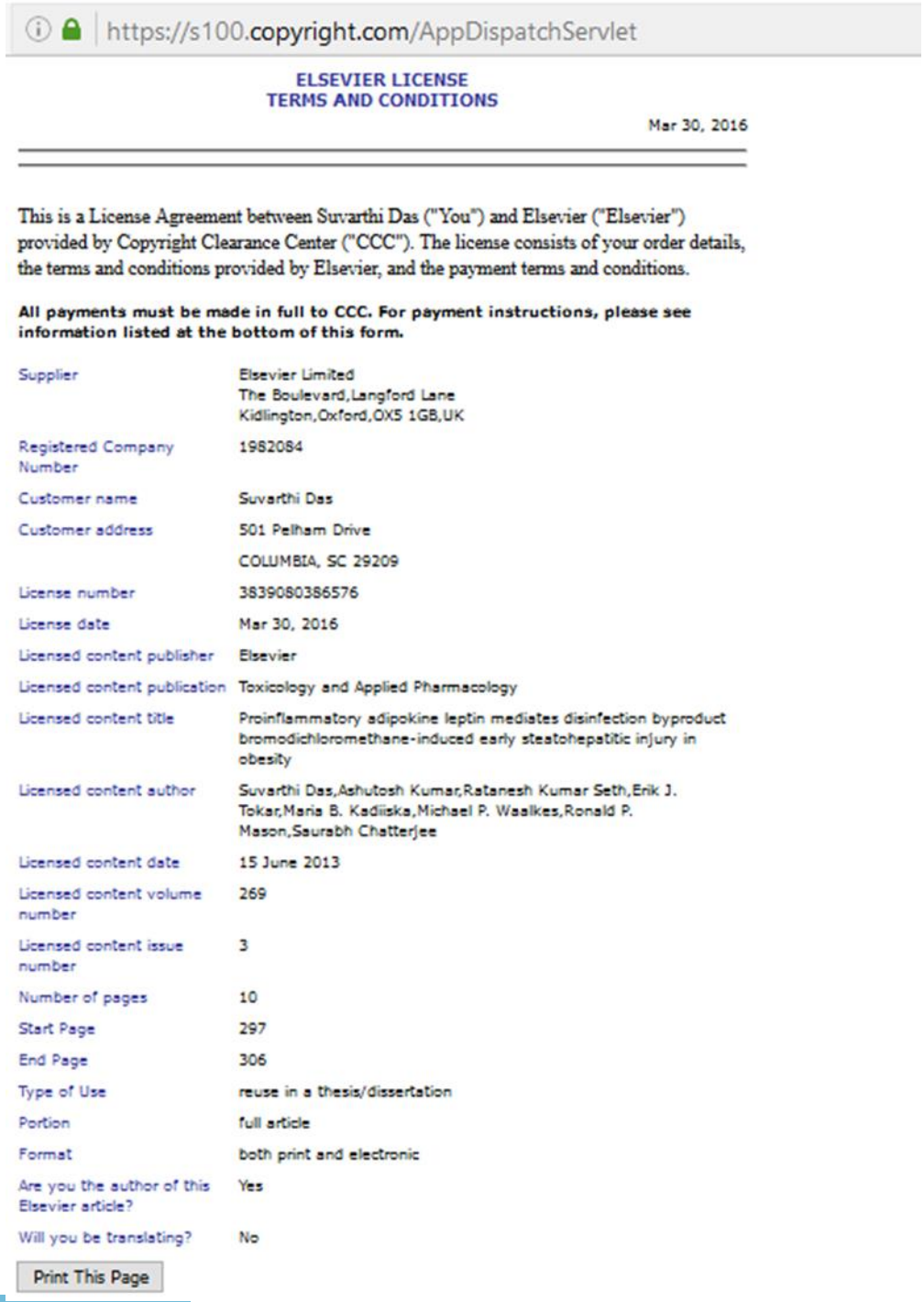

https://s100.copyright.com/AppDispatchServlet

ELSEVIER LICENSE
TERMS AND CONDITIONS

Mar 30, 2016

This is a License Agreement between Suvarthi Das ("You") and Elsevier ("Elsevier") provided by Copyright Clearance Center ("CCC"). The license consists of your order details, the terms and conditions provided by Elsevier, and the payment terms and conditions.

All payments must be made in full to CCC. For payment instructions, please see information listed at the bottom of this form.

Supplier	Elsevier Limited The Boulevard,Langford Lane Kidlington,Oxford,OX5 1GB,UK
Registered Company Number	1982084
Customer name	Suvarthi Das
Customer address	501 Pelham Drive COLUMBIA, SC 29209
License number	3839080386576
License date	Mar 30, 2016
Licensed content publisher	Elsevier
Licensed content publication	Toxicology and Applied Pharmacology
Licensed content title	Proinflammatory adipokine leptin mediates disinfection byproduct bromodichloromethane-induced early steatohepatitic injury in obesity
Licensed content author	Suvarthi Das,Ashutosh Kumar,Ratanesh Kumar Seth,Erik J. Tokar,Maria B. Kadiiska,Michael P. Waalkes,Ronald P. Mason,Saurabh Chatterjee
Licensed content date	15 June 2013
Licensed content volume number	269
Licensed content issue number	3
Number of pages	10
Start Page	297
End Page	306
Type of Use	reuse in a thesis/dissertation
Portion	full article
Format	both print and electronic
Are you the author of this Elsevier article?	Yes
Will you be translating?	No

Print This Page

www.manaraa.com

APPENDIX B: LICENSE AGREEMENT FOR CHAPTER 3

https://s100.copyright.com/AppDispatchServlet#formTop

Copyright Clearance Center RightsLink®

Home | Account Info | Help | Live Chat

Title: Purinergic receptor X7 is a key modulator of metabolic oxidative stress-mediated autophagy and inflammation in experimental nonalcoholic steatohepatitis

Author: Suvarthi Das,Ratanesh Kumar Seth,Ashutosh Kumar,Maria B. Kadiiska,Gregory Michelotti,Anna Mae Diehl,Saurabh Chatterjee

Publication: Am J Physiol-Gastrointestinal and Liver Physiology

Publisher: The American Physiological Society

Date: Dec 15, 2013

Copyright © 2013, The American Physiological Society

Logged in as:
Suvarthi Das
Account #:
3001014280
LOGOUT

Permission Not Required

Permission is not required for this type of use.

BACK | CLOSE WINDOW

Copyright © 2016 Copyright Clearance Center, Inc. All Rights Reserved. Privacy statement. Terms and Conditions.
Comments? We would like to hear from you. E-mail us at customercare@copyright.com

www.manaraa.com

APPENDIX C: LICENSE AGREEMENT FOR CHAPTER 4

ELSEVIER ORDER DETAILS

Apr 17, 2016

This is an Agreement between Suvarthi Das ("You") and Elsevier ("Elsevier"). It consists of your order details, the terms and conditions provided by Elsevier ("Elsevier"), and the payment terms and conditions.

Order Number	501132673
Order Date	Apr 17, 2016
Licensed content publisher	Elsevier
Licensed content publication	The American Journal of Pathology
Licensed content title	NADPH Oxidase–Derived Peroxynitrite Drives Inflammation in Mice and Human Nonalcoholic Steatohepatitis via TLR4-Lipid Raft Recruitment
Licensed content author	Suvarthi Das,Firas Alhasson,Diptadip Dattaroy,Sahar Pourhoseini,Ratanesh Kumar Seth,Mitzi Nagarkatti,Prakash S. Nagarkatti,Gregory A. Michelotti,Anna Mae Diehl,Balaraman Kalyanaraman,Saurabh Chatterjee
Licensed content date	July 2015
Licensed content volume number	185
Licensed content issue number	7
Number of pages	14
Start Page	1944
End Page	1957
Type of Use	reuse in a thesis/dissertation
Intended publisher of new work	other
Portion	full article
Format	both print and electronic
Are you the author of this Elsevier article?	Yes
Will you be translating?	No
Title of your thesis/dissertation	MOLECULAR CUES OF PATTERN-RECOGNITION-RECEPTOR PATHWAYS IN REDOX-TOXICITY-DRIVEN ENVIRONMENTAL NAFLD
Expected completion date	Apr 2016
Estimated size (number of pages)	
Elsevier VAT number	GB 494 6272 12

www.manaraa.com